THE PROCEEDINGS OF THE PHYSICAL SOCIETY

Section B

VOL. 62, PART 9 1 September 1949 No. 357 B

CONTENTS

Price to non-members 10*s*. net, by post 6*d*. extra. Annual subscription: £5 5*s*.
Composite subscription for both Sections A and B: £9 9*s*.

Published by
THE PHYSICAL SOCIETY
1 Lowther Gardens, Prince Consort Road, London S.W.7

Laboratory Precision in Production Testing

A direct-reading capacitance bridge that will measure capacitance and power factor with laboratory precision but is built to withstand the heavy usage encountered in production testing.

The quartz insulated variable air capacitance standard guarantees the highest accuracy and stability under all working conditions.

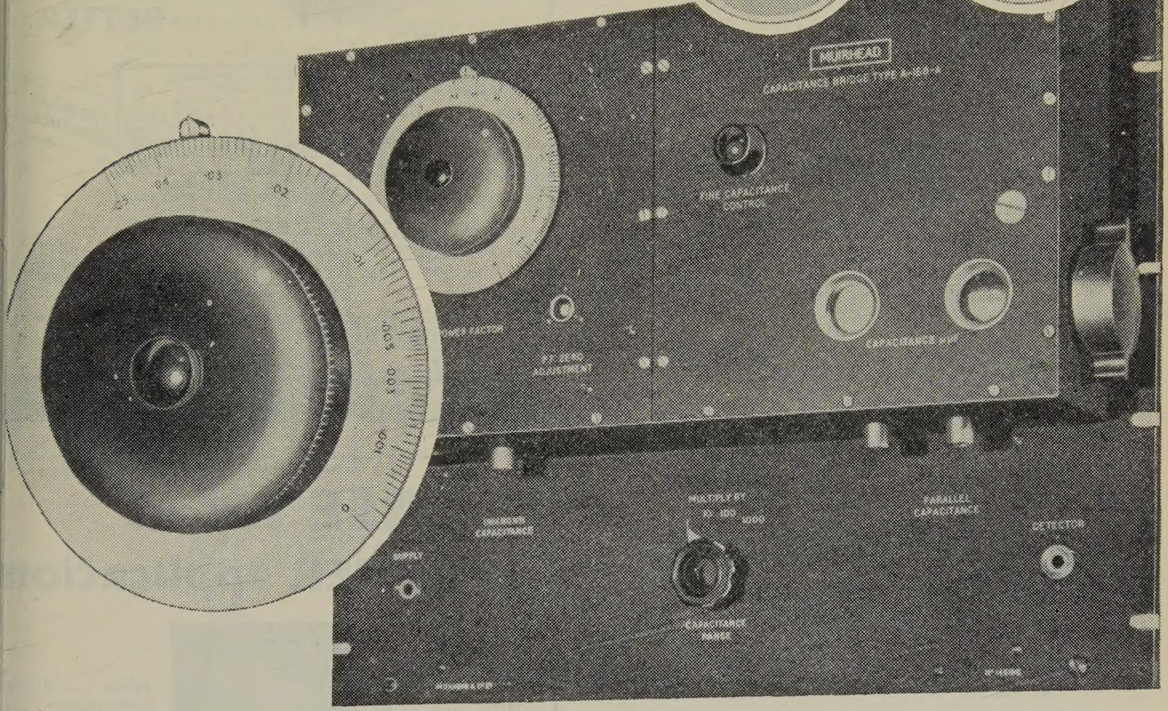

SPECIFICATION:

Modified Schering Bridge, double screened and direct reading in capacitance at any frequency between 50c/s and 10 kc/s. Direct reading in power factor at 1 Kc/s; a simple correction is necessary at other frequencies.

RANGES:

Capacitance: 100 $\mu\mu$F to 1 μF on 4 ranges.

Power Factor: 0 to 0.05 at 1 kc/s.

CAPACITANCE STANDARD:

High quality quartz insulated variable air condenser with precision worm drive gives discrimination to 0.2 $\mu\mu$F Directly calibrated in $\mu\mu$F from 100 to 1000; measurements outside the normal ranges may be made by the substitution method.

ACCURACY:

Capacitance; $\pm$ 0.1% of full scale reading on all ranges.

Power Factor:

by direct reading: $\pm$ 0.0003 $\pm$ 3% of scale reading.

by substitution: $\pm$0.00005 $\pm$ 3% of scale reading.

May we send you Publication C-104 giving full details of this and other A.C Bridges?

MUIRHEAD

Muirhead & Co. Limited, Elmers End, Beckenham, Kent. Tel: Beckenham 0041-2

FOR OVER 60 YEARS DESIGNERS AND MAKERS OF PRECISION INSTRUMENTS

CRC80a

THE PHYSICAL SOCIETY

Founded 1874. Incorporated 1878.

OFFICERS OF THE SOCIETY, 1949-50

President: Professor S. Chapman, M.A., D.Sc., F.R.S.

Hon. Secretaries: C. G. Wynne, B.A. (*Business*). H. H. Hopkins, Ph.D. (*Papers*).

Hon. Foreign Secretary: Professor E. N. da C. Andrade, Ph.D., D.Sc., F.R.S.

Hon. Treasurer: H. Shaw, D.Sc.

Hon. Librarian: R. W. B. Pearse, D.Sc., Ph.D.

SPECIALIST GROUPS

COLOUR GROUP

Chairman: W. S. Stiles, O.B.E., D.Sc., Ph.D.
Hon. Secretary: R. G. Horner, B.A.

OPTICAL GROUP

Chairman: Professor L. C. Martin, D.Sc.
Hon. Secretary: G. S. Speak.

LOW-TEMPERATURE GROUP

Chairman: Professor F. E. Simon, C.B.E., M.A., D.Phil., F.R.S.
Hon. Secretary: G. G. Haselden, Ph.D.

ACOUSTICS GROUP

Chairman: H. L. Kirke, C.B.E., M.I.E.E.
Hon. Secretaries: W. A. Allen, B.Arch., A.R.I.B.A., and A. T. Pickles, O.B.E., M.A

Secretary-Editor: Miss A. C. Stickland, Ph.D.
Offices and Library: **1 Lowther Gardens, Prince Consort Road, London S.W. 7.**
Telephone: KENsington 0048, 0049

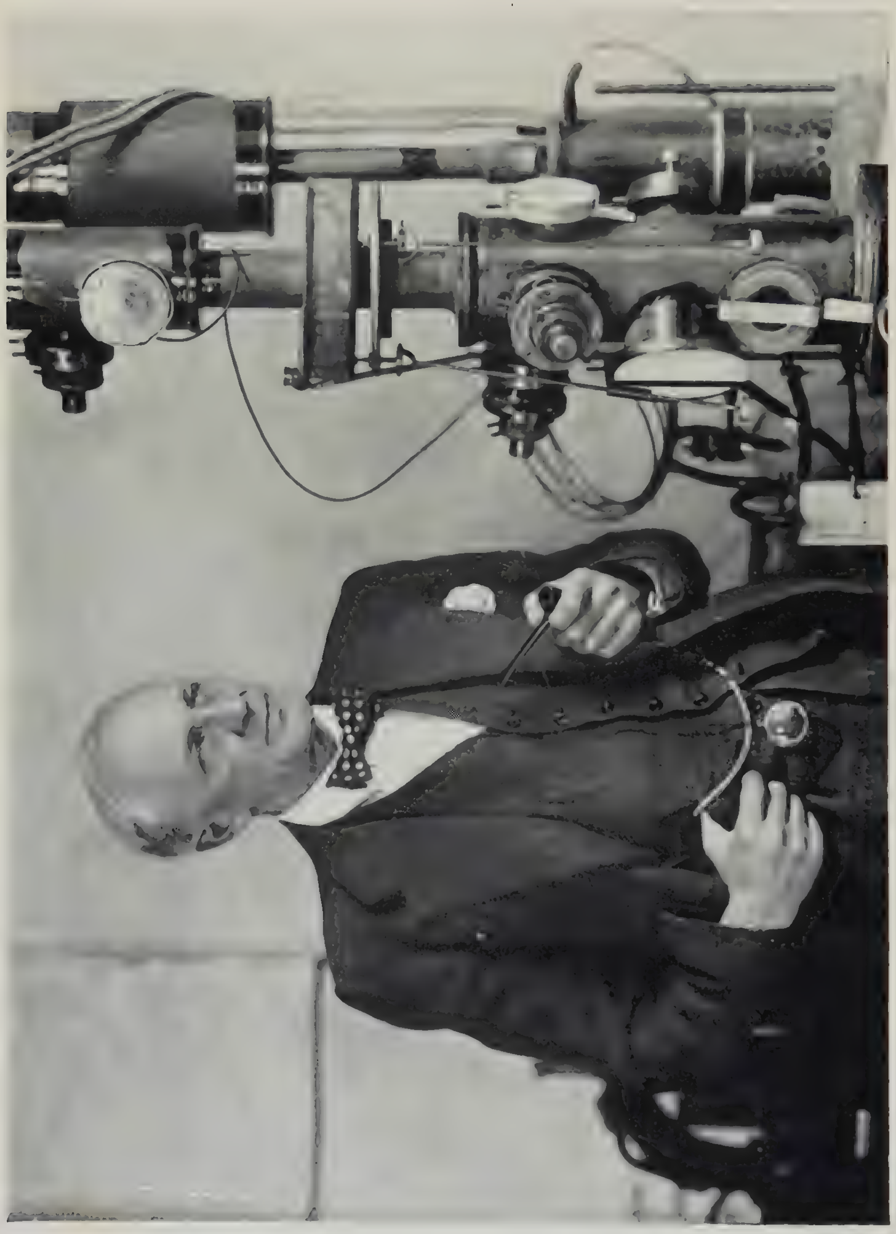

PROFESSOR G. I. FINCH, M.B.E., D.Sc., F.R.S.,
President of the Physical Society, 1947-1949.

THE PROCEEDINGS OF
THE PHYSICAL SOCIETY

Section B

VOL. 62, PART 9 | 1 September 1949 | No. 357 B

Steam in the Ring Discharge

By G. I. FINCH*

Presidential Address, delivered 6th May 1949

ABSTRACT. The behaviour of steam and its decomposition products in the ring discharge has been examined.

Dry hydrogen is not dissociated. The production of atomic hydrogen is dependent upon the presence of steam which dissociates into hydroxyl and atomic hydrogen. A secondary source of atomic hydrogen is then afforded by the interaction of hydroxyl with molecular hydrogen.

The escape from the discharge of atomic hydrogen, a long-lived species, favours the dissociation of steam. Mercury vapour, on the other hand, inhibits the formation of atomic hydrogen and thus leads to a high equilibrium steam concentration.

Unlike dry hydrogen, dry oxygen is dissociated into atoms, but these have a short life as such and recombine in the discharge to form molecular oxygen and ozone.

The reaction mechanisms occurring in the discharge are discussed in the light of spectrographic results.

§ 1. INTRODUCTION

BETWEEN 1926 and 1935 my collaborators and I carried out a systematic study of the combustion of hydrogen and carbon monoxide by oxygen in the cathode glow of the electric discharge maintained between metallic electrodes. Our object was to elucidate the nature of the mechanisms of these combustion processes, and the results and conclusions drawn therefrom were summarized in the *Journal of the Chemical Society* (Finch 1935). It may be remarked that, during the progress of this work, it became apparent that the results were also of practical interest, in that they threw fresh light on the chemistry of the thermionic valve, particularly in relation to the electron emissivity of the cathode.

Whilst certain phenomena arising out of the use of metallic electrodes in our experiments had helped towards an understanding of some aspects of the general mechanism of combustion, it became evident that, in other directions, they tended to obscure the issues. Indeed, as regards the undoubtedly complex mechanism of the homogeneous combustion of hydrogen by oxygen to steam, we could, in 1935, say no more than that, when the combustible mixture was rigidly dried, the initial step was the formation of the hydroxyl radical and that, in the undried mixture, steam was first dissociated into atomic hydrogen and hydroxyl, whereupon the hydroxyl somehow acted as a powerful promoter in the succeeding stages, leading ultimately to the formation of steam. No positive rôle in the combustion

* This article also appears in the August issue of *Proc. Phys. Soc.* A (p. 465).

process could be assigned to atomic hydrogen. This was remarkable since, under the conditions of our experiments, atomic hydrogen was known to be produced in considerable quantities. Accordingly it was decided to examine the equilibrium between steam and its dissociation products in the electrodeless discharge under conditions which would eliminate surface effects, or at least permit of an adequate appreciation of the part played by them.

§ 2. APPARATUS AND GENERAL PROCEDURE

The gas (steam, $2H_2+O_2$, H_2, O_2 or rare gas, or various mixtures thereof) was contained in the closed circulation system shown in Figure 1. This was assembled from the cleaned components using a dry, filtered, glass-blowing air supply, and was so constructed that the circulating gas came into contact only with glass, mercury or quartz, thus avoiding the contaminations introduced by

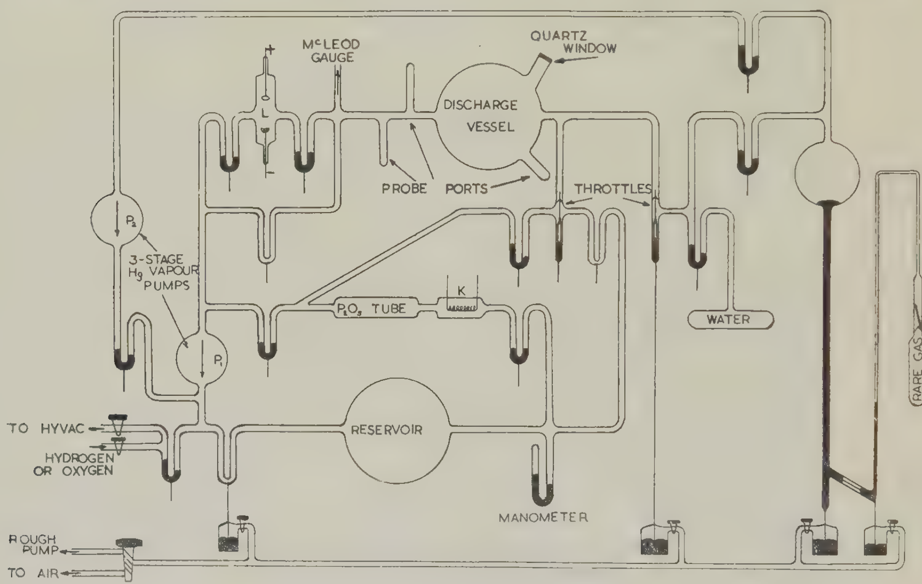

Figure 1.

lubricated stopcocks and rubber joints which have in the past so often vitiated the results of work on the combustion of hydrogen. The glass and quartz components were cleaned with chromic acid and distilled water ; the mercury, previously washed in the usual manner and distilled, was redistilled into the appropriate vessels ; and the phosphoric oxide was redistilled in oxygen until free from the lower oxides (Finch and Fraser 1926). The major remaining sources of impurity (other than mercury vapour) were the gases, chiefly carbon monoxide and nitrogen, dissolved in the glass of the discharge vessel. As will be seen later, getting rid of these gases presented no difficulty.

In Figure 1 the apparatus is shown with the barometric cut-offs and throttles set for the passage of the gas through the main circulation system consisting of the discharge vessel (10 cm. diameter), the three-stage mercury vapour pump, P_1, and the reservoir (10 cm. diameter). In L a high-tension arc could be maintained between a nickel anode and a molten lithium cathode for the purification of the rare gas admitted to the system. By a suitable setting of the

appropriate cut-offs, the vessel K and the phosphoric oxide tube could be inserted into the circulation system between the reservoir and discharge vessels for the purpose of the quantitative analysis of steam-hydrogen-oxygen mixtures. Thus, with the platinum wire coil in K cold, the steam was removed with a corresponding change in the manometer level. Next, with the coil heated, hydrogen and oxygen in their combining proportions were removed, with a further change in the manometer level, the remaining gas being excess hydrogen, oxygen or known added inert diluent such as, for example, neon. The gaseous contents of the discharge vessel–reservoir circulation system could be well dried by circulation through the interposed phosphoric oxide tube, though that degree of rigid drying which exerts a marked effect in increasing the resistance of hydrogen to ignition could not be achieved. It is well known to workers in this field that, despite all precautions, the use of mercury seals and cut-offs invariably introduces traces of moisture.

The normal working pressure of gas in the reservoir during circulation was between about 7 and 10 mm., whilst that in the discharge vessel was maintained at between 0·026 and 0·03 mm. Hg by means of the pump, P_1, and the appropriate throttle. The rate of circulation through the discharge vessel was rather over 200 cm^3 per second ; this was measured in a manner which will be obvious from Figure 1. Owing to the fall in pressure at the throttle, the partial pressure of mercury vapour in the discharge vessel could not exceed 3×10^{-6} mm., the rate of circulation being more than sufficient to prevent diffusion of mercury from the McLeod gauge, cut-offs or pump towards the discharge vessel.

Short sealed-off tubes were fused, as shown, into the discharge vessel and the 1·2 cm. bore tube, nearly 1 metre long, between the discharge vessel and the McLeod gauge entry tube. These tubes served for the sealing in of probes projecting into the discharge or gas stream. Three probe tubes, two of which are shown in Figure 1, were situated at 5, 20 and 50 cm. respectively beyond the discharge vessel outlet. In all other respects Figure 1 is self-explanatory.

The discharge was maintained by means of a high-frequency current in a solenoid, 13 cm. in length and internal diameter, mounted coaxially with the discharge vessel, and consisting of seven turns of 4 mm. diameter copper tubing. The current was obtained from a valve (Mullard S.W.9) oscillator in a modified Hartley circuit. The valve filament was run at its rated value and, unless otherwise stated, the input to the oscillator was 160 watts. The frequency was 26 Mc/s. as measured by a Southworth-Lecher (Southworth 1920) wire system. Further, the gas pressure in the discharge vessel was maintained at between about 0·026 and 0·03 mm. Hg, preferably nearer the former, the McLeod gauge readings being corrected for the experimentally determined equilibrium steam contents when moist gaseous mixtures were in use.

Under these conditions the discharge in steam consisted of a bright rose-pink annulus coaxial with the discharge vessel, from the cool walls of which it was separated by a dark sheath about 2 or 3 mm. thick. In cross section the diameter of the bright core of the annulus was about 4 cm., the intensity of the glow decreasing considerably near the centre of the discharge tube. It will be evident that this was a ring discharge, the theory of which was outlined in the 13th Guthrie Lecture by J. J. Thomson (1928). In such a discharge the currents form closed circuits in the gas, though it is possible that, under the conditions of these experiments, the actual initiation of the discharge was effected by the electrostatic field across

the ends of the solenoid (Mackinnon 1929, Esclangen 1934). It will be appreciated that conditions in this ring discharge closely resemble those in the positive column.

The evacuated discharge vessel was finally cleansed and gases absorbed in its walls sufficiently removed, first by prolonged baking at about 350° C. and then by maintaining the discharge in a stream of steam drawn from the vessel containing CO_2-free water, past the appropriate throttle, through the cool discharge vessel and the pump P_1 backed by the 'Hyvac' pump. This also served to free the water in its storage vessel from dissolved air. After evacuation following upon such cleansing, the main circulation route was restored and the system filled with the appropriate gas to the desired pressures in the discharge and reservoir vessels.

A mixture of hydrogen and oxygen in combining proportions was frequently used in the experiments to be described below. It was conveniently prepared in a high state of purity by drawing pure steam through the discharge and drying the products accumulated in the reservoir by subsequent circulation through the phosphoric oxide tube. Oxygen was obtained by heating recrystallized potassium permanganate and then washing with a caustic potash solution. Hydrogen was prepared by electrolysis of a saturated recrystallized baryta solution and, when necessary, was subsequently freed from oxygen and hydrogen oxides by circulation past the heated platinum spiral K and through the phosphoric oxide tube.

§ 3. EXPERIMENTAL RESULTS AND CONCLUSIONS

Series 1—*Dry and moist hydrogen.* A puzzling feature of our work on the cathodic combustion of hydrogen was that, as has already been remarked, no evidence was found to justify the assigning of a direct rôle in combustion to the atomic hydrogen, which was known to be produced in considerable quantities. Accordingly it was decided to examine first the behaviour of hydrogen, dried as well as possible by circulation over phosphoric oxide, in the electrodeless discharge.

After a preliminary drying of the discharge tube walls by means of a prolonged circulation of dry hydrogen with the phosphoric oxide tube in the circuit, the filament K glowing and the discharge in action, the apparatus was evacuated and charged with dried hydrogen. It was then found that the hydrogen could be circulated through the discharge for long periods without any change in pressure and that, in the early stages of circulation, the spectrum (Figure 2*) of the bluish-white discharge consisted mainly of the secondary spectrum due to neutral molecular hydrogen. The hydroxyl bands (2808 and 3064 A.) and the more intense lines (H_α 6563, H_β 4861 and H_γ 4350 A.) of the Balmer series, due to neutral atomic hydrogen, were visible but, with the exception of H_α, were feeble compared with those of the secondary series. Also in evidence were a few mercury lines, in particular 2536, 3650 and 4358 A. With increasing time of circulation and drying, during which precautions were taken to avoid shaking or otherwise disturbing the mercury in the McLeod gauge and the cut-offs associated with the main circulation system, the degree of dryness of the gas evidently improved until, except for the brilliant secondary series and the few mercury lines mentioned above, only the 3064 A. hydroxyl band-head region and the red H_α line still remained

* For Figures 2 to 6 see Plates.

visible. Thus it seems likely that, had it been possible to achieve a rigid drying of the hydrogen, the Balmer series and hydroxyl bands would have been eliminated.

These results confirm, in all essential respects, the experimental findings of Wood (1920, 1921, 1922 a, b), Copeland (1930), Poole (1937) and other workers. Wood concluded that atomic hydrogen was copiously formed in the discharge passing through dry hydrogen and attributed the virtual non-appearance of the Balmer series to a catalytic recombination of the atomic hydrogen to the molecular form at the dry walls of the vessel. Other workers have since accepted this hypothesis.

For the three following reasons, however, I have not been able to subscribe to this view without submitting it to the test of further experiment. In the first place, Wood and others worked with gas pressures of the order of 1 mm. ; it seems improbable, therefore, that any considerable proportion of hydrogen atoms formed in the discharge could arrive at the walls of the vessel without being excited and radiating, and thus giving rise to the Balmer series. Next, the catalytic inertness of cool, clean dry glass is well known, particularly to workers in the field of gaseous reactions in closed vessels. Thus Strutt (1911) found that the greenish glow of active nitrogen in a clean glass vessel persisted for several minutes after excitation, although it was extinguished almost instantaneously on introducing into the vessel a superfically oxidized copper wire. Finally, although the quantum theory indicates the possibility of the dissociation of the hydrogen molecule by electron impact, the necessary excitation energy would be 18 ev. (Mott and Massey 1933), and it is doubtful if such high energies were available in the ring discharge maintained under the conditions set forth above. The matter is one which was put to the test of crucial experiment as follows.

The pointed end of a glass needle was wetted to a length of about 3 mm. with diluted waterglass, dusted with yellow mercuric oxide powder, dried *in vacuo* and sealed into the discharge vessel probe port. The tip of the needle was about level with the contour of the discharge vessel so that, if any hydrogen atoms were formed in the discharge, some would reach the mercuric oxide-coated needle tip directly. The circulation system with the phosphoric oxide tube in circuit and the wire K at red heat was then filled with hydrogen which was circulated for 26 hours. The discharge was then started in the, by this time, relatively well-dried, oxygen-free hydrogen, and the circulation continued. At first no change could be seen in the appearance of the mercuric oxide ; it was not until after 20 minutes that the first signs of reduction, consisting in a blackening due to the formation of mercurous oxide, could be detected. The drying tube was then by-passed out of the circulation system and a little oxygen admitted to the reservoir contents, whereupon, within a few seconds, the yellow changed to black oxide and this, in turn, was quickly further reduced to minute droplets of mercury which slowly evaporated. In another experiment a similar procedure was followed, except that instead of oxygen about 2 per cent by volume of steam was added to the reservoir vessel contents. Here again the same remarkable acceleration in the rate of reduction of the mercuric oxide occurred. As will be shown later, the agent responsible for the reduction of both mercury oxides was atomic hydrogen.

It is difficult to resist drawing from these experimental results the conclusion that, apart from traces due to imperfect drying and revealed spectrographically, atomic hydrogen is not formed when an electrodeless discharge passes through dry hydrogen. Hence, the hitherto generally accepted view that the hydrogen

molecule is atomized by the discharge in dry hydrogen and that the absence of the Balmer spectrum is to be accounted for by a recombination to the molecular state at the surface of the discharge vessel is untenable. These experiments, of course, afford no information as to the relative activities of dry and moist glass surfaces in causing the recombination of hydrogen atoms to molecules ; but they do show that dry hydrogen is not dissociated by the discharge, and that the minute amount of atomic hydrogen formed is attributable to that trace of moisture which can hardly be eliminated in an experiment of this kind carried out in an apparatus equipped with barometric mercury cut-offs.

Series 2—The steam equilibrium. Preliminary experiments in which steam had been circulated through the discharge, primarily with a view to outgassing the discharge vessel, had shown that much of the steam was decomposed and that the only other products received into the reservoir vessel consisted of hydrogen and oxygen in their combining proportions. In further such experiments steam was drawn through the discharge, and the products accumulated to a pressure of about 10 mm. in the previously evacuated reservoir, the cut-off between this and the discharge vessel being closed. On interrupting the steam supply and restoring the main circuit, no further change in pressure occurred, even after several hours' circulation. Analyses immediately before resumption of, or after, prolonged circulation revealed no change in the steam concentration, the remaining products always consisting of hydrogen and oxygen in their combining proportions. It is clear, therefore, that the steam dissociation equilibrium was attained in a single passage of the steam through the discharge and, further, that no gas was lost by, for example, combination with mercury.

In the course of these and other exploratory experiments it was also found that the extent of this dissociation was much affected by the state of the surface of the walls of the discharge vessel. For example, with clean walls and starting with either steam or the equivalent mixture of hydrogen and oxygen, the products at equilibrium contained between 16·5 and 19 per cent by volume of steam. On repeating such an experiment, but with a fine (37 S.W.G.) copper wire protruding into the discharge through the appropriate port, the wire glowed and the equilibrium steam concentration rose progressively in the course of five two-hour runs to between 38 and 40 per cent. By this time the walls of the discharge vessel near the wire were faintly discoloured, presumably by evaporated copper which may or may not have been oxidized. The glowing of the wire was due to some energetic surface reaction, and not merely to eddy-current heating, as was shown by the fact that on reducing the pressure in the discharge vessel, by closing the throttle and thus extinguishing the gas discharge, the wire at once ceased to glow. The wire was then removed and the port sealed off, whereupon further runs, in which equilibrium was approached sometimes from one side and sometimes from the other, continued to yield equilibrium steam concentrations approaching 40 per cent as before. Thus there was no tendency for this concentration to increase, as had been the case when the copper wire protruded into the discharge.

The discharge vessel was now cut out of the apparatus, cleaned with fuming nitric acid followed by chromic acid, washed with distilled water and finally dried with warm filtered air. The vessel was then re-sealed into the circulation apparatus, using dry filtered air for glass-blowing purposes. It was then found that this cleaning had restored the discharge vessel to its original state, equilibrium steam concentrations of about 18 per cent being once more obtained.

These results point to a promotion, by the copper stain on the discharge vessel walls, of some surface reaction or reactions which, either directly or through the products formed, favoured the formation of steam.

The reactants concerned must be relatively long-lived, because they survive passage from the discharge region to the vessel walls across the intervening discharge-free dark zone. Further, bearing in mind the evidence afforded by the glowing copper wire of the highly energetic nature of the reaction, and the testimony of the mercuric oxide probe experiments with moist hydrogen to the arrival of atomic hydrogen at the discharge vessel walls, it seems likely that the surface reaction is the recombination of atomic to molecular hydrogen, and that this may be, indeed, the dominating reaction increasing the equilibrium steam concentration. In other words, the formation of atomic hydrogen seems, somehow or other, to hinder the formation of steam.

Further light was thrown on these matters by the spectrograms (Figure 3) of the discharge in steam and its decomposition products. These are striking in that, apart from the relatively weak mercury spectrum, they consist of the Balmer series (3771, 3797, 3835, 3890, 3970, 4102, 4340, 4861 and 6562 A.), the hydroxyl bands with heads at 2808 and 3064 A., and the rather weak lines, 3947 and 4368 A., due to atomic oxygen. The secondary molecular hydrogen spectrum is absent. Further, the presence or otherwise of copper deposited on the discharge vessel walls had no appreciable effect on the appearance of the spectrograms or on the relative intensities of the hydroxyl band and Balmer spectra, despite the profound effect exerted by the copper stain in the equilibrium steam concentration.

Wood and other workers have obtained spectra under conditions comparable to those outlined above, except that, instead of pure steam, they used moist hydrogen, the steam concentration being in general about $2\frac{1}{2}$ per cent. Apart from the absence of all atomic oxygen lines, their spectra are essentially similar to those obtained in the present experiments. Thus, while Wood and others have shown that copious supplies of long-lived atomic hydrogen are obtained from the discharge in moist hydrogen, the above experiments demonstrate that atomic hydrogen is also freely produced when steam alone is fed to the discharge.

Series 3—Steam–hydrogen mixtures. In order to gain further insight into the mechanism of the formation of atomic hydrogen, experiments were now carried out in which a wide range of mixtures of hydrogen with steam, or with hydrogen and oxygen in their combining proportions, were circulated through the discharge. Before each such experiment, however, the circulation system was prepared in the following manner. Glass needles, the points of which had been coated with ash (mainly tin oxide and lime) by calcining a thin smear of sealing wax, were sealed into the three ports with their tips projecting into the tube between the discharge vessel and the McLeod gauge. Another ash-coated probe was sealed into the discharge tube port with its tip level with the contour of the vessel. Dry oxygen was then circulated under standard pressure conditions through the discharge. The reaction product reacted with mercury vapour to deposit in a few minutes broad rings or, rather, bands of yellow mercuric oxide about the openings leading to the McLeod gauge and the rare gas purifier, and just above the entry to the pump, P_1. The apparatus was then evacuated and the circulation system, with the phosphoric oxide tube in circuit, swept out and finally charged with roughly dried hydrogen, which was then still further dried by prolonged circulation during which the platinum spiral, K, was glowing. Throughout

these operations the mercuric oxide films remained unchanged. The discharge was now started and spectrographed. Apart from the strong secondary molecular spectrum and the usual lines due to traces of mercury, only the H_α (moderate to weak), H_β (weak) and H_γ (very weak) lines of the Balmer series and the hydroxyl 3064 A. band-head region were visible. The circulating gas had no visible effect on any of the probes coated with sealing-wax ash ; likewise, the mercuric oxide films near the McLeod gauge and the pump were unchanged, even after two hours' circulation.

The apparatus was now evacuated, and the normal circulation route restored and filled to the usual pressures with the required mixture of hydrogen and steam. After a sufficiently prolonged circulation to ensure thorough mixing of the gases, the discharge was started. The range of mixtures examined extended from steam alone to steam (or the equivalent hydrogen–oxygen mixture) diluted with up to 95 per cent of hydrogen. Spectrograms were obtained in each case under uniform conditions of exposure and development. The sealing-wax ash probe inserted through the discharge vessel port was withdrawn after the first experiment and was not replaced.

The results of this series are illuminating. In the first experiment, carried out with steam alone, the mercuric oxide films, including that near the mercury vapour pump inlet, about $1\frac{1}{2}$ metres beyond the discharge vessel, were completely reduced within a few minutes of starting the discharge. The progress of such reduction could, however, be immediately arrested by interrupting the discharge. Further, the particles of ash on the discharge vessel probe and on the two probes nearest to the discharge vessel flashed into incandescence immediately the discharge was started, but ceased to glow when this was interrupted. From time to time glowing fragments of ash would fly off the probes, particularly that in the discharge vessel, and these continued to incandesce after lodging on the wall of the vessel or in the tube beyond it. Indeed, owing to this stripping-off of the ash, the section of tubing carrying the first two ports beyond the discharge vessel had to be removed for cleaning after each experiment and fresh ash-coated probes inserted in preparation for the next. As stated above, the discharge vessel probe was removed and not replaced after the first experiment.

The incandescence of the ash on the second probe beyond the discharge vessel was less brilliant than that of the first probe and, in the case of the third probe some 50 cm. beyond the discharge vessel, an ash particle would sometimes glow, but only in mixtures containing initially between about 30 and 60 per cent of hydrogen.

The spectrograms were similar to those obtained with pure steam (Figure 3), except that the atomic oxygen lines, 3947 and 4368 A., seemed to weaken with increasing hydrogen concentration ; they no longer appeared in a spectrogram from the discharge in a mixture of steam and hydrogen in equal volumes. Visual comparison of the spectrograms, more particularly of the hydroxyl band 2808 A. with H 3797 and H 3835 A., and of the hydroxyl band 3064 A. with H 3890 and H 3970 A., revealed no change with increasing hydrogen concentration in the relative intensities of the hydroxyl band and Balmer series spectra.

Finally, it was found that the steam equilibrium constant decreased with increasing dilution of the mixture by hydrogen. For example, with steam alone the constant $K = (H_2O)^2/[(H_2)^2.(O_2)] = 0{\cdot}46$, but was 0·38 and 0·25 in the case of mixtures diluted with 55 and 69 per cent of hydrogen respectively. Thus,

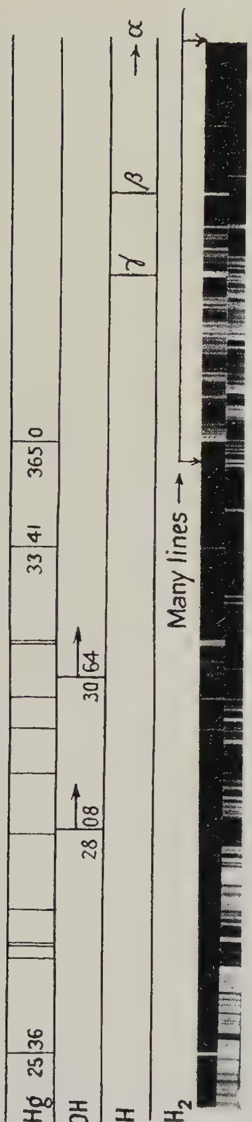

Figure 2. Roughly dried hydrogen.

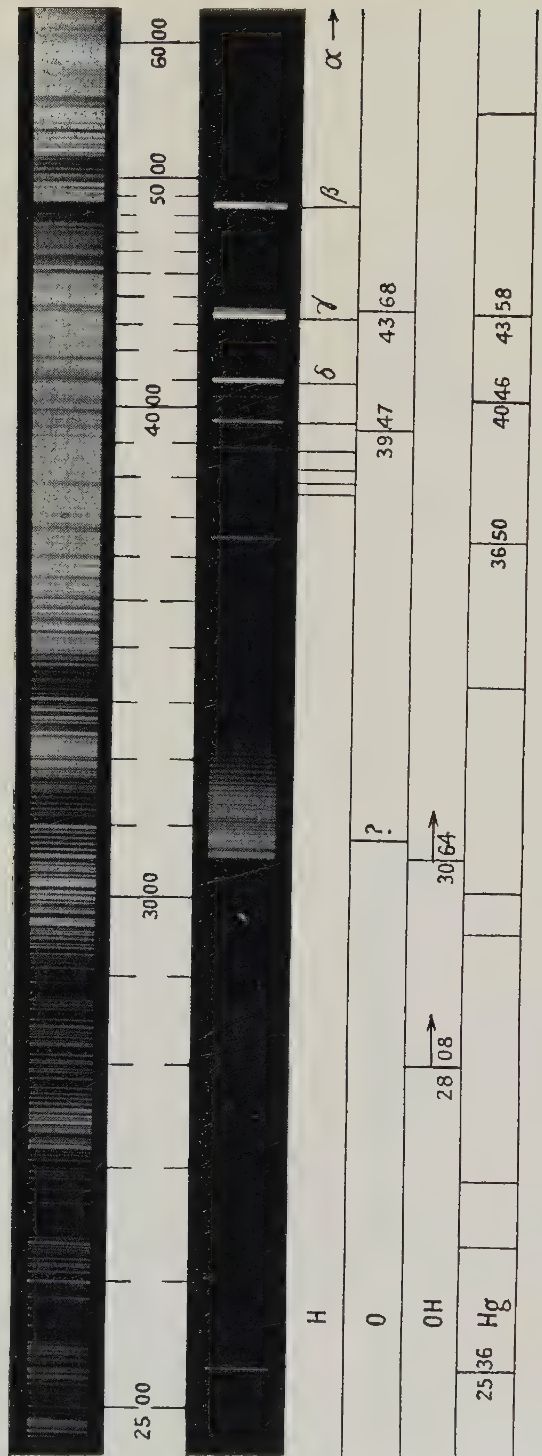

Figure 3. Steam.

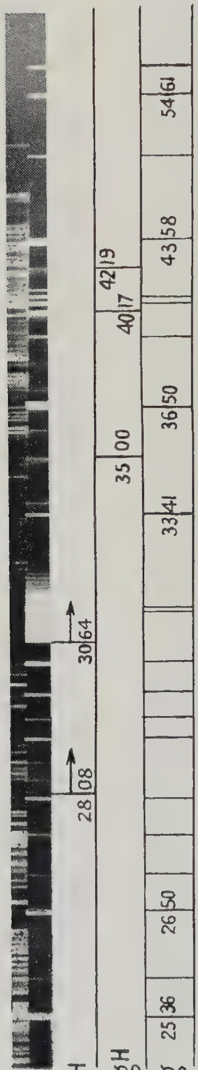

Figure 4. Steam and mercury vapour.

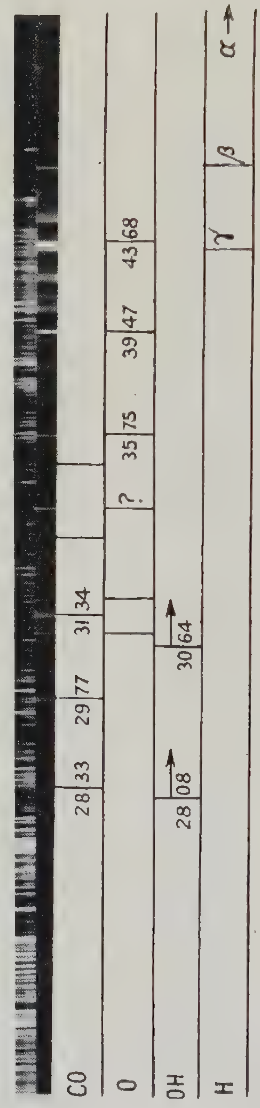

Figure 5. Roughly dried oxygen.

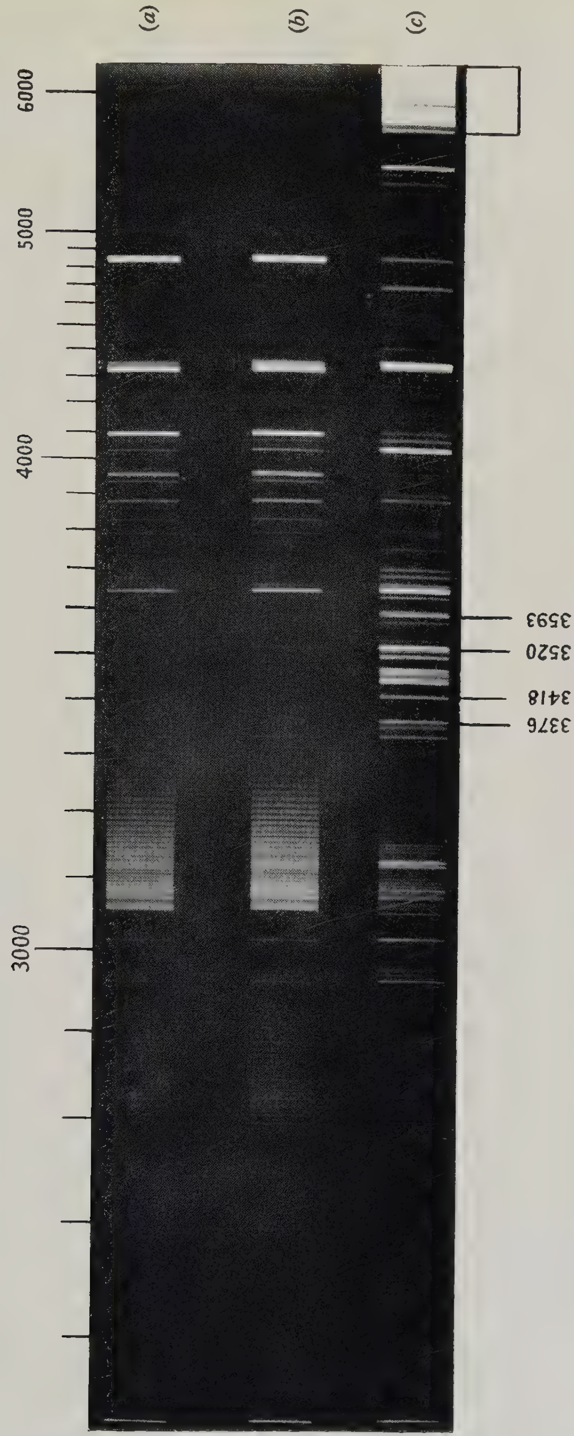

Figure 6. (a) Steam; (b) 50% steam and 50% neon; (c) neon.

although dilution with hydrogen did, in fact, greatly reduce the dissociation of the steam by the discharge, it did not do so to the extent required by the law of mass action.

The reason is not far to seek. The results of these experiments as a whole now afford overwhelming evidence that the first step towards equilibrium in steam or in a steam–hydrogen mixture is the direct dissociation of the steam into hydroxyl and atomic hydrogen. The molecular hydrogen as such is not dissociated by the discharge and, when steam is present in adequate supply (which may possibly be considerably less than 5 per cent), either the hydrogen is not excited or it reacts in some way before it can radiate. This dissociation of steam must be practically irreversible in the gaseous phase, because quantum energy considerations forbid the reverse reaction by which atomic hydrogen and hydroxyl might recombine to form steam, except as a result of necessarily infrequent three-body collisions. Similar considerations apply in the case of the union of hydrogen atoms to the molecular state. On the other hand, the life of the hydroxyl radical (Bonhoeffer and Pearson 1931, Geib and Harteck 1934, Oldenberg 1937) can be terminated by two-body collision processes such as, for example, $2OH = H_2O + O$, and $OH + H_2 = H_2O + H$. Thus the fall in the steam dissociation equilibrium constant with increasing dilution by hydrogen is to be accounted for by the practically irreversible formation, and hence escape, of atomic hydrogen from the reaction zone.

There is evidence from the above experiments that the hydroxyl reacted in the discharge in both the ways suggested. That the first reaction occurred is supported by the appearance of oxygen atom lines in the spectrograms from the discharge in steam, and by their weakening and final disappearance on progressive dilution with hydrogen. As for the second reaction, in which hydroxyl interacts with hydrogen, the likelihood of its occurrence is supported by the following facts and considerations. In the first place, the relative intensities of the hydroxyl and Balmer spectra (Figure 3) were independent of hydrogen dilution of steam over a wide range. This strongly supports the previous conclusion, that the sole primary source of atomic hydrogen is the direct dissociation of steam in the discharge. Next, the fact that the third sealing-wax ash probe glowed only in mixtures of steam diluted by a roughly equal proportion of hydrogen shows that the yield of atomic hydrogen was increased by such dilution. Hence the diluent hydrogen must itself contribute in some way to the ultimate yield of atomic hydrogen. Since, as has already been shown, atomic hydrogen cannot have been produced by direct dissociation of molecular hydrogen, the probable source of this contribution lies in the interaction in the discharge of hydroxyl and molecular hydrogen, whereby atomic hydrogen and steam are formed. This view received strong support from the results, which showed that the recombination of atomic hydrogen at the copper-stained walls of the discharge vessel increased the steam equilibrium concentration by returning molecular hydrogen to the discharge and thus reducing the amount escaping in the atomic state from the reaction zone. The possibility of a surface reaction between hydroxyl and atomic hydrogen in similarly affecting the steam equilibrium will be considered later.

The results of this series of experiments furnish ample evidence of the significance to be attached to the probe and mercuric oxide reactions. Thus, when the discharge was fed with steam, steam diluted with hydrogen, or the equivalent hydrogen–oxygen mixtures, the mercuric oxide films were rapidly reduced, and

the sealing-wax ash probes incandesced with a brilliancy which increased as the discharge vessel was approached. Further, all these phenomena ceased immediately the discharge was interrupted, irrespective of whether the circulating gas was steam (or the equivalent hydrogen–oxygen mixture) alone or diluted with hydrogen. Therefore the agent reducing the mercuric oxide could not have been molecular hydrogen, nor could the reaction catalysed by the ash have been the union of hydrogen and oxygen to steam. In addition to the normal equilibrium products entering the reservoir vessel, the only other products for which there is evidence of formation in the discharge are atomic hydrogen, hydroxyl and hydrogen peroxide (Finch and Mahler 1931). Atomic oxygen can be excluded because, although revealed spectrographically in the case of steam traversing the discharge, it was eliminated by sufficient dilution of the reaction mixture with hydrogen. Hence, whereas the reduction of the mercuric oxide films can only be attributed to atomic hydrogen, the incandescence of the ash-coated probes might be ascribed either to the formation of molecular hydrogen or to the interaction of atomic hydrogen with hydroxyl to form steam. The heat evolutions of these reactions are similar, being about 103,000 kcal/gm. mol (see Steacie 1946). Whilst there is no doubt about the longevity of atomic hydrogen, the situation in regard to the life of hydroxyl, though known to be much shorter than that of atomic hydrogen, is less clear. Thus, while Bonhoeffer and Pearson (1931) were unable to find the radical in the gas flowing from a discharge through water vapour, Frost and Oldenberg (1936), using a 21-foot grating, detected hydroxyl for as long as $\frac{1}{8}$ second after their discharge in steam was interrupted. Thermal conditions may, however, have contributed to this result. The reduction of the mercuric oxide probe in the discharge vessel port, when the discharge took place in moist hydrogen, would be difficult to explain if hydroxyl arrived at the probe, and hence also at the surface of the vessel, at a rate comparable with that of the atomic hydrogen. Thus the evidence so far supports the view that the incandescence of the ash-coated probes was due to the recombination of atomic hydrogen. This issue was further tested in the next series of experiments.

Of the three ash-coated probes, all of which were much nearer to the discharge vessel than were the mercuric oxide films, the first two incandesced regularly, whilst the third did so spasmodically, and then only under the most favourable conditions. It would seem that, whilst the reduction of the mercuric oxide film formed a sensitive test for the presence of atomic hydrogen, the sealing-wax ash probes could respond only to a relatively high concentration.

Series 4—*Further probe experiments.* In the first experiment of this series a closely wound spiral nearly 1 cm. in diameter, of 28 S.W.G. copper wire, was inserted into the exhaust tube leading from the discharge vessel. The spiral, previously cleaned and reduced by hot hydrogen, extended from near the second port, which was fitted with a mercuric oxide-coated probe, to within 0·5 cm. from the discharge vessel. The equilibrium steam concentration was then determined, starting with steam or the equivalent hydrogen–oxygen mixture. The mean steam yield from eight such runs was 19·2 per cent, a value which did not differ significantly from that (18·9 per cent) afforded by a similar series of runs carried out before inserting the spiral. The presence of the copper spiral, however, practically inhibited the reduction of the mercuric oxide, thus showing that the bulk of the atomic hydrogen leaving the discharge vessel was, on passing through the spiral, transformed to the molecular state. This, together with the fact that the steam yield was virtually unaffected by the presence or otherwise of

the spiral, proves conclusively that hydroxyl could not have survived long enough after leaving the discharge to reach the spiral in appreciable quantities ; otherwise the equilibrium steam concentration must have increased, which it did not do. Hence these results confirm that the ash incandescence observed in the previous experiments was due solely to recombination of atomic hydrogen.

The spiral was now removed and the corresponding tube section cleaned and re-fused into the apparatus. The glass pinch of a tungsten filament lamp was then sealed into the first probe port beyond the discharge vessel, the lamp filament having been replaced by a 2·5 cm. long fine (37 S.W.G.) platinum wire and the current-carrying posts shrouded with quill tubing. The wire projected in the form of a hoop into the path of the gas stream from the discharge vessel.

In the next experiment a mixture of hydrogen and oxygen was circulated under normal conditions but without the discharge, the phosphoric oxide tube being included in the circulation path. After drying the gas in this manner until the manometer readings were steady, the platinum filament was brought to a bright red heat and circulation continued. The McLeod gauge readings then fell from the steady value of 0·027 mm., obtained before heating the filament, to 0·019 mm., thus clearly indicating that steam was being formed as a result of a surface union of hydrogen and oxygen on the heated platinum wire. This was further confirmed by a progressive fall in the reservoir manometer readings as circulation proceeded. On interrupting the heating current, the wire immediately cooled and the McLeod gauge reading rose to its previous steady value of 0·027 mm. Evidently the rate of heat evolution during the formation of steam at this low pressure was not sufficient to compensate for the heat losses from the wire, which in consequence cooled and ceased to catalyse the reaction. Immediately the discharge was started, however, the platinum filament began to glow brightly, but cooled at once when the discharge was switched off. That the heating of the wire must have been due solely to the recombination of atomic hydrogen, and not to heating of the filament by the high-frequency field exciting the discharge, was shown by tha fact that the wire cooled immediately the discharge was interrupted by closing the throttle admitting gas into the discharge vessel.

The difference in behaviour of the platinum wire in atomic hydrogen and in a mixture of hydrogen and oxygen in equivalent proportions finds a natural explanation in the heat evolution of the appropriate reactions, the heat of formation of molecular hydrogen being 103,000 kcal/gm. mol, while that of steam is only about 59,000.

Further experiments were carried out with, in place of the platinum filament, a probe consisting of a straight length of either 36 S.W.G. tungsten or 37 S.W.G. copper wire protruding into the gas stream from a glass rod sealed into the port adjacent to the discharge vessel. When steam was fed to the discharge, these wires glowed dull red. With a mixture of steam and hydrogen in equal proportions, the copper wire became bright red and the tungsten wire was even hotter.

Wood (1922 a) also found that a tungsten wire glowed in atomic hydrogen ; he did not however obtain such an effect with a platinum wire. This may have been due to the state of the surface of his wire. It is a common experience that catalysing the combustion of a mixture of hydrogen and oxygen at a bright red heat not only cleans and activates a platinum surface but also roughens it.

Series 5—Steam–mercury vapour mixtures. At the conclusion of the experiments of Series 3 the question was left open as to whether or not the effect of the copper-staining of the discharge vessel walls in promoting a high yield of

steam might be due, not only to the returning of molecular hydrogen to the reaction zone, but also to a surface reaction between atomic hydrogen and hydroxyl. In previous work on cathodic combustion (Finch 1935) it had been suspected that mercury vapour facilitated the combustion of hydrogen. This, and the fact that mercury vapour can play an important rôle in photosynthesized reactions involving hydrogen (Taylor and Bates 1926, Rieke 1936, Olsen 1938), suggested that its use might throw light on the present problem. Accordingly arrangements were made to examine the effect of mercury vapour additions to steam passing through the ring discharge.

About 0·5 cm^3 of mercury was distilled into the discharge vessel port tube through a branch tube, which was then sealed off close to the port tube. A few turns of resistance wire wrapped round the port tube and immersed in an oil-filled jacket enabled the mercury to be warmed. An ash-coated probe was inserted through the first port beyond the discharge vessel. Mercuric oxide films were then formed, in the manner previously described, at the usual places where the circulating gas stream came in contact with stagnant mercury vapour. A similar deposit also formed about the entry to the discharge-vessel port tube.

Steam (or the equivalent hydrogen–oxygen mixture) was then circulated along the usual path under the normal pressure distribution of 0·026 mm. in the discharge vessel and 7 or 10 mm. in the reservoir, according to the nature of the gas mixture used. The mercury in the discharge port vessel was then gently heated and maintained at between 40 and 45° C. When steady conditions had been attained, the discharge was started. Instead of a rose-pink ring, it now formed an apparently uniform bluish-green sphere. A rough estimate afforded by the increased damping of the oscillation circuit suggested that the partial pressure of mercury vapour was between 0·005 and 0·012 mm., probably nearer the former. Despite this, no condensation occurred anywhere between the discharge vessel and the pump though, with time, a barely perceptible brownish band formed on the discharge vessel walls coaxial with the solenoid.

The mercury vapour exerted a profound effect on the results. The ash-coated probe did not incandesce and, although the mercuric oxide film near the discharge vessel port had disappeared within five minutes of starting the discharge, the more remote films were only very slowly reduced. Also, the equilibrium steam concentration, which previously had been between 18 and 19·4 per cent, was now practically 100 per cent, irrespective of the direction of approach to equilibrium. Finally, the spectrogram (Figure 4) of the discharge differs strikingly from that obtained with steam or steam–hydrogen mixtures (Figure 3). Apart from the strong, well-developed mercury line spectrum, its main features are the 2808 and 3064 A. hydroxyl bands, the latter being intense, and the three mercurous hydride line groups 3500, 4017 and 4219 A. Neither the secondary hydrogen nor the Balmer spectra appear.

These results show that the effect of the mercury vapour was largely to suppress the formation of atomic hydrogen, thereby shifting the equilibrium so far towards the steam side that the reaction products consisted almost wholly of steam. Thus the evidence suggests that steam is reduced, reversibly, by mercury to mercurous hydride and hydroxyl. In view of the high intensity of the 2536 A. mercury line [$Hg(6^3P_1)$] the reduction of mercury by hydrogen to mercurous hydride and atomic hydrogen is also likely to occur. Again, since mercury is

oxidized by ozone to mercuric oxide, and this in turn is reduced in the cold by atomic hydrogen and by molecular hydrogen at about 120° c. (Manchot and Kampschulte 1907, 1910), further probable reactions are the oxidation of mercurous hydride to mercuric oxide and hydroxyl, and the reduction of mercuric oxide by atomic or molecular hydrogen to mercury and hydroxyl or steam respectively. In addition, the short life of hydroxyl is terminated in the manner set forth in Series 3 and 4 of the above experiments.

The question is still left open as to whether the survival life of hydroxyl is sufficient for it to interact with atomic hydrogen at the walls of the discharge vessel ; the results of Series 4 show, however, that this reaction does not occur at surfaces beyond the discharge vessel.

Series 6—*Dry and moist oxygen mixtures.* The behaviour of oxygen, both dry and moist (or diluted with hydrogen), in various types of discharges, including the ring discharge, has been the subject of much experimental work. In general, a broad measure of agreement has been reached as to findings and conclusions. In one respect, however, a conflict of views does exist. Harteck and Kopsch (1931), Geib and Harteck (1934), Geib (1938) and others incline to the belief that, like atomic hydrogen, atomic oxygen has a relatively long life. On the other hand, Strutt (1910) and Finch and Bradford (1934) froze out ozone from the gas issuing from a discharge fed with dry oxygen, but found no evidence of the survival of atomic oxygen. All these workers appear to have used discharges between electrodes. Copeland (1930), however, used an electrodeless discharge, and concluded that atomic oxygen not only has a life comparable with that of atomic hydrogen but is also formed in the discharge by a mechanism similar to that postulated by Wood, whereby a poisoning of the discharge vessel walls by moisture was supposed to be necessary for the survival of the atomic species. It has, however, already been mentioned above that mercuric oxide films were formed after a brief circulation of oxygen through the discharge. These films were as readily obtained with dry as with moist oxygen. Thus if, as Copeland held, they were due to the interaction of mercury vapour and atomic oxygen, their formation with dry oxygen conflicted with his hypothesis. It was therefore decided to examine the matter further.

Owing to the difficulty of removing stains, caused by the experiments of Series 5, from the discharge vessel without etching the glass and thus impairing its smooth surface, a new vessel was fitted. It had previously been cleaned in the usual way but not baked out or degassed by circulating steam through the discharge. After fitting the first port beyond the discharge vessel with an ash-coated probe and the discharge vessel port with a 36 s.w.g. tungsten wire protruding into the discharge region, the normal circulation system was filled with oxygen previously washed with concentrated caustic potash and roughly dried by a single passage over phosphoric oxide. The gas was then circulated through the discharge under the normal conditions of pressure.

Rapid formation of the mercuric oxide films again occurred and was followed more slowly by a "tailing" of the mercury in the pump boiler. Neither the ash-coated nor the tungsten probe showed any signs of incandescence. The "tailing" and mercuric oxide films were easily removed by reduction, in the manner previously described, with atomic hydrogen formed from a hydrogen–steam mixture in equal proportions. A spectrogram, taken about half an hour after

starting the discharge, is reproduced in Figure 5. It reveals, *inter alia*, a fairly strong atomic oxygen spectrum, faint hydroxyl bands, the first three lines of the Balmer series, and prominent bands due to carbon monoxide.

On repeating this experiment, a spectrogram similar to Figure 5 was obtained, but without the carbon monoxide spectrum. It would appear, therefore, that in the first experiment of this series the circulation of oxygen through the discharge had effectively out-gassed the discharge vessel walls. A fresh charge of oxygen was circulated for several hours past the heated spiral K and through the drying tube before starting the discharge, and a further spectrogram taken. This was again similar to Figure 5, except that, in addition to the absence of the carbon monoxide spectrum, the 3064, but not the 2808 A., hydroxyl band-head region was visible. H_β of the Balmer spectrum was very faint.

It will be evident at once that, in affording the primary (atomic) spectrum, the behaviour of dry oxygen in the ring discharge differed radically from that of dry hydrogen which, in the main, yielded the secondary spectrum, with weak hydroxyl bands and a few faint lines of the Balmer series attributable to traces of moisture.

It is noteworthy that, despite the spectrographic evidence of the production of atomic oxygen in the discharge, the tungsten and ash-coated probes remained cool throughout. Since the heat of formation of molecular oxygen ($>117{,}000$ kcal/gm. mol.) is greater than that of hydrogen, it is plain that little or no atomic oxygen survived to reach the ash probe, only 5 cm. beyond the discharge vessel, or even the tungsten wire probe. It is most unlikely, therefore, that the mercuric oxide films, which had formed so rapidly, could have been due to the interaction of mercury vapour and atomic oxygen, as Copeland has supposed. Rather must this phenomenon be ascribed to some other active modification of oxygen.

In the next experiments the effect of the dilution of oxygen by steam was examined. A wide range of mixtures was used containing between 5 and 96 per cent steam, the remainder being oxygen. The results have so much in common that it will suffice to summarize them as follows:

(i) Mercuric oxide films were formed, as with dry oxygen, at the usual sites, and "tailing" in the pump also occurred. The rate of formation of the mercuric oxide, as estimated from the growth in density of the film near the McLeod gauge, was roughly proportional to the oxygen concentration.

(ii) The ash-coated probe incandesced to some extent in all cases, but did so most vigorously in mixtures rich in steam. The tungsten wire probe glowed brightly in all cases.

(iii) The spectrograms reveal a progressive weakening of the atomic oxygen spectrum with increasing steam concentration, but a few lines, notably 3947 and 4368 A., remain, even in the case of pure steam. The hydroxyl band and Balmer spectra are prominent throughout.

It has already been shown in the case of dry oxygen that the formation of the mercuric oxide films was due to some active form of oxygen, other than atomic oxygen, which was incapable of exciting either the ash-coated or tungsten wire probe to incandescence. Hence, the fact that this oxidation process was slowed down by progressive dilution of the oxygen with steam strongly suggests that in the cases of both dry and moist oxygen the same agent was responsible for the oxidation of mercury. The results obtained by Strutt (1911) and Finch and Bradford (1934), taken into consideration with the fact that ozone is known to form

yellow mercuric oxide with mercury (Manchot and Kampschulte 1907, 1910), justify the assumption that ozone was the long-lived, active form of oxygen produced in these experiments.

Since the ash probe and, to a lesser extent, the tungsten wire incandesced more brightly with increasing dilution with steam, it is evident that this could only have been due to recombination of atomic hydrogen. That the phenomena of the probe incandescence and mercuric oxide formation occurred simultaneously, even in mixtures containing as little as 5 per cent of oxygen, suggests that atomic hydrogen and ozone interact in the gas phase only relatively slowly, if at all, under the conditions of our experiments.

In the light of these results we are forced to conclude that, unlike atomic hydrogen, atomic oxygen does not survive as such on escaping from the discharge. There is a ready explanation for this. Thomson and Thomson (1928) point out that, unlike hydrogen, the oxygen molecule readily captures an electron to form a negative ion. It is to be expected that the oxygen atom is even more efficient in this respect. There is ample opportunity for such capture to occur within the discharge, where the electron population is of the same order as that of the molecules present (Thomson 1928). Under these circumstances, two-body collision reactions, such as the recombination of oxygen atoms to molecular oxygen, or of oxygen atoms with molecules to form ozone, are no longer subject to quantum-mechanical restrictions, provided one or both of the reactants is a negative ion.

Series 7—Neon–steam mixtures. This series of experiments forms, in a sense, a continuation of Series 6, the oxygen component being, however, replaced by a rare gas. It was hoped that a comparison of the results of the two sets of experiments would throw further light on, *inter alia*, the apparent strange reluctance of atomic hydrogen and ozone to interact. The experiments were carried out with mixtures covering a range from well-dried neon to pure steam.

The essential results can be summarized briefly by stating that (i) the intensity of the incandescence of the ash and tungsten wire probes increased with increasing steam concentration in a manner which closely paralleled that observed in the case of the corresponding oxygen–steam mixtures and, (ii) unlike the case of steam-diluted oxygen, the spectrograms (Figure 6) show that on increasing the steam concentration the neon spectrum was quickly suppressed. For instance, in a mixture of neon and steam in equal proportions only the hydroxyl and Balmer series spectra are visible.

The parallel behaviour of the probes in the two series supports the conclusion that in the case of both oxygen and neon–steam mixtures incandescence of the probes was caused solely by atomic hydrogen and, further, that atomic hydrogen and ozone are, for some unknown reason, slow to react with each other. It is also not difficult to see that, except for the formation or otherwise of mercuric oxide, the experimental results which led Copeland to suppose that atomic oxygen of long life is formed by the action of the electrodeless discharge on moist oxygen could equally well have been obtained with moist neon.

§4. SUMMARIZED FINDINGS AND CONCLUSIONS

The behaviour of steam or a mixture of hydrogen and oxygen in combining proportions, and their mixtures with hydrogen or oxygen, ranging from dry hydrogen to dry oxygen, have been studied in the ring discharge. The effect of mercury vapour and of neon on the steam equilibrium was also examined.

The principal facts established were as follows :

(i) *Dry hydrogen.* The secondary hydrogen spectrum was strongly emitted. The hydroxyl-band and Balmer spectra were weak and tended to disappear with progressive drying. Apart from traces attributable to incomplete drying, no agent capable of reducing yellow mercuric oxide at room temperature reached the walls of the discharge vessel.

(ii) *Moist hydrogen.* On adding to dry hydrogen about 1 per cent of oxygen or 2 per cent of steam (and possibly much less) the spectrum changed radically, the secondary hydrogen spectrum being replaced by the hydroxyl-band and Balmer spectra. Mercuric oxide at the wall of the discharge vessel was rapidly reduced.

(iii) *Steam.* The emission consisted mainly of the hydroxyl-band and Balmer spectra, together with a few lines due to atomic oxygen.

The stable end-products obtained from steam (or the equivalent hydrogen–oxygen mixture) consisted of steam, hydrogen and oxygen, the last two in their combining proportions. With a clean discharge vessel, the final steam concentration was between 16·5 and 19 per cent, but partial contamination of the vessel's walls by a barely visible film of copper sufficed to more than double the steam yield, which, however, returned to its previous value after removal of the copper film.

Glass needles, coated with sealing-wax ash (SnO and CaO) and inserted into the exhaust tube through ports situated 5 and 20 cm. beyond the discharge vessel, incandesced brightly. Films of yellow mercuric oxide deposited in the exhaust tube were rapidly reduced to metallic mercury. Copper, tungsten or platinum wire probes in the discharge vessel or in the exhaust tube glowed. The insertion of a copper wire spiral into the exhaust tube between the discharge vessel and an ash-coated probe suppressed the incandescence of the probe and practically stopped the reduction of the mercuric oxide films. The spiral did not appreciably affect the equilibrium steam concentration. With the ring discharge interrupted, an electrically heated platinum wire probe, situated in the exhaust tube near the discharge vessel, catalysed the formation of steam from the equivalent hydrogen–oxygen mixture, but ceased to do so and cooled when the heating current was stopped. The wire glowed spontaneously, however, immediately the ring discharge was restored.

(iv) *Steam-hydrogen and the equivalent hydrogen–oxygen mixtures.* The hydroxyl-band and Balmer spectra were prominent in all mixtures containing up to 95 per cent (and possibly more) diluent hydrogen, and their relative intensities appeared to be independent of such dilution. On increasing dilution with hydrogen, the atomic oxygen lines observed with steam alone weakened and eventually disappeared.

Dilution with hydrogen reduced the dissociation of steam, but not to the extent required by the law of mass action.

The ash-coated probes incandesced and the mercuric oxide films were reduced in all mixtures examined, incandescence being most pronounced in the case of mixtures containing hydrogen and steam in roughly equal proportions.

(v) *Steam–mercury vapour.* Apart from an intense mercury spectrum, the emission from the ring discharge in a mixture of steam (or the equivalent hydrogen–oxygen mixture) with roughly one-third its volume of mercury vapour consisted chiefly of the hydroxyl-band and mercurous-hydride spectra. The Balmer and secondary hydrogen spectra were absent. The ash probes did not incandesce.

The mercuric oxide films in the exhaust tube were only slowly reduced. In contrast to the steam yield of about 18 per cent obtained with pure steam, the equilibrium steam concentration rose to nearly 100 per cent.

(vi) *Dry oxygen.* The emission consisted mainly of the atomic oxygen spectrum, with faint hydroxyl-bands and a few faint lines of the Balmer series attributable to traces of moisture.

Yellow mercuric oxide was formed in the exhaust tube at all those sites where the gas stream issuing from the discharge came into contact with stagnant mercury vapour. The wire and ash-coated probes remained cool.

(vii) *Oxygen–steam.* The atomic oxygen spectrum weakened with increasing dilution by steam, but a few lines remained even with pure steam. The hydroxyl-band and Balmer spectra were prominent throughout.

Mercuric oxide films were formed, as with dry oxygen, even in mixtures containing only 5 per cent of oxygen. The ash-coated probes incandesced in all mixtures containing up to 95 per cent oxygen, but were brightest in steam-rich mixtures.

(viii) *Neon–steam.* The hydroxyl-band and Balmer spectra only gave way to the neon spectrum as the neon concentration approached 100 per cent. The behaviour of the ash-coated and wire probes was similar to that observed in the case of the corresponding oxygen–steam mixtures, in that the incandescence effect increased with increasing steam concentration.

The following conclusions have been drawn:

Dry molecular hydrogen is not dissociated but only excited in the ring discharge. The generally accepted view, according to which atomic hydrogen is formed and the absence of the Balmer spectrum is due to recombination of the atoms on the walls of the discharge vessel, is therefore untenable.

Atomic hydrogen issues in considerable quantity from the discharge in steam, hydrogen–steam or hydrogen–oxygen mixtures. The incandescence of ash-coated probes, and the spontaneous glowing of copper, tungsten, or platinum wires in the gases drawn from the discharge testify to a high concentration of atomic hydrogen, whilst the reduction of mercuric oxide films serves as a more sensitive test. It is unlikely that moisture adsorbed on the walls of the discharge vessel materially affects the yield of atomic hydrogen; for, if it did, it should also cloak the catalytic activity of a thin copper film, which it does not do.

The following reactions take place in hydrogen–steam and the equivalent hydrogen–oxygen mixtures. Steam is dissociated into hydroxyl and atomic hydrogen. The reverse reaction cannot proceed except through three-body collisions, and is therefore practically excluded. The same is true of the union of hydrogen atoms to molecules; consequently atomic hydrogen has a long survival life. On the other hand, the life of hydroxyl is short and is terminated by reacting with molecular hydrogen to form steam and atomic hydrogen, and with hydroxyl to form steam and atomic oxygen. Owing to the ease with which oxygen atoms form negative ions, they revert quickly to the molecular state. Finally, hydrogen reacts with oxygen to form steam and atomic oxygen. Some hydrogen peroxide may also be formed, but mainly at surfaces.

Dry oxygen, unlike dry hydrogen, is dissociated directly into atomic oxygen, which has a short life and quickly reacts within the discharge to form molecular oxygen and ozone. With stagnant mercury vapour, ozone forms films of yellow mercuric oxide. All the reactions occurring in oxygen and in hydrogen–steam mixtures also take place in oxygen–steam and the equivalent oxygen–hydrogen

mixtures ; thus ozone and atomic hydrogen appear together in the effluent gases and interact, if at all, very slowly. The phenomena of the formation of mercuric oxide and the heating of ash-coated probes and wires in oxygen–steam mixtures are due to ozone and atomic hydrogen respectively, and are not evidence, as hitherto supposed, of a long life of oxygen in the atomic state.

The products leaving the ring discharge fed with a mixture of steam (or the equivalent hydrogen–oxygen mixture) and sufficient mercury vapour consist almost wholly of steam ; only traces of atomic hydrogen are present. In this case the steam is no longer directly dissociated into hydroxyl and atomic hydrogen, but reacts with mercury to form hydroxyl and mercurous hydride. Other reactions occurring are the oxidation of mercurous hydride to form mercuric oxide and hydroxyl, the reduction of mercuric oxide by atomic (or molecular) hydrogen to mercury and hydroxyl (or steam), the reduction of mercury by molecular hydrogen to mercurous hydride and atomic hydrogen, and the formation of steam and atomic oxygen from hydroxyl.

In neon–steam and the equivalent neon–hydrogen–oxygen mixtures, the reactions are similar to those occurring in steam.

ACKNOWLEDGMENTS

I have received much help in this study and wish to thank in particular Dr. E. E. Thompson and Dr. A. E. W. Austen, who carried out much of the experimental work, and Dr. R. W. B. Pearse, who checked the analyses of the spectrograms. My thanks are also due to Messrs. Ferranti for financial support of the work.

REFERENCES

Bonhoeffer, K. F., and Pearson, T. G., 1931, *Z. phys. Chem.* **B14**, 1.
Copeland, L. C., 1930, *Phys. Rev.*, **36**, 1221.
Esclangen, F., 1934, *Ann. Phys., Paris*, **11**, 267.
Finch, G. I., 1935, *J. Chem. Soc.*, 32.
Finch, G. I., and Bradford, B. W., 1934, *J. Chem. Soc.*, 360.
Finch, G. I., and Fraser, R. P., 1926, *J. Chem. Soc.*, 117.
Finch, G. I., and Mahler, E. A. J., 1931, *Proc. Roy. Soc.* A, **133**, 173.
Frost, A. A., and Oldenberg, O., 1936, *J. Chem. Phys.*, **4**, 642.
Geib, K. H., 1938, *Z. Elektrochem.*, **44**, 81.
Geib, K. H., and Harteck, P., 1934, *Trans. Faraday Soc.*, **30**, 134.
Harteck, P., and Kopsch, U., 1931, *Z. phys. Chem.*, **B12**, 327.
Mackinnon, K. A., 1929, *Phil. Mag.*, **3**, 605.
Manchot, W., and Kampschulte, W., 1907, *Chem. Ber.*, **40**, 2891; 1910, *Ibid.*, **43**, 750.
Mott, N. F., and Massey, H. S. W., 1933, *Atomic Theory of Collisions* (Oxford : Clarendon Press), p. 214.
Oldenberg, O., 1937, *J. Phys. Chem.*, **41**, 293.
Olsen, L. O., 1938, *J. Chem. Phys.*, **6**, 307.
Poole, H. G., 1937, *Proc. Roy. Soc.* A, **163**, 404.
Rieke, F. F., 1936, *J. Chem. Phys.*, **4**, 513.
Southworth, G. C., 1920, *Radio Rev.*, **1**, 583.
Steacie, E. W. R., 1946, *Atomic and Free Radical Reactions* (New York : Reinhold).
Strutt, R. J., 1910, *Proc. Phys. Soc.*, **23**, 66; 1911, *Proc. Roy. Soc.* A, **85**, 226.
Taylor, H. S., and Bates, J. R., 1926, *Proc. Nat. Acad. Sci., Wash.*, **12**, 714.
Thomson, J. J., 1928, *Proc. Phys. Soc.*, **40**, 79.
Thomson, J. J., and Thomson, G. P., 1928, *Conduction of Electricity through Gases* (Cambridge : University Press), 3rd ed., p. 242.
Wood, R. W., 1920, *Proc. Roy. Soc.* A, **97**, 455; 1921, *Phil. Mag.*, **42**, 729 ; 1922 a, *Ibid.*, **44**, 538 ; 1922 b, *Proc. Roy. Soc.* A, **102**, 1.

The Electron Optical Properties of the Focal Isolation β-Ray Spectrometer

By D. K. BUTT
Department of Natural Philosophy, The University, Edinburgh

Communicated by N. Feather ; *MS. received* 15*th February* 1949

ABSTRACT. An attempt is made to show theoretically how the performance of a lens spectrometer depends upon the degree of spherical aberration present in the lens. In particular, curves of resolving power and transmission are plotted against radius and area of the central lens annulus, for source and counter window on the axis and of equal diameter.

The resolving properties of a circular source and counter window placed at equal distances off the axis are determined. The arrangement is found to be impracticable.

Lastly, an investigation is made into the resolving properties of a line source placed at right angles to the axis of the spectrometer, the image of which is focused into a slit-shaped window in a counter. The arrangement is shown to be advantageous particularly when long solenoids are employed, as in high energy β-spectroscopy.

§1. INTRODUCTION

Rubens and Wood (1911) utilized the principle of focal isolation in the design of a light spectrometer. Although the idea was not further developed for light spectroscopy, the application of a magnetic lens to give spectroscopic resolution of β-rays is now a general practice. Tricker (1924) first constructed an instrument employing this principle, and since then many different types have been designed.

A detailed theoretical treatment of the resolving properties of such an instrument is extremely hard to give, since no exact analytical expressions exist by which one can determine the paths of the rays through the system. An exception must be made in the special case of a homogeneous lens field, for which Tricker's original treatment is adequate. Approximate methods do exist,

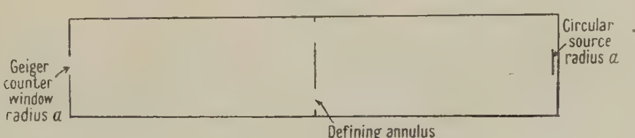

Figure 1.

however, the utilization of which gives one a very good idea of the processes taking place in the general case. Using such a method, Deutsch, Elliot and Evans (1944) made the first systematic attack on the problem. In the present paper their method is extended and a more complete picture of the characteristics of the focal isolation instrument is given.

The essential requirement of a magnetic electron lens spectrometer is a magnetic lens of axial symmetry which will produce a focusing of the electrons emitted from a source placed somewhere in the object field of the lens. Usually the source is disc shaped, and placed on the axis of the lens, as shown in Figure 1. Some sort of electron detecting device (usually a Geiger counter on this type of spectrometer) is placed at the electron image to register the intensity of the focused beam. A stop is placed, usually in the middle of the lens. As will be

seen later, different annular zones of the lens possess different focusing properties. The stop has to define a zone which will give the maximum gathering power for the resolution that is desired.

For simplicity, a thin lens is chosen for the analysis which follows. This type of lens, although considerably different from those generally used on β-ray spectrometers, is sufficiently characteristic to give results which will show the general properties.

§ 2. GENERAL CONSIDERATIONS

The focal length of an electron lens can be expressed by the formula

$$f = K(p/i)^2, \qquad \ldots\ldots (1)$$

where p is the momentum of the focused electrons, i is the focusing current and K is a constant depending only upon the geometry of the lens. This is in effect a generalization of the Busch thin lens formula for a lens of any type. It is not strictly valid, since in the general case, the principal planes of an electron lens change slightly for different focal lengths, and the expression for the chromatic aberration obtained from it on the assumption that the lens is thin, is usually larger than is found in practice. However, in this paper, this fact will simply distort the results by a constant factor.

The lens used in the following analysis is considered as having a paraxial focal length of 22·5 cm. with a focusing current of 1·5 amperes for electrons of $H\rho = 1385$ gauss. cm. A magnification of unity is assumed throughout.

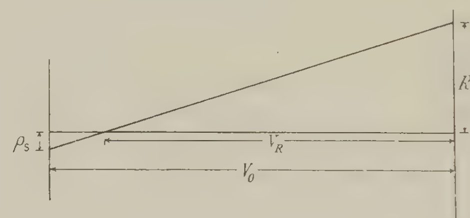

Figure 2.

Many kinds of aberration are present in an electron lens, but for the present analysis by far the most important is the spherical aberration. This is usually of such a magnitude that it overshadows all other aberrations ; here it will be considered as the only defect. The lens, apart from spherical aberration, therefore, will be considered to be perfect.

Consider a ray passing through an annular zone of radius R in the middle of the lens (Figure 2). Since it passes through an outer zone, it behaves as if the focal length of the lens is less than that for the paraxial ray. If it cuts the paraxial image plane at a distance ρ_s from the axis, to a first degree of approximation ρ_s can be expressed by the formula

$$\rho_s = C\theta^3, \qquad \ldots\ldots (2)$$

where θ is the angle which the ray in question makes with the axis, and C is a constant depending upon the lens geometry and the object and image positions. C is called the constant of spherical aberration. Obviously an analysis based upon this formula is true only so long as second order spherical aberration is negligible.

Although an expression does exist for the calculation of the constant C for any given field distribution, the calculation, except for special cases, is a long one, and usually C is determined practically (such a determination has been described by Deutsch, Elliot and Evans (1944)).

In the present analysis values of C equal to 0, 250 and 500 cm. have been used and the results for many different cases compared. The values of 250 and 500 cm. are somewhat high for modern lenses. From the results quoted by Deutsch, Elliot and Evans it can be deduced that for a lens system of dimensions similar to those of the one we are here considering, the value of C is approximately ·92 cm.

If the paraxial image distance in Figure 2 is V_0 and the image distance for the "annular" ray is V_R, then $\rho_s/R=(V_0-V_R)/V_R$. But

$$\frac{1}{f_R}-\frac{1}{f_0}=\frac{1}{V_R}-\frac{1}{V_0} \quad \text{and hence} \quad \frac{\rho_s}{R}=V_0\left(\frac{1}{f_R}-\frac{1}{f_0}\right),$$

and substituting for ρ_s from equation (2),

$$\frac{C\theta^3}{R}=V_0\left(\frac{1}{f_R}-\frac{1}{f_0}\right). \qquad \ldots\ldots(3)$$

In order that equation (2) may be valid, $R \ll V_0$, and we may therefore write $\theta=R/V_0$ approximately, when equation (3) becomes

$$\frac{CR^2}{V_0^3}=V_0\left(\frac{1}{f_R}-\frac{1}{f_0}\right).$$

Thus, for a given paraxial focal length, the focal length for any other ray may be calculated :

$$\frac{1}{f_R}=\frac{1}{f_0}-\frac{CR^2}{V_0^4}. \qquad \ldots\ldots(4)$$

Consider now a beam of electrons passing through an infinitely narrow annulus (Figure 3). If the plane of the Geiger counter window is at a distance

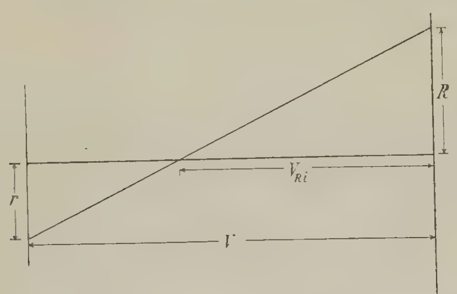

Figure 3.

V from the middle of the lens, and the electrons are brought to a focus at a distance V_{Ri} from the lens annulus, they will form a circle on the plane of the Geiger counter window of radius

$$r_{Ri}=R\left(\frac{V-V_{Ri}}{V_{Ri}}\right)$$

$$=RV\left(\frac{1}{f_{Ri}}-\frac{1}{f}\right), \qquad \ldots\ldots(5)$$

where f is the corresponding focal length for the image distance V. Since the annulus is assumed infinitely narrow, these electrons will be concentrated on the infinitely narrow circumference of the circle.

§3. CASE OF A DISC SOURCE COAXIAL WITH THE LENS

It is now possible to calculate the fraction of the electrons falling on the Geiger counter window from a disc source, after passing through such an annulus.

Let the radii of the source and counter window each be a. Consider any point on the source at a distance x from its centre. If x is small compared with the radius of the annular zone, we may assume that the electrons from this point will fall on a circle on the Geiger counter window plane, this image circle having radius

$$r_{Ri}=RV\left(\frac{1}{f_{Ri}}-\frac{1}{f}\right)$$

and its centre being at a distance x from the centre of the window.

The fraction of the transmitted electrons received by the counter is therefore the fraction of the image circle that falls on the counter window, that is δ/π (see Figure 4). This fraction will be denoted by t_{Ri}. If the source is divided into

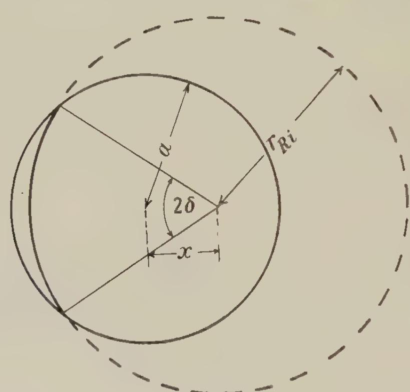

Figure 4.

elementary areas $x\,dx\,d\alpha$, each of these elementary areas will act as a point source as above considered. For the complete source, for a given annular radius R, and any focusing current i, the fraction T_{Ri} of the electrons received is given by

$$T_{Ri}=\frac{2\pi}{A}\int_0^a t_{Ri}\,x\,dx, \qquad \ldots\ldots(6)$$

since t_{Ri} is independent of α owing to the cylindrical symmetry of the system. Here A is the area of the source. For convenience the integration has been carried out graphically for a series of values of R and i. As an example of the results, graphs of T_{Ri} against R for constant i are shown in Figure 5 for $2a = 1$ mm., and $C = 250$ cm.

The next stage in the analysis is to find the effect of a finite lens aperture. If an aperture of finite width is considered, we have instead of (6) the expression

$$T_{(R_1R_2,\,i)}=\frac{2\pi}{(R_2^2-R_1^2)}\int_{R_1}^{R_2} R\,T_{Ri}\,dR \qquad \ldots\ldots(7)$$

approximately, assuming $R \ll V$.

This expression can be quickly evaluated if the ordinates of Figure 5 are multiplied by R. $T_{(R_1R_2,\,i)}$ is then given in terms of the area under the (RT_{Ri}, R) curve. This can be found with sufficient accuracy for this analysis by the use of a planimeter.

It is of interest to find which annulus, when the current is adjusted for optimum utilization, will give the best resolution, and also how the resolution depends on the area of the annulus.

If the transmission curve * is of a simple shape, an estimate of the resolution can be made by stating the fractional spread of the curve at half its height. Thus

$$S = \frac{\Delta i}{i} = \frac{\Delta(H\rho)}{(H\rho)}. \qquad \ldots\ldots(8)$$

This of course is only a very crude way of defining resolution since no account is taken of the shape of the curve. However, in the present case, such a definition

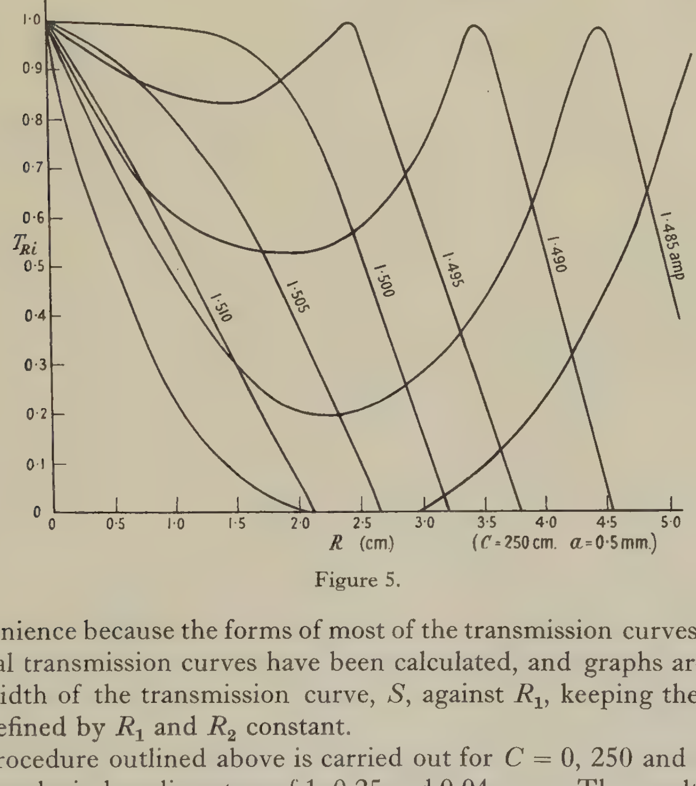

Figure 5.

is of convenience because the forms of most of the transmission curves are similar. Theoretical transmission curves have been calculated, and graphs are plotted of the half width of the transmission curve, S, against R_1, keeping the area of the annulus defined by R_1 and R_2 constant.

The procedure outlined above is carried out for $C = 0$, 250 and 500 cm. and for source and window diameters of 1, 0·25 and 0·04 mm. The results are shown in Figure 6. Ω is numerically equal to the area of the annulus in cm² divided by π. Thus the solid angle subtended by the annulus at the source is $\pi\Omega/V^2$ approximately when the object distance is large compared with R_1 and R_2.

When the disc of least confusion is larger than the counter window, all the electrons passing through the annulus $R_2 - R_1$ do not enter the window, so that only a fraction of the solid angle is usefully employed. This fraction is shown on the graphs. The optimum diameter of the counter window for any given annulus is, as Deutsch, Elliot and Evans pointed out, equal to the diameter of the disc of least confusion.

* This is the curve obtained by plotting counting rate against focusing current for a constant source of electrons of a single energy.

It can be seen from these graphs that, quite generally, as an annular zone of given aperture is moved outwards from the axis, the resolution improves, although only slowly after a certain value of R_1 is reached. The fraction of any solid angle that is utilized (that is, the fraction of the electrons passing through any given annulus that is transmitted), however, steadily decreases. This is

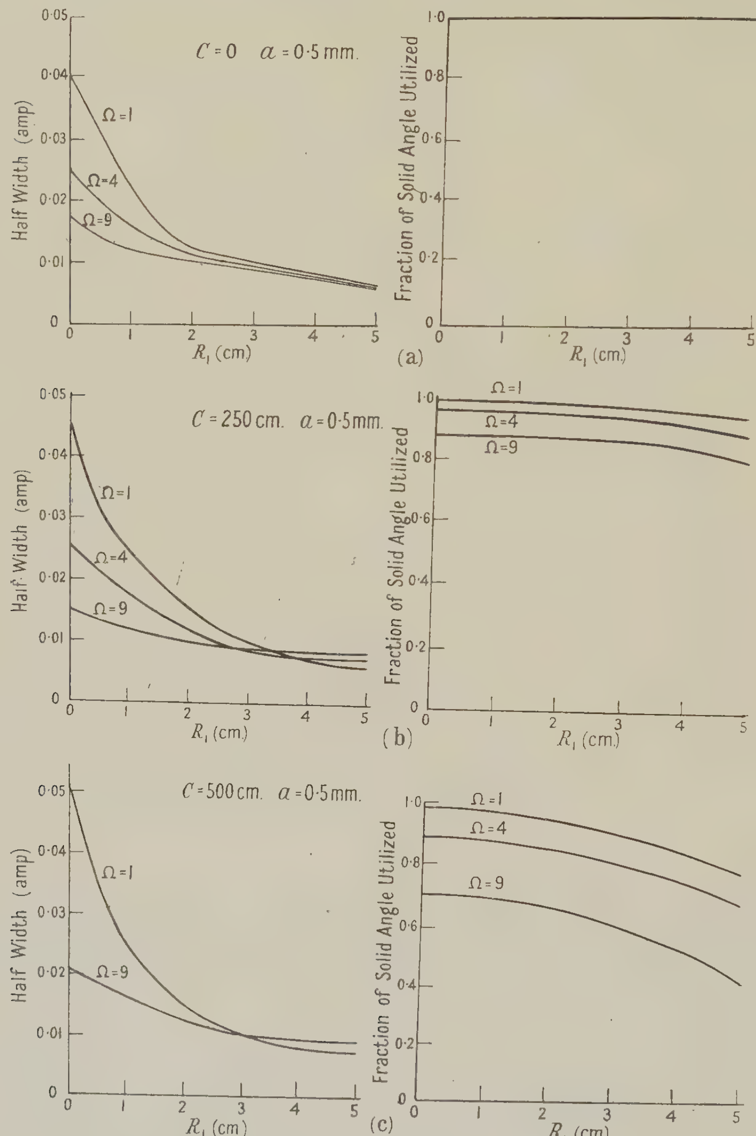

Figure 6. (*a*, *b*, and *c*).

due to the fact that as any annulus of a given area is increased in diameter, the circle of least confusion is enlarged, and if the counter window is of a constant diameter, a smaller fraction of the total incident beam of electrons will go through it.

From Figures 6 (*a*), (*b*) and (*c*), it can be seen that for any given value of Ω the spherical aberration has no great effect on the resolution, but, as would be

expected, the fraction of any solid angle that is utilized becomes smaller as the value of C increases.

In Figures 6 (d) and (e) it is seen that for small diameter sources and counter

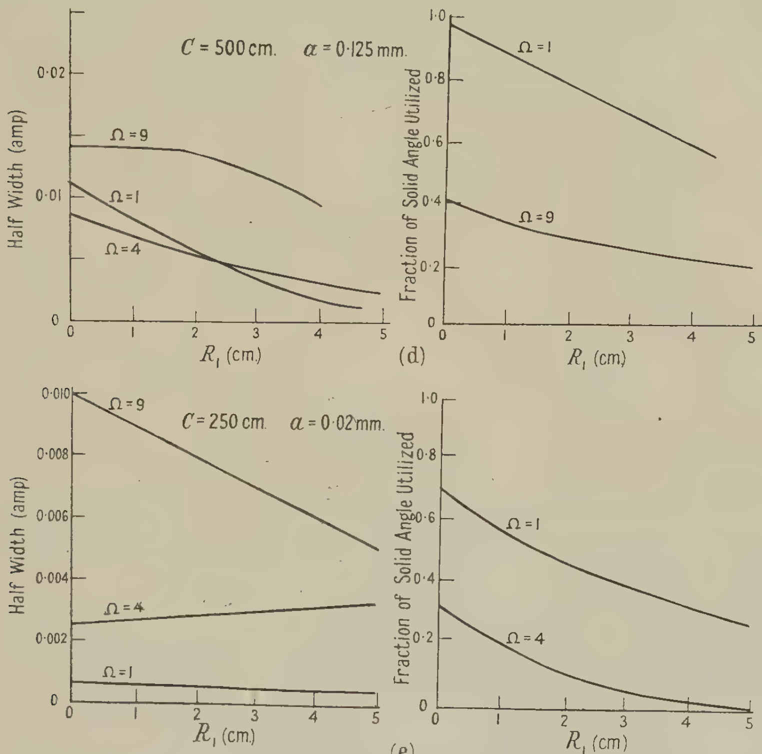

Figure 6. (d and e).

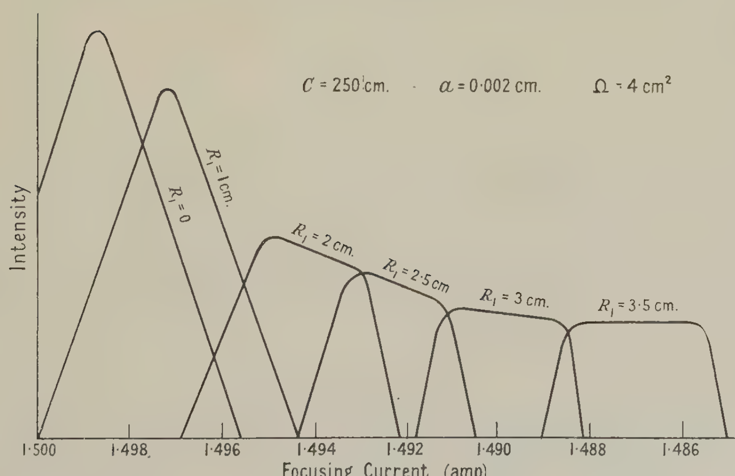

Figure 7.

windows the resolution can be made very high, but this is at the expense of a very low gathering power ; when the diameter of the source is small the spherical aberration almost entirely determines the diameter of the image (that is, the disc

of least confusion), and when the diameter of the counter window is small compared with this, only a very low gathering power can be obtained.

When the disc of least confusion is much larger than the counter window, flat topped transmission curves are obtained. Figure 7 shows some of the transmission curves calculated for the rather extreme case of $a=0{\cdot}002$ cm.

Experimental verification of the results given in Figure 6 has been attempted.

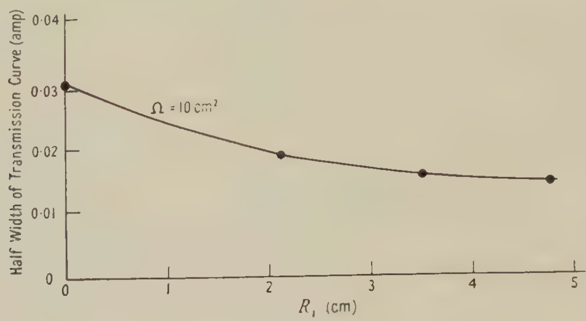

Figure 8.

The practical spectrometer had a thick lens, composed of an unshielded solenoid of diameter 14 cm. and length 20 cm. The magnification was unity (as in the theoretical calculations) and the focal length of the system 21·1 cm. The principal planes of the lens were crossed and 2 cm. apart.

It is obvious that only approximate agreement between experiment and theory can be expected in this comparison. The experimental curve for R_1 against half-width is shown in Figure 8, for $\Omega=10\,\mathrm{cm}^2$, and $a=0{\cdot}5$ mm.

§4. THE CASE OF AN OFF-AXIAL SOURCE

It is well known that the electron image formed by a magnetic lens is rotated with respect to the object. The angle through which the image is rotated is given by the formula

$$\phi=\frac{1}{H\rho}\int H_z\,dz,$$

where the z axis coincides with the axis of the lens.

It is interesting to enquire whether use can be made of this phenomenon to increase the resolving power of the lens.

Obviously for a disc-shaped source that is axially symmetrical with the lens the rotation does not affect the image at all. If, however, the source is moved off the axis a distance v say, the image is rotated as shown in Figure 9. It is not at first obvious what is the resultant effect.

Assume the lens to be perfect. As seen from Figure 5, any elementary area around point P on the source gives rise to an image circle in the plane of the Geiger counter window (assuming the electrons to pass through an elementary lens zone), the centre of which, P', is rotated through a certain angle about the axis, with respect to P. Hence corresponding to any elementary area at P on the object, there is the corresponding centre of its image circle at P′. The total of all such elementary areas P, i. e. the complete disc source, will give rise to a similarly shaped distribution of points P′, which is called here the constructional image.

Obviously, as the focusing current is changed, so the rotation of the constructional image changes, and when the focusing current is of such a value that $r_{Ri}=0$ (remembering that $C=0$), the constructional image coincides with the real image. The Geiger counter window is adjusted so that this real image lies exactly over it. As seen from Figure 9, the fraction of the electrons that are transmitted, having come from an elementary area P and passed through an elementary zone R, is $\delta/2\pi$.

The integration for a circular source of radius $a = 0{\cdot}5$ mm. is carried out graphically. The coordinates are taken as shown in Figure 10. From the centre of the window, suppose an arc of radius b is drawn to cut the constructional image

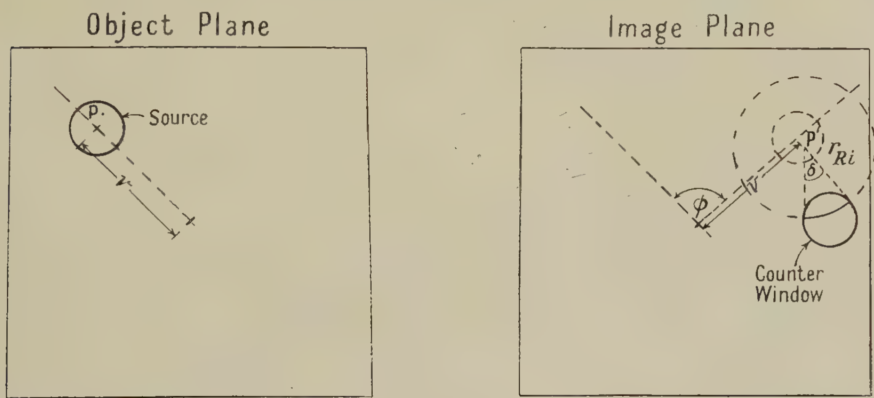

Figure 9.

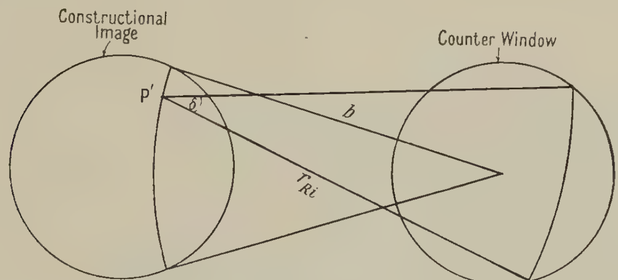

Figure 10.

as indicated. Corresponding to every point on this arc, a constant fraction t_{Ri} of the electrons will be received and this fraction can be found by drawing an arc of radius r_{Ri} centred somewhere on the arc of radius b, and measuring off the angle δ (see Figure 10). The fraction of the total transmission received will then be given by

$$T_{Ri} = \frac{1}{2\pi A}\int b\alpha\,\delta\,db.$$

The rotation is assumed to be 100° per ampere. This is a somewhat liberal value, giving the total image rotation a value of 150° ; v is assumed to be 2 cm.

The graphs of T_{Ri} against R for various focusing currents * are shown in Figure 11. In dotted lines are included the graphs for the source on the axis (as calculated for Figure 6 (a)).

* Δi represents the amount of current by which the lens is defocused for the energy of the electrons considered.

It is seen that, roughly, for values of R less than 1·5 cm. the rotational effect is advantageous, and that for values of R greater than 1·5 cm. the source on the axis will give the better resolution. This result depends in detail upon the arbitrary value of the image rotation that is chosen. If it were possible to have a greater

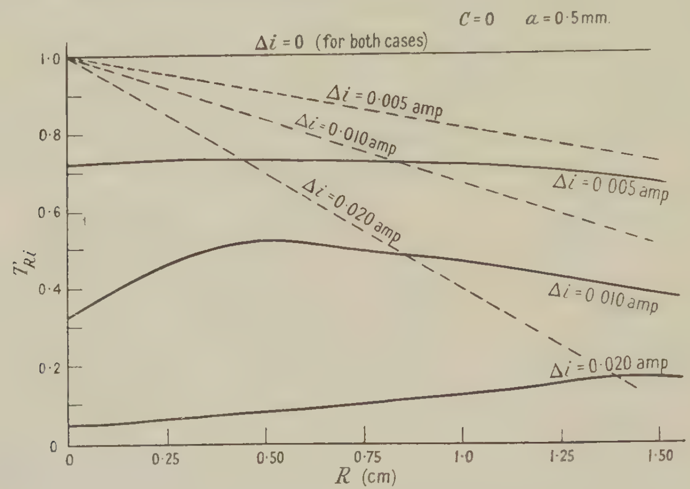

Figure 11. Dotted curves represent transmission for source on axis, and full curves source 2 cm. off axis.

rotation, the focal length remaining constant, the gain would be greater. This is not realizable in practice, but another manner in which the image rotation may be made of greater effect is by use of a source (and counter window) of smaller diameter.

§ 5. THE CASE OF A LINE SOURCE

It was seen in the last section, that the rotation of the image in an electron lens could be used with advantage only when the diameter of the source (and counter window) is small. Obviously in practice, sources much less than 1 mm. in diameter will not give sufficient intensity, so that this requirement is too severe for the idea of off-the-axis focusing to be profitable. A way of overcoming this difficulty is to use a line source, with a slit for a counter window. This arrangement was originally suggested to the author by Siday (1942) ; afterwards it was found that Siegbahn (1944) has already considered the case for practical application, although theoretically he took the matter no further than the Cosslett (1940) formula for the resolution for a disc-shaped source on the axis.

We consider here the case of a line source 0·05 mm. broad and 2 cm. long, placed symmetrically at right angles to the axis of the spectrometer, and a Geiger counter window of the same dimensions. The method of dealing with the problem is similar to that used in the previous section. Initially curves are plotted of the radius of the image circle r against the focusing current i, for different zonal radii R. The curves, calculated from equations (1) and (5), are shown in Figure 12. The fact that r is not zero at the same focusing current for all values of R is due to the fact that spherical aberration is present in the lens. A value of $C = 500$ cm. is used. If from these graphs, a line is drawn parallel to the r axis, for any given focusing current i, the values of r can be deduced for any value of R.

Consider the zone of radius R, for which the line image is in focus for a given value of i. The line image is assumed to be straight and its rotation to be fixed by

this current. Here we assume the rotation to be 60° per ampere. To begin with suppose we fix the counter window in such a direction that the image of the line due to electrons passing through the zone $R = 2{\cdot}5$ cm. is fully received. If the current remains constant at this value, for any other value of R, every point on the image will have expanded into a circle of radius r, obtainable from the graph. The fraction of the electrons passing through any zone apart from the

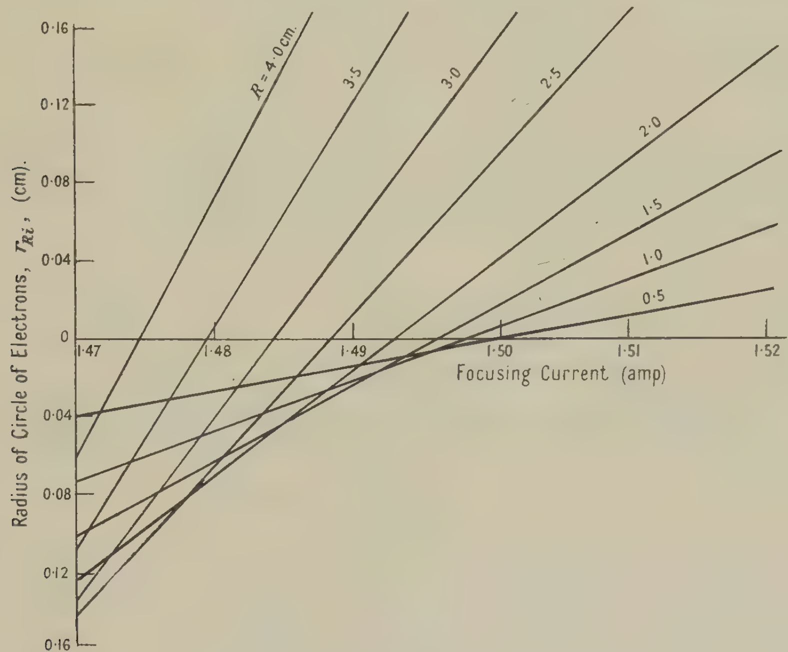

Figure 12.

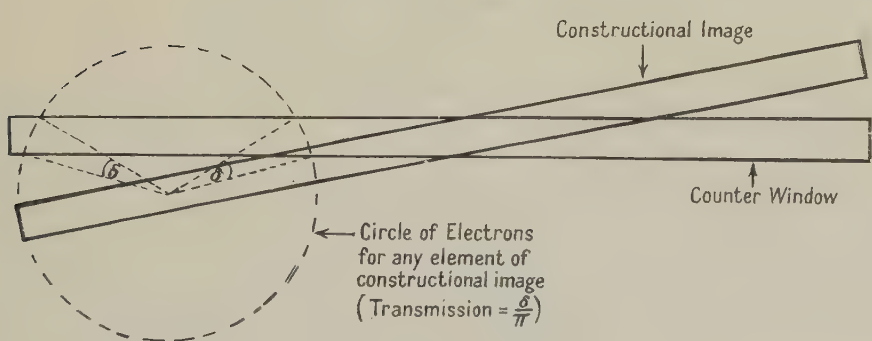

Figure 13.

one $R = 2{\cdot}5$ cm. can then be obtained by purely graphical methods (see Figure 13). The calculation is repeated for other values of i, the counter slit remaining constant in position. In general it will be seen that for any value of i there is a value of R for which the image will be in focus, but this focused image will be rotated with respect to the slit, except for the special case mentioned above.

The transmission curves obtained are shown in Figure 14. From these or similar curves, the most suitable annular dimensions may be deduced for any

given problem, simply by graphical integration. The results for a few annular sizes are shown in Figure 15. It is seen that, after a certain range, very little intensity is gained by further opening of the annulus, but the resolving power is

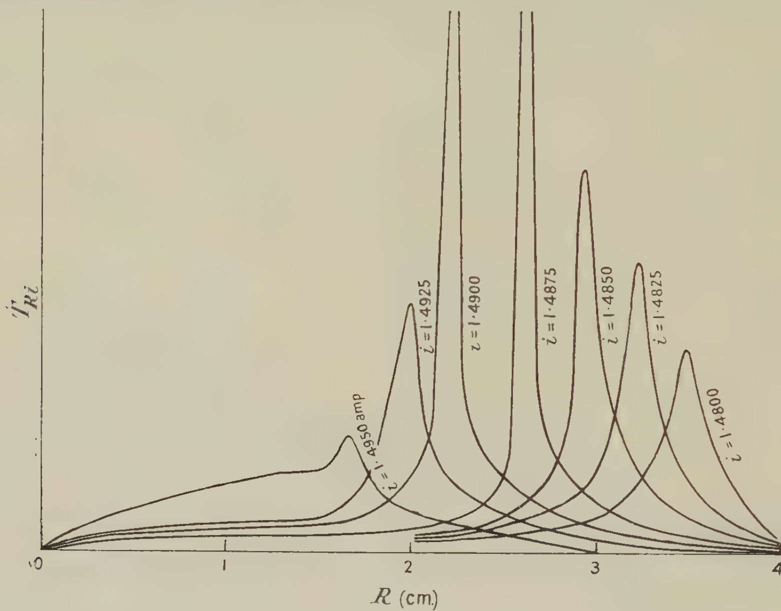

Figure 14.

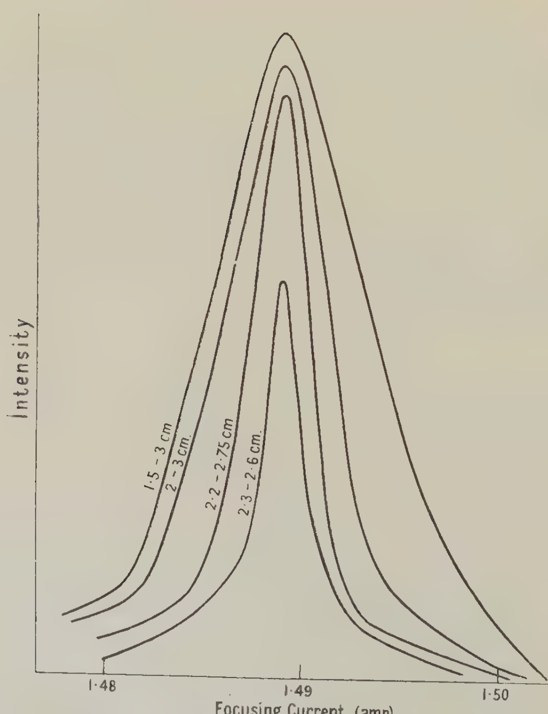

Figure 15. Resolution curves for a line source.

decreased. The fraction of the solid angle, subtended by the 2–2·75 cm. annulus at the source, which is utilized by the counter is 0·37 in the arrangement considered.

One noticeable feature of the type of source considered in this section is that it gives a β-ray line with a long low-intensity "tail". As can be seen, the presence of this "tail" will not appreciably affect the resolution of the instrument, since its intensity is relatively small. The "tail" is due to the fact that the image circle for out-of-focus electrons must be of diameter at least equal to the length of the counter slit before any electrons are received. In the case of a circular source the least diameter for the image circle for no reception is the diameter of the counter window. This, of course, is very much smaller than the length of the counter slit in any equivalent arrangement.

The chief advantage in the line source lies in the fact that a relatively high resolving power can be obtained from a lens of small diameter. As can be seen from Figure 15, a resolving power * of approximately 250 can be obtained

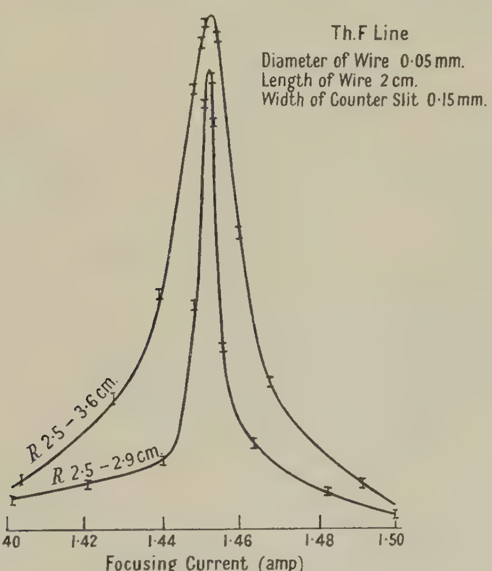

Figure 16.

although the radius of the annulus is only 2·75 cm., and it is to be expected that this value would not rapidly decrease with decreasing annular radius as is the case for a circular source on the axis.

The effect of spherical aberration on the shape of the transmission curve is greater for a line source than for a circular source on the axis. According to Siday (1942) lenses giving the lowest spherical aberration have small values of the diameter-to-length ratio, so that it is possible that very high resolutions can be obtained by the use of a line source together with a long narrow lens.

The main drawback to the use of a line source is the difficulty of the preparation of the long narrow sources themselves. In the few cases in which it is possible to deposit the activity electrically or electrochemically, a wire or metal foil may be used, but in such cases work must be confined to the higher energy region of the spectrum. With sources deposited even on thin metal foils backscattering will be appreciable at energies much below 100 kev.

* Defined by $i/\Delta i$, cf. equation (8).

A practical investigation of possibilities using a wire source of Th(B+C) was carried out with the spectrometer described earlier. A comparison of Figure 16 with Figure 15 shows that the general characteristics of the transmission agree quite well with those predicted theoretically fot the F line.

§ 6. CONCLUSION

It is seen from Figure 6, that the practical limit to the resolving power of a lens spectrometer is brought about by the presence of spherical aberration. As seen from Figure 6 (*d*) and (*e*), very high resolutions are obtainable from small diameter sources, but owing to the presence of spherical aberration, the collecting powers are far too small for the cases to be of practical interest. The same effect is also evident with the line source, as, in the case quoted, only 0·37 of the electrons that go through the central annulus also go through the counter slit. To use a lens spectrometer as a high resolution instrument, therefore, attention must be paid to the further reduction of spherical aberration.

ACKNOWLEDGMENTS

The author's thanks are due to Professor N. Feather, for his continued support and kind interest throughout this work, and to Mr. R. E. Siday, who introduced him to the problems, and with whom he had many stimulating discussions.

REFERENCES

Cosslett, V. E., 1940, *Proc. Phys. Soc.*, **52,** 511.
Deutsch, M., Elliot, L. G., and Evans, R. D., 1944, *Rev. Sci. Instrum.*, **15,** 178.
Rubens, H., and Wood, R. W., 1911, *Phil. Mag.*, **21,** 249.
Siday, R. E., 1942, *Proc. Phys. Soc.*, **54,** 266.
Siegbahn, K., 1944, *Arkiv. Mat. Ast. Fys.*, **30** A, No. 20.
Tricker, R. A. R., 1924, *Proc. Camb. Phil. Soc.*, **22,** 454.

A Unit-Magnification Optical System for the Attainment of Long Working Distances in Microscopy

By J. DYSON
Research Laboratory of the Associated Electrical Industries Ltd., Aldermaston, Berks.

Communicated by T. E. Allibone ; MS. received 24th December 1948

ABSTRACT. To fill an application for a microscope with a long working distance, several optical systems are reviewed. Of these, a system giving unit magnification to be used in conjunction with a conventional microscope is selected as suitable. This consists of a spherical mirror used with the object near its centre of curvature.

The aberrations of such a system are discussed and means of correcting them described. Modifications necessary to enable vertical illumination to be used are also described, and photographs taken by means of an experimental system are shown.

Other applications of the same system are suggested and designs given for a miniature system capable of being used on an ordinary microscope for an immersion objective for " nuclear plate " work and for a water immersion system for biological applications.

§ 1. INTRODUCTION

THERE are many applications, metallurgical and others, requiring the use of a microscope having a working distance much greater than that given by conventional objectives. These include the observation of metal specimens at high temperatures for the investigation of phase transformations and grain growth, the study of sintering and the behaviour of surface films. Other applications include the investigation of conditions inside vacuum tubes and the study of nuclear plates, which may involve working through considerable thicknesses of glass and emulsion.

As the Physical Metallurgy section of this Laboratory wished to undertake work of the nature outlined above an investigation was made of optical systems suitable for this purpose.

In addition to the obvious difficulties introduced by the high temperature, it is usually necessary for the specimen to be enclosed in a vacuum vessel; hence it must be observed through a substantial glass or silica window.

§ 2. CHOICE OF SYSTEM

Suitable optical systems fall into two categories: (*a*) objectives of long working distance giving initial magnification, as in the case of ordinary microscope objectives, and (*b*) systems of approximately unit magnification, having a long working distance and producing a real image which can then be examined by a conventional microscope.

Category (*a*) can include

(1) scaled-up versions of conventional microscope objectives;
(2) Burch's reflection objective, employing aspherical surfaces (Burch 1947);
(3) mirror-lens systems employing spherical surfaces, as used by certain Dutch workers (Bouwers 1946).

Systems of category (*b*) can be divided into

(4) lens systems;
(5) mirror systems.

The relative merits and disadvantages of these systems were considered and are reviewed below.

The smallest numerical aperture which can usefully be employed for a magnification of 400 is about 0·4, corresponding roughly to an 8 mm. objective. The working distance of this is normally less than two millimetres, hence to be of use such an objective would have to be scaled up many times. This would lead to serious difficulties in the correction of such a system, for the residual aberrations grow linearly with the focal length. In any case, the system would be complex and would be costly to produce. Hence alternative (1) was ruled out.

Burch's microscope has a working distance of the order of 1 cm. and would thus not require much scaling up. It is already large, and would need re-designing to counteract the effect of the plane-parallel window. The aspherical surfaces are difficult and slow to produce.

Alternative (3) appears the best possibility in the first category. The system consists of a spherical mirror and a meniscus correcting lens of almost zero power. The latter is somewhat difficult to make, and the accurate centring required presents further difficulties.

A system of type (4) may consist of either a lens specially designed for equal conjugates, or two similar lenses of the photographic type used back to back. The design of a lens for equal conjugates presents even greater difficulties than a scaled-up objective, because of the greater refractive power. The use of two photographic lenses might seem attractive until it is realized that a numerical aperture of 0·4 corresponds to a relative aperture of f/1·25, and that axial corrections much better than those given by a photographic lens are required.

Alternative (5) is much more attractive, as it can consist of a spherical mirror with the object almost at its centre of curvature and the image can be brought out to an accessible position by means of a plane mirror. If no plane-parallel plates were required, the object could be exactly at the centre of curvature, and in this case the system would be perfectly corrected for spherical aberration and for coma varying with the first power of the field.

We are left, therefore, with alternatives (3) and (5) as possibilities. As (5) is much the simpler to construct, it was decided to investigate this.

§3. PHYSICAL ARRANGEMENT

Two alternative forms of the system are shown in Figures 1 and 2. The arrangement in Figure 1 presents some advantages; the full aperture of the system is used, and light coming directly from the illuminated specimen does not enter the microscope as glare. On the other hand, the plane mirror must be of appreciable thickness, as it is quite large, and this will introduce a considerable amount of astigmatism which will need to be corrected by means of additional optical elements.

For this reason, the arrangement shown in Figure 2 is to be preferred. Here a small portion is cut out of the centre of the aperture. The amount of light lost is, however, negligible, and the effect on the image can be shown to be very small.

§4. ABERRATIONS

If it were not for the presence of the vacuum cell window and the half-silvered mirror, the system as shown in Figure 2 would be free from spherical aberration. However, the combined thickness of these two elements cannot well be less than

8 mm. and it can readily be shown that the primary longitudinal spherical aberration introduced by a plate of thickness t and refractive index n is

$$\frac{tu^2}{2n}\left[\frac{1}{n^2}-1\right], \qquad \ldots\ldots(1)$$

where u is the angle of slope of the ray in air. This corresponds to a path difference of

$$\frac{tu^4}{8n}\left[\frac{1}{n^2}-1\right] \qquad \ldots\ldots(2)$$

which, for $t=8$ mm., $n=1{\cdot}5$, $u=0{\cdot}5$ gives a path difference of 0·0232 mm., or 42·5 wavelengths for the green mercury line. This is a gross error and must be corrected.

The spherical aberration thus introduced is of negative sign and could be corrected bv using the spherical mirror with the image somewhat displaced

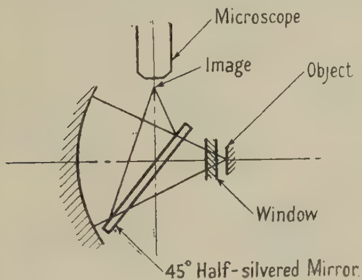

Figure 1.

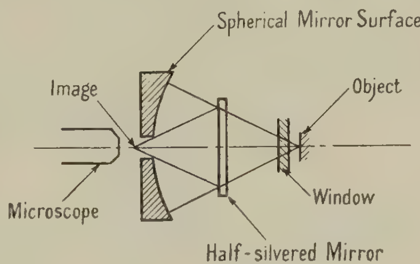

Figure 2.

axially from the centre of curvature. If the radius of curvature be R and the object be displaced by a distance kR from the centre of curvature away from the mirror, the primary longitudinal aberration is given by

$$\frac{Rk^2(1+k)^2}{(1+2k)^4}u^2, \qquad \ldots\ldots(3)$$

where u is the slope of the ray at the image side.

Equating (1) and (3) gives very reasonable ranges of values for k and R, and further investigation shows that, taking into account the next order of spherical aberration, a numerical aperture of 0·54 can be realized.

Unfortunately conditions are not so favourable when off-axis aberrations are considered, as will be done in the next section.

§ 5. OFF-AXIS ABERRATIONS

The off-axis aberrations of this very simple system can be easily discussed with the help of the concept of "aspheric plates" situated at the centres of curvature of the various surfaces. This concept has already been used by Burch (1943) in the design of aspherical systems.

Consider a point P on the axis of the spherical mirror (Figure 3) situated a short distance kR from the centre of curvature. Taking angular coordinates x, y for the ray from the object-point, and restricting the aperture so that x, y can be considered to form a Cartesian system, the path-difference introduced by the spherical aberration will be

$$A(x^2+y^2)^2 \qquad \ldots\ldots(4)$$

where A is a constant which can be calculated with the help of (3).

If, now, another point P′ be considered at an equal distance from the centre of curvature and separated by a small distance from the axis in the plane $y=0$, an auxiliary optical axis can be drawn from this point through the centre of curvature, making an angle θ with the principal optical axis. The spherical aberration figure for this point will be centred on the auxiliary optical axis.

Evidently, the aberrations can be regarded as if caused by an aspheric plate located at the centre of curvature causing a retardation given by (4). The strength of this plate varies, of course, with the distance of the object point from the centre of curvature.

Now, the spherical aberration due to the plane-parallel plates can be regarded in the same way as that due to an aspheric plate, but, as the axis of the plate is

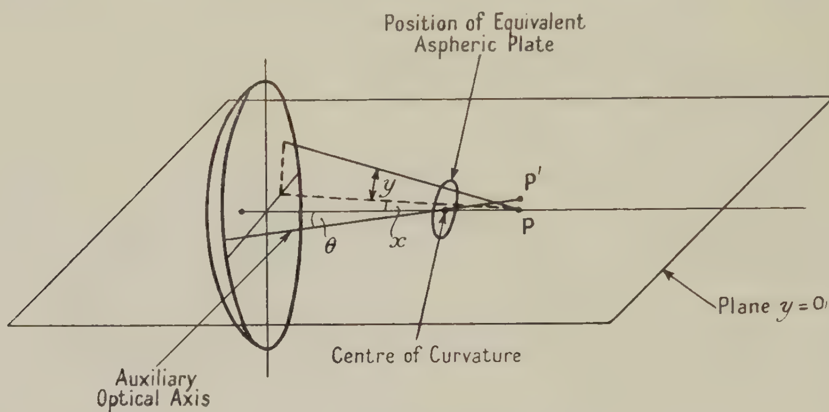

Figure 3.

unchanged in direction as the object-point moves off the axis of the system, this plate is located at infinity. The retardation introduced by this plate may be represented by

$$A'(x^2+y^2)^2. \qquad \ldots\ldots(5)$$

For the spherical aberration to be zero, $A'=-A$. Then for a point distant h from the axis, so that $\theta=h/kR$, the retardation p is the sum of that due to the two plates:

$$p=A\left[\left(x-\frac{h}{kR}\right)^2+y^2\right]^2-A[x^2+y^2]^2.$$

This expression when expanded gives rise to the following terms:

$$\left.\begin{array}{ll} 2A(x^2+y^2)h^2/k^2R^2 & \text{change of focus} \\ -4A(x^2+y^2)hx/kR & \text{coma} \\ Ah^4/k^4R^4 & \text{change of phase} \\ -4Ah^3x/k^3R^3 & \text{lateral shift} \\ 4Ah^2x^2/k^2R^2 & \text{astigmatism} \end{array}\right\}. \qquad \ldots\ldots(6)$$

The most serious of these for small h is the coma term, as this is linear in h. The value of A is found by calculation to be 0·371 and $k=0{\cdot}3$, $R=60$. The greatest path difference in the image is twice the expression given above, since the

expression is odd in x. The limit of the sharp field is given by equating this to the Rayleigh limit:

$$8A(x^2+y^2)\frac{hx}{kR}=\frac{\lambda}{4}, \qquad \ldots\ldots(7)$$

which gives $h=5{\cdot}8$ microns for N.A. $=0{\cdot}5$. This is much too small a field to be useful in a microscope of this nature.

This treatment of the errors brings out the fact that the off-axis errors arise out of the shearing of the equivalent aspheric plates across each other as the object point moves off the axis. This in itself suggests a remedy, for obviously the aspheric plate arising from refraction at the plane-parallel plates can only be satisfactorily cancelled by another plate at a great distance, if only two elements are to be used. This suggests that a surface of very small curvature be used, and it is found that if the surface next to the object of the half-silvered mirror be made slightly convex, a good correction of spherical aberration up to N.A. $=0{\cdot}5$ can be achieved. The dimensions of the resulting system are shown in Figure 4. The nearest aspheric plate is now situated at the centre of curvature of the spherical refracting surface, i.e. over a metre away. Coma is now certainly negligible over a field a millimetre in diameter.

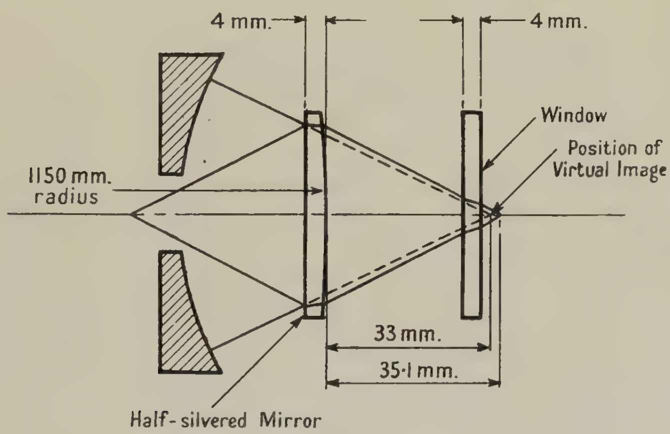

Figure 4.

The virtual image produced is free from spherical aberration and so can be placed at the centre of curvature of the spherical mirror. This does not introduce any coma, since the sine condition is exactly satisfied. The only other troublesome Seidel aberrations are curvature of field and astigmatism.

It will be noted that the simple theory given above is valid so long as the angle θ is small compared with the aperture angle, i.e. for cases where the field radius is small compared with the distance of the object or image from the centre of curvature. It breaks down, however, if the object is at the centre of curvature, and hence the astigmatism must in this case be calculated by other means.

The radius of curvature of the Petzval surface is $R/2$, convex towards the mirror. The sagittal surface is easily seen from elementary considerations to be flat, and hence the tangential surface has a radius of $R/4$, concave towards the mirror. The surface of least confusion has therefore a radius of $R/2$, concave towards the mirror. This unfortunately is of the wrong sign to suit most microscope objectives, but the departure is not serious.

The physical depth of focus is given by $\pm\lambda/2u^2$ where u is the slope of the marginal ray. The distance between tangential and sagittal surfaces for an image height h is given by $2h^2/R$. Equating this to the whole range of depth of focus gives $h^2=\lambda R/2u^2$, or $h=0{\cdot}23$ mm. This is satisfactory for most purposes.

It will be seen from Figure 4 that the total working distance with a 4 mm. window in position is 35·1 mm. Of this, the mounting takes up one or two millimetres, but even so the working distance is sufficient for many purposes.

§ 6. ALIGNMENT OF THE VACUUM WINDOW

It is essential that the window of the vacuum cell be adjusted to be square with the axis of the system. The tolerance can be calculated by equating the coma, calculated from the second expression of (6), to the Rayleigh limit. This gives

$$-\frac{t}{n}\left[\frac{1}{n^2}-1\right]u^3\theta=\frac{\lambda}{4},$$

from which $\theta=0{\cdot}64\times10^{-3}$ radians, or 2·2 minutes of arc. This very high precision demands either levelling screws and an optical device for indicating correct orientation, or integral construction of the microscope and vacuum chamber.

§ 7. ILLUMINATION OF THE SPECIMEN

In the above form the system is only suitable for the examination of translucent objects. The required application, however, calls for vertical illumination of the specimen. An ordinary vertical illuminator cannot be used, for in its two passages through the system the light is attenuated by a factor of 16 due to two reflections and two transmissions at the half-silvered mirror. As a result the image is swamped by glare produced by direct reflection from the back of the objective.

The object could be illuminated by a narrow cone of light reflected from a small 45° mirror cemented to the centre of the half-silvered mirror, without introducing any glare. This is undesirable, however, for due to the smallness of the illuminating cone the specimen shows pronounced interference effects giving rise to spurious structure. Better results would be obtained by a hollow cone surrounding the system, but this would give rise to the need for an undesirably large hole in the side of the vacuum furnace.

The remaining alternative is to intersect the cone of rays converging to the microscope objective with a very thin half-silvered mirror at 45° to the axis, as shown in Figure 5. This reflects into the system a divergent cone formed by a condenser lens and the system forms an image of the light source on the specimen.

As this mirror is situated in a strongly convergent beam it is essential that it be very thin. Fortunately, however, the requirements for its flatness are not very stringent, so this mirror can be a pellicle of collodion. Pellicles of this nature can be prepared only a few microns thick and of sufficient uniformity not to disturb the definition of the system to a perceptible extent. It has been found that if the pellicle be stretched on a frame the surface of which has been ground flat its flatness is sufficient to allow a sharp image of the source to be focused on the specimen.

The pellicle is illuminated by a beam of very high intensity as compared with that from the specimen; its scattering powers must therefore be kept very low.

It has been found possible to achieve very satisfactory results by carefully excluding dust during preparation of the pellicle and by casting it on an optically worked glass surface.

Even when this is done, it is found that glare is still present, for the system forms an image of the light source, after two reflections at the half-silvered mirror and one at the concave mirror, in coincidence with the image of the specimen.

However, the cone of light forming this image is hollow, because of the hole in the concave mirror. If the specimen be displaced a distance of about 1·5 mm. along the axis of the system, the image of the light source is separated axially by 3 mm. from the image of the specimen, while still keeping the light source sharply focused on the specimen. If the viewing microscope be focused on the image of the specimen, the image of the light source is out of focus to such an extent that all except the central hole in the beam is outside the field. The specimen is thus viewed, as it were, through the hole in the illuminating beam. If these precautions be taken, together with the obvious one of carefully blackening the internal surfaces of the mount, an excellent view of the object is seen, comparable in every way with that obtained in a metallurgical microscope.

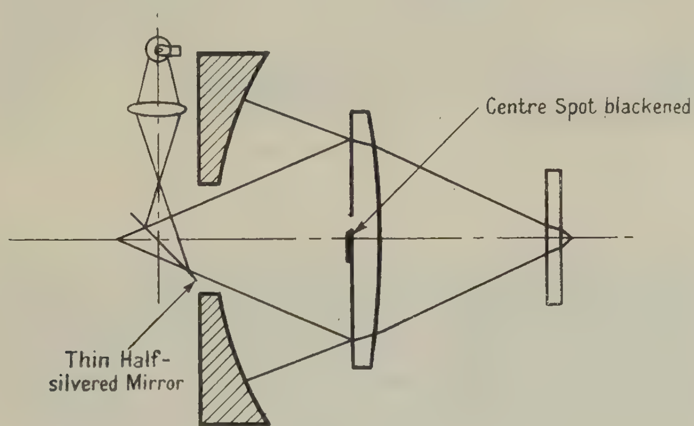

Figure 5.

The above step of displacing the image axially from the centre of curvature of the mirror will, of course, introduce spherical aberration. This can be corrected by slightly increasing the thickness of the window of the vacuum cell or of the half-silvered mirror, but coma is introduced once more; a calculation on the lines of that above shows that it reaches the Rayleigh limit at a field diameter of about 0·036 mm. If the doubled Rayleigh limit be allowed, the field diameter is 0·072 mm., which is just usable at high magnifications if interest is concentrated at the centre of the field. The microscope has actually been used satisfactorily in this form.

It is desirable, however, to be able to correct the spherical aberration without introducing coma. From the discussion above it is evident that this can only be done satisfactorily without too many additional elements by using spherical surfaces concentric with the concave mirror.

As the sign of the aberration to be corrected is positive, this can be done by using a meniscus lens both surfaces of which are concentric with the mirror. This expedient has been used for various purposes by several workers (Burch

1947, Hawkins and Linfoot 1945, British Patent 1944). As there is little room for this lens in the system, it can most conveniently be introduced on the opposite side of the microscope objective, concentric with the image of the centre of curvature of the concave mirror. The system is then as shown in Figure 6. The proportions of the correcting lens are best determined by trial and error, as trigonometrical tracing is very simple and quick with this type of lens.

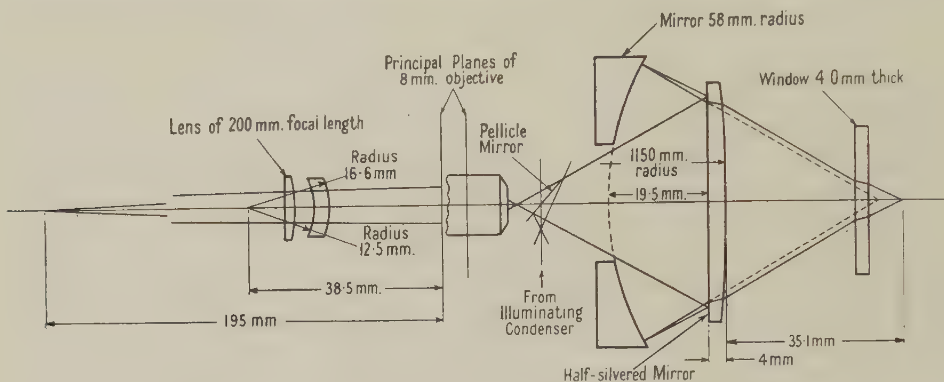

Figure 6. Refractive index of meniscus lens taken as 1·530.

To maintain the effective tube-length at which the objective is working at the correct value, it is convenient to introduce a positive lens after the meniscus lens as shown. The aberrations introduced by this are negligible.

Chromatic Aberration

A certain amount of chromatic aberration is introduced by the plates in the system and is aggravated by the meniscus lens. It is found experimentally that if a mercury lamp is used and an Ilford "Iso" filter is used to cut out the blue lines, the green and yellow lines can be used together satisfactorily. If, however, it is desired to use white light the aberration can be corrected by making the positive lens shown in Figure 6 into a doublet.

§ 8. PERFORMANCE

A model of this system without the meniscus lens has been made up and tested. The concave mirror consisted of the concave surface of the flint member of an achromatic doublet and was slightly astigmatic. In spite of this, however, the photographs shown in Figures 7 and 8 were obtained (see Plate I). Figure 7 is of an electron microscope specimen grid (× 250) stuck to a glass plate and illuminated by transmission. As the grid was of appreciable thickness it was not possible to focus the edges, but small particles may be detected in the clear spaces down to about 0·5 micron diameter, which is equal to the theoretical resolving power of an objective of 0·5 N.A. (The N.A. of this objective was actually about 0·45.)

Figure 8 is of an etched steel specimen, viewed with vertical illumination, showing the pearlite pattern (× 500). Here the resolution is not much below the theoretical value.

These photographs were taken by the light of a B.T.H. compact source mercury vapour lamp of 250 watts rating with an Ilford "Iso" filter. Exposures were 5 seconds on Ilford Special Rapid Panchromatic plate for Figure 7 and

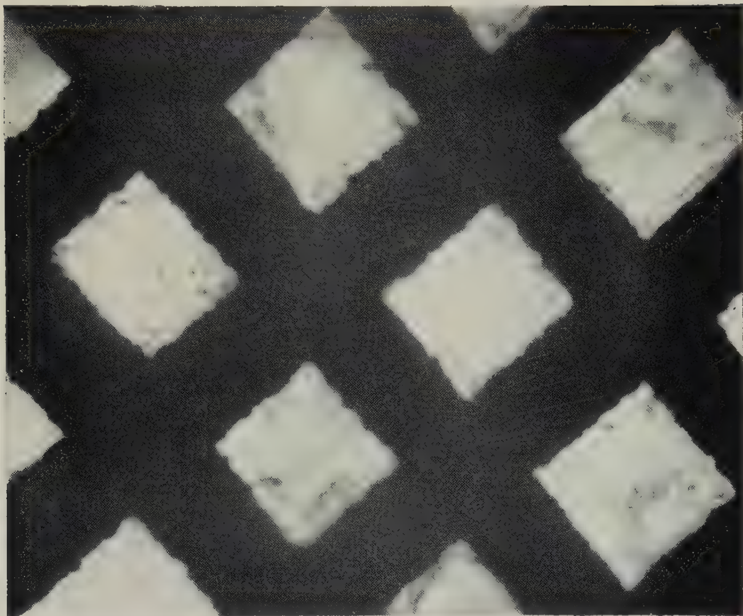

Figure 7. Copper grid (200 mesh) cemented to glass and viewed by transmission. (250×)

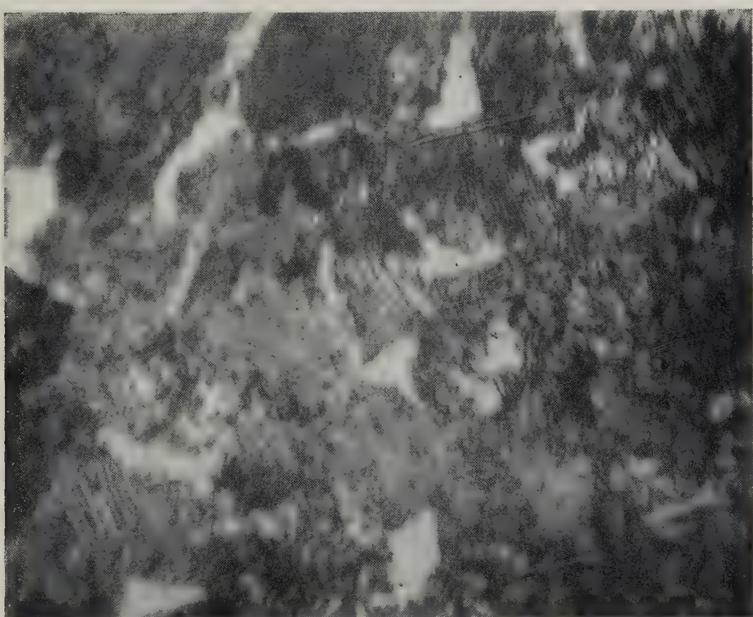

Figure 8. Pearlite structure in steel specimen. (500×)

Plate I.

To face page 572

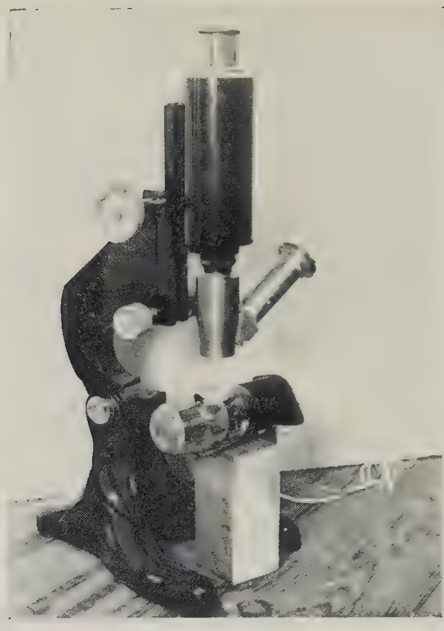

Figure 10. System with N.A. of 0·2 mounted on Beck microscope.

Figure 11. Heater wires of rectifier valve photographed in their own radiation.

Plate II.

30 seconds on Ilford H.P. 3 plate for Figure 8. In the latter case the pellicle was used without aluminizing; with a good half-reflecting coating the exposure required should be reduced by a factor of at least 2·5.

With vertical illumination the contrast was good and compared very favourably with that obtained with a conventional vertical illuminator in the usual way.

§ 9. FURTHER APPLICATIONS

There are a number of applications other than the above where a long working distance is desirable. These include carrying out of dissection of biological specimens under the microscope, examination of the surface finish of metals by inspecting the shadow of a straight edge thrown on the surface, and examination of any object inside an enclosure. For some of these applications it is not necessary to have such a long working distance as in the example quoted above. An example has been worked out giving a working distance of 12·8 mm. The system is in this case small enough to mount in a normal microscope. Dimensions are shown in Figure 9. If vertical illumination is not required, the hole in the concave mirror can be made quite small.

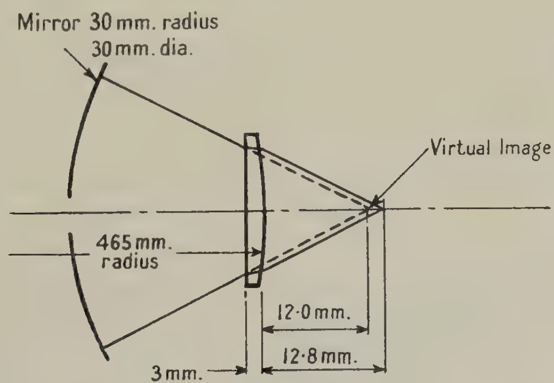

Figure 9.

Another system has been constructed with a N.A. of 0·2 and a working distance of 34·0 mm. This is shown in Figure 10 (see Plate II) mounted on a Beck microscope with the stage removed. Vertical illumination in this case is supplied by a small lamp and lens in the side tube, and the light is directed to the object via a small prism cemented to the centre of the half-silvered mirror. This method is suitable for many applications, such as the inspection of the electrodes of radio valves.

Figure 11 is a photograph of the heater wires of a rectifier valve, taken with the system shown in Figure 10. Vertical illumination was not used in this case, the hot wires being photographed in the light of their own radiation. A series of small cracks is visible on the surface of the left-hand wire just as it enters the cathode sheath. These were not visible when the heater was cold.

In this case the glass envelope of the valve acts as a cylindrical lens and introduces a considerable amount of astigmatism. This was eliminated by introducing two plane-parallel glass plates about 1 mm. thick into the light path between valve and objective, and tilting them symmetrically in opposite directions

about an axis parallel to that of the valve. This introduces a compensating degree of astigmatism.

The reason for using two such plates is that one plate will also introduce coma. The second plate introduces an equal amount of coma of opposite sign, but the astigmatism produced by each plate is of the same sign. These plates are not shown in Figure 10.

Another application where a similar principle can be used is in the examination of "nuclear plates". It is sometimes desired to examine the interior of a very thick emulsion through the glass of the plate, and inconvenience is caused by the short working distance of normal objectives. However, the system illustrated

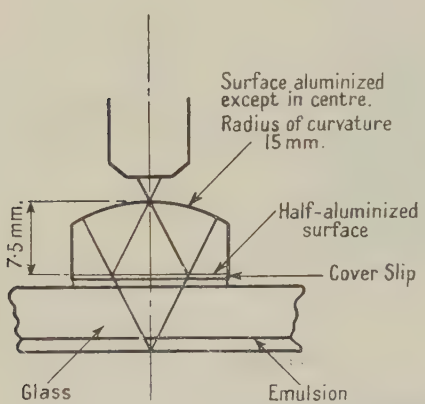

Figure 12.

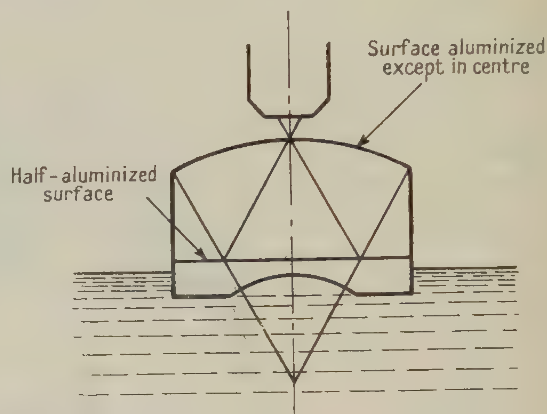

Figure 13.

in Figure 12 can be used. The mirror system is constructed as a solid glass block with its outside surfaces aluminized. A thin cover slip is cemented on to the front surface to protect the aluminizing and the space between the cover slip and the glass of the plate is filled with immersion oil.

In this case there is no plane-parallel plate to cause spherical aberration, and the object can be placed at the centre of curvature of the spherical mirror. The image is practically coincident with the rear surface of the block, so that chromatic aberration is very small. If desired, the central part of the rear surface can be worked to a curvature suitable for matching the field curvature to that of the microscope objective. Owing to the near coincidence of the image with this surface this expedient prevents the introduction of troublesome oblique aberrations.

A numerical aperture of 0·75 can easily be achieved, so that a 4 mm. objective is suitable for use with this system. In view of the very small size of the system it can be mounted directly on the tip of the objective or built integrally with it. A working distance of about 7 mm. is attainable with the dimensions shown.

For some biological applications a "water immersion" system may be desirable, for such purposes as observing aquatic life when it is not desired to restrict the volume of water surrounding the specimen. A system for doing this is shown in Figure 13. This is generally similar to the last, save that to overcome the difficulty of refraction at the glass–water surface the front face is made spherical with the centre of curvature at the object. If a glass such as a borosilicate crown,

whose refractive index is sensibly proportional to that of water throughout most of the spectrum, be used, chromatic difference of both focus and magnification is avoided. A numerical aperture of about 0·67 can be attained readily.

The concave front surface of the glass block will, of course, tend to trap a bubble of air when lowered into the water, but this may be removed by means of a small bent pipette.

§ 10. CONCLUSIONS

An optical system has been described which, used in conjunction with a microscope of conventional optical design, enables the examination under powers of the order of 500 of specimens which would normally be inaccessible due to enclosure in a vacuum chamber or under other conditions requiring a large clearance between the specimen and the nearest optical element. The aberrations of this system have been discussed and shown to be satisfactory for the use of powers of this order.

The system is constructed throughout of elements having spherical or flat surfaces and thus avoids the difficulties in construction due to the use of non-spherical surfaces. The price paid for this simplicity is the loss of three-quarters of the available light because of the use of a half-silvered mirror and, in the case where vertical illumination is essential, the introduction of a small amount of spurious detail. This arises due to the necessity for a large hole in the spherical mirror. This does not adversely affect the resolution, but gives rise to the appearance of false diffraction effects. Thus, in the case of an object consisting of parallel equidistant lines, a second set of faint lines may appear midway between them. This effect is not obtrusive, however, and is in many cases acceptable in view of the increased working distance obtained.

If vertical illumination is not required the hole in the mirror may be made very much smaller and the objection disappears.

A smaller scale version of the system is suitable for objects which are not enclosed in a chamber and, giving a working distance of about half-an-inch, is small enough to be used in a conventional microscope.

"Immersion" objectives using the same principle are suitable for the examination of nuclear plates or for examination of biological material under several millimetres of water.

ACKNOWLEDGMENT

The author wishes to express thanks to Dr. T. E. Allibone, for permission to publish this article.

REFERENCES

Bouwers, A., 1946, *Achievements in Optics* (Amsterdam : Elsevier Publishing Co. Ltd.).
Burch, C. R., 1943, *Proc. Phys. Soc.*, **55**, 433 ; 1947, *Ibid.*, **59**, 41.
British Patent 1944, No. 586851 (B.T.H. Co. and J. Dyson).
Hawkins, D. S., and Linfoot, E. H., 1945, *Mon. Not. R. Astr. Soc.*, **105**, 334.

The Optical Constants of Thin Metallic Films

BY R. WEALE*
S.W. Essex Technical College, London, E.17

Communicated by H. Lowery ; MS. received 13th April 1949

ABSTRACT. The optical constants of thin films are shown to depend on the thickness of the films due to the variation of the electrical conductivity with thickness. Good and bad conductors both exhibit maxima in the curves relating absorption coefficient and film thickness : in the two groups these peaks are due to two entirely different causes. The mean free paths of the conducting electrons are calculated from data found in the literature.

POGÁNY (1916), Haringhuizen, Was and Kruithof (1937), Planck (1914), and others have investigated the optical properties of thin metallic films as functions of the film thickness D, and have observed maxima in the curves relating the absorption coefficient nk with D for small values of D. It will be recalled that the optical properties are linked with the electrical by the formulae due to Mott and Zener (1934):

$$\left.\begin{aligned} n^2-k^2&=1-\frac{4\pi N\boldsymbol{e}^2/\boldsymbol{m}}{\omega^2+\nu^2}, \\ 2nk&=4\pi N\boldsymbol{e}^2\frac{\nu}{\omega}\frac{1}{\omega^2+\nu^2}, \end{aligned}\right\} \qquad \ldots\ldots(1)$$

where n is the refractive index, k the extinction coefficient, N the number of free electrons per cm^3, $\boldsymbol{e}$ and $\boldsymbol{m}$ the electronic charge and mass respectively, $\omega=2\pi\boldsymbol{c}/\lambda$, where $\boldsymbol{c}$ is the velocity of light, and λ its wavelength. ν is half the frequency of relaxation, related to the resistivity by

$$\rho=\frac{\boldsymbol{m}}{N\boldsymbol{e}^2}\nu. \qquad \ldots\ldots(2)$$

It is assumed that the conductivity σ_F of the film is connected with that of the metal σ_B by an expression of the form

$$\sigma_F/\sigma_B=R=f(D/l), \qquad \ldots\ldots(3)$$

where l is the mean free path of the electrons in the bulk metal. R will be less than unity. It follows from (2) that the expressions (1) are to be corrected by means of (3). When this is done, and these expressions are differentiated with respect to D, it will be found that

$$\frac{d}{dD}(n^2-k^2)=-2a\frac{\nu_B^2}{[\omega^2R^2+\nu_B^2]^2}R\frac{dR}{dD}, \qquad \ldots\ldots(4)$$

$$\frac{d}{dD}(2nk)=-\frac{a\nu_B}{\omega}\frac{\omega^2R^2-\nu_B^2}{[\omega^2R^2+\nu_B^2]^2}\frac{dR}{dD}, \qquad \ldots\ldots(5)$$

where $a=4\pi N\boldsymbol{e}^2/\boldsymbol{m}$.

* Now at the Vision Research Unit, Institute of Ophthalmology, Judd St., London, W.C.1.

It will be seen below that dR/dD can never be zero. Therefore n^2-k^2 plotted as a function of D will not exhibit any extremum. Expression (5), on the other hand, will be zero when

$$R=\frac{\nu_B}{\omega}=\frac{\lambda}{\lambda_\tau}, \qquad \ldots\ldots(6)$$

since $\nu_B=2\pi c/\lambda_\tau$.

Gold and silver have extremely large values of $\lambda_\tau(\simeq 160\mu)$, and it is clear that, at least in the visible part of the spectrum, these metals should show nk curves without any extremum whatever. Poorer conductors should exhibit a maximum in the nk curve but none in the graph relating n^2-k^2 to D. This has actually been observed by Pogány for platinum and palladium.

Now λ_τ for platinum and palladium is $9{\cdot}5\,\mu$ if one free electron per atom is assumed. R can be calculated from the wavelength of light used in the experiment. When substituted in Lovell's (1936) expression

$$R=(D/l)\,[1+\ln D/l], \qquad \ldots\ldots(7)$$

values for R yield data for l when the appropriate measurement for D is used. These results for l are given in column A of the Table.

Values of l

	A	B	C	D	E
Pt	5×10^{-5}	$1{\cdot}9\times10^{-5}$	$1{\cdot}1\times10^{-6}$	$2{\cdot}59\times10^{-6}$	$8{\cdot}8\times10^{-7}$
Pd	5×10^{-5}	$1{\cdot}9\times10^{-5}$	2×10^{-6}	—	$8{\cdot}93\times10^{-7}$
Au	—	—	$6{\cdot}32\times10^{-6}$	—	$4{\cdot}51\times10^{-6}$
Ag	—	—	$3{\cdot}2\times10^{-6}$	$8{\cdot}3\times10^{-6}$	$6{\cdot}25\times10^{-6}$
Cu	—	—	—	$5{\cdot}65\times10^{-6}$	$4{\cdot}6\times10^{-6}$

A, from equations (6) and (7) ; B, from equations (6) and (8) ; C, from Pogány's measurements ; D, from Riede's measurements ; E, from equation (10).

When deriving an expression in a manner similar to that used by Thomson (1901), the writer found for $D<l$

$$R=(2/\pi)\{\tfrac{1}{2}\cos\phi\ln(\sec\phi+\tan\phi)-1/(\sec\phi+\tan\phi)+\pi/2-\phi\} \qquad \ldots\ldots(8)$$

where $\phi=\cos^{-1}D/l$, and for $D>l$

$$R=1-l/\pi D. \qquad \ldots\ldots(9)$$

The values obtained for l from (6) and (8) are shown in column B. Also using (9) to calculate l from Pogány's and Riede's (1914) resistivity measurements when $D>l$, the writer obtained approximate values given in columns C and D respectively. The values for copper, silver and gold are shown for purposes of comparison; l is given in centimetres. It should be stated in this connection that equation (9) becomes equivalent to Planck's empirical expression when $D\gg l$; the writer (1949) derived the latter by a less rigorous method. It will be noted that the former constant of proportionality $4/\pi$ is replaced by $1/\pi$; Thomson's value is $1/4$.

Finally, column E contains values for l calculated from the expressions

$$\left.\begin{aligned} \boldsymbol{h}&=(8\pi/3)^{\frac{1}{3}}N^{\frac{2}{3}}\boldsymbol{e}^2\bar{\lambda}\rho, \\ \text{and}\qquad \bar{\lambda}^2&=2l^2, \end{aligned}\right\} \qquad \ldots\ldots(10)$$

where $\boldsymbol{h}$ is Planck's constant of action. Again, the assumption is made that there is one free electron per atom.

It is seen that the film thicknesses are too great for Lovell's expression to be strictly applicable; it will be recalled that it is valid for very thin films only. The disagreement between columns B and C is not due to anything but the substitution of λ_τ in equation (6). Mott and Jones (1936) have made it quite clear that, in order to explain the optical constants of metals in the visible, it is necessary to assume D.C. resistivities as much as ten times the accepted values. If this is done the values for R become correspondingly larger. They will yield larger values for $D\,l$; the values for l obtained are now in good agreement with those in column C. Riede's results are in better agreement with those given in column E: the latter are somewhat low because N has been assumed to be equal to the number of atoms per cm^3.

There arises this question: why do both gold and silver exhibit extrema not only in the curves for nk but also in those for n^2-k^2? The answer is to be found in a paper by Blackman (1934). He shows in connection with thin films that also when k is large interference effects will take place, and give rise to a double bend in the curve connecting the reflectivity of the film with its thickness. Such a double bend will, of course, find its counterparts in the corresponding curves for n^2-k^2 and nk. Since both gold and silver exhibit rapidly increasing values of k as the red parts of the spectrum are approached, these extrema should be observed. Further, as the bend in the n^2-k^2 curve is the flatter of the two, it may escape the attention of those who work, say, only at about $0{\cdot}5\,\mu$. It is evident that this fact makes it possible to differentiate between the nk maximum due to the increased resistivity and that due to interference. The former will become flatter in the near infra-red, because as R is increased dR/dD becomes less. The latter, however, becomes more pronounced as k increases when the wavelength is increased. This has been demonstrated by Pogány.

It is thus apparent that good and relatively poor conductors will exhibit maxima in the nk curves at very small film thicknesses, but their respective causes are entirely different. The confusion which exists in the interpretation of the data obtained by the authors mentioned at the beginning is solely due to that fact.

REFERENCES

Blackman, M., 1934, *Phil. Mag.*, **18**, 262.
Haringhuizen, P. J., Was, D. A., and Kruithof, A. M., 1937, *Physica*, **4**, 695.
Lovell, B., 1936, *Proc. Roy. Soc.* A, **157**, 311.
Mott, N. F., and Jones, H., 1936, *Theory of the Properties of Metal Alloys* (Oxford: Clarendon Press), Chapter 3.
Mott, N. F., and Zener, F., 1934, *Proc. Camb. Phil. Soc.*, **30**, 249.
Planck, W., 1914, *Phys. Z.*, **5**, 563.
Pogány, B., 1916, *Ann. Phys., Lpz.*, **49**, 531.
Riede, A., 1914, *Ann. Phys., Lpz.*, **45**, 563.
Thomson, J. J., 1901, *Proc. Camb. Phil. Soc.*, **11**, 120.
Weale, R., 1949, *Proc. Phys. Soc.* A, **62**, 135.

The Displacement–Frequency Characteristic of Elastically Coupled Mechanical Systems with Two Degrees of Freedom

By D. H. PEIRSON*
Royal Aircraft Establishment, Farnborough

MS. received 9th February 1948, and in amended form 3rd March 1949

ABSTRACT. The displacement–frequency characteristic of elastically coupled mechanical systems with two degrees of freedom is calculated. Conditions are obtained for independence of deflection and frequency. The practicability of these conditions is considered and a determination made of the extent of the range for displacement independent of frequency.

The relations between the fundamental constants of the systems are illustrated graphically and the application to galvanometer and accelerometer design is discussed.

§ 1. INTRODUCTION

The response of elastically coupled systems of two degrees of freedom to a force of constant amplitude has been theoretically investigated by Den Hartog (1940), with particular reference to application as a vibration absorber. In the present paper the treatment is extended to include the effect of damping in both systems, the displacement–frequency and phase–frequency relations being expressed as functions of non-dimensional quantities. The conditions obtained for independence, to a required accuracy, of displacement and frequency establish relations between the mass, damping and natural frequency of the two systems.

§ 2. THE MECHANICAL SYSTEMS

The coupled systems, referred to by suffixes 1, 2 are illustrated schematically in Figure 1. The constants of the two systems are: mass m_1, m_2, damping

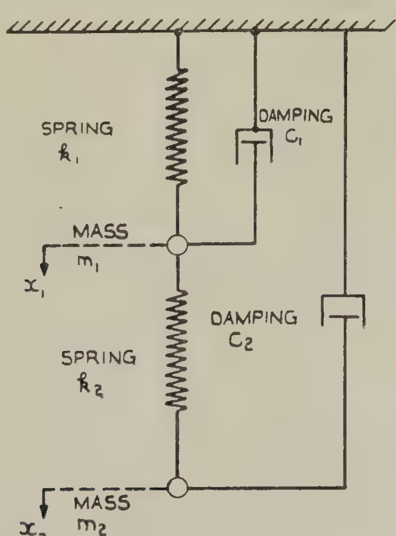

Figure 1. Definition of coupled systems.

coefficient (assuming velocity damping) c_1, c_2, spring constant (restoring force per unit displacement) k_1, k_2. The masses and spring constants are combined to

* Now at Atomic Energy Research Establishment, Harwell.

determine the natural angular frequencies ω_1, ω_2 of the two systems, considered separately. $\delta = \omega_2/\omega_1$; $\mu = m_2/m_1$.

The damping factors may be expressed as the non-dimensional quantities α_1, α_2, where these quantities represent the ratio of each damping coefficient to the coefficient for critical damping in the particular system. Critical damping defines the condition when the transient motion of a system changes from an oscillatory to a non-oscillatory type.

Equations of Motion. The mass m_1 is excited by a periodic force of amplitude F_0 and angular frequency ω producing displacements x_1 and x_2 of the masses m_1 and m_2 from the equilibrium positions. The simultaneous equations of motion in x_1 and x_2, with coupling terms due to the restoring action of the spring k_2, are solved for the amplitude x_2 in terms of the non-dimensional quantity $\beta = \omega/\omega_1$.

The damping terms in the equations involve the absolute and not the relative velocities of the masses, implying that the equivalent damping forces are external and associated with the movement of the masses and not internal and associated with that of the springs.

§3. RELATION BETWEEN DISPLACEMENT AND FREQUENCY

The expression relating displacement and frequency (see Appendix) involves the quantities, δ, μ, α_1 and α_2. The non-dimensional character of the equation is preserved by writing the displacement as y, the ratio of x_2 to F_0/k_1 the static displacement (i.e. displacement at zero frequency). The nature of the displacement–frequency curve is illustrated schematically in Figure 2 showing in the general case two maxima in the relevant positive section of the curve.

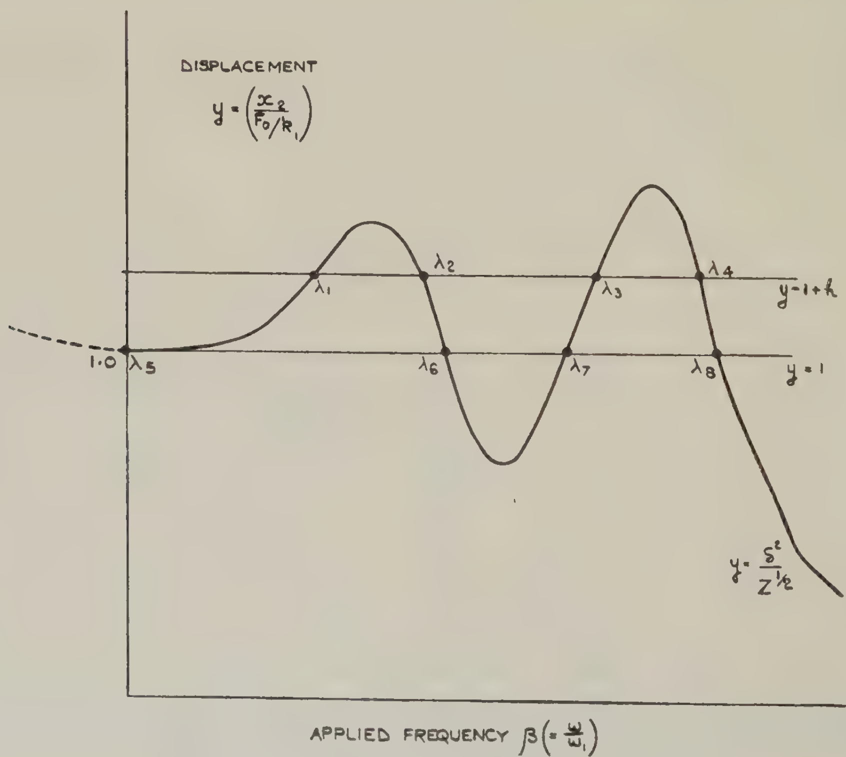

Figure 2. General displacement–frequency curve.

(i) *Conditions for Independence of Displacement and Frequency*

For independence of displacement and frequency y must lie between the values 1 and $1+h$ over a frequency range from zero ($\beta=0$) to a value to be determined, which includes the two maxima.

This restriction is applied by considering, in Figure 2, the conditions that (i) the straight line $y=1+h$ shall be tangential to the positive section of the curve at two points; (ii) the straight line $y=1$ shall be tangential to the positive section of the curve at one point. It follows that the limit of y independent of β is given by the non-tangential intersection (λ_8) of $y=1$ with the curve.

These three tangency conditions determine the relations between the four quantities δ, μ, α_1, α_2. These relations may be plotted for $h=0{\cdot}05$ using α_2 (from 0 to 1·0) as independent variable. The variation of δ and λ_8 with α_2 is shown in Figures 3 and 4.

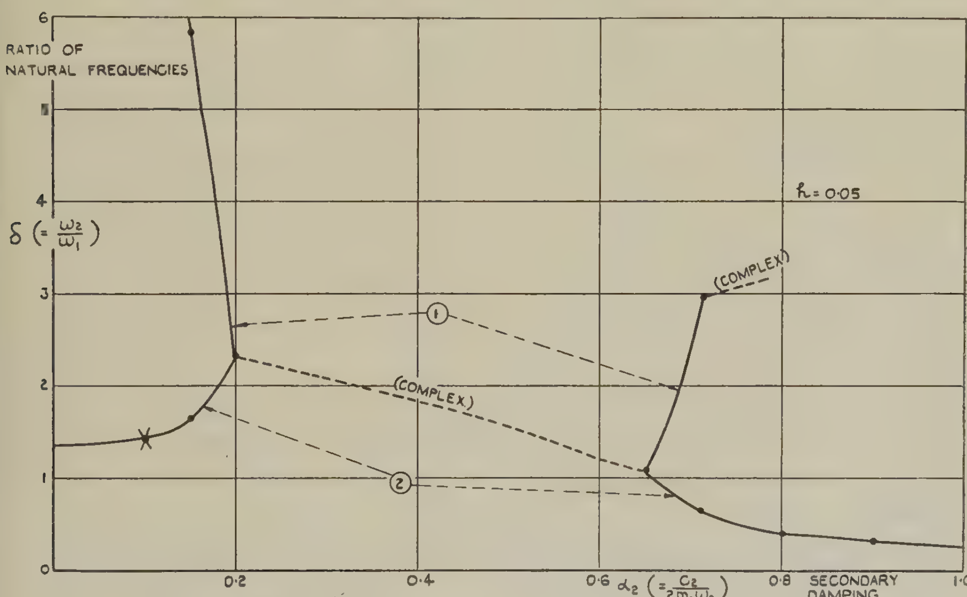

Figure 3. Curve of natural frequency ratio and secondary damping.

Inspection of these graphs shows two real branches (1 and 2) in the positive quadrant interrupted by an intermediate complex region extending from $\alpha_2=0{\cdot}20$ to 0·65. From practical considerations the most useful portion of the curve is that of branch 2 for values of α_2 less than 0·20.

(ii) *Single Degree of Freedom*

A comparison may be obtained with a system having a single degree of freedom by considering the case when $\mu=0$ and $\delta=\infty$ (i.e. $m_2=0$, $\omega_2=\infty$). The expression for y degenerates into one involving β and α_1 and it is found that the tangency condition is satisfied by a unique value of α_1. Then, the limit of displacement independent of frequency may be compared, as in Figure 6, with that of the corresponding case for two degrees of freedom. Thus for a possible practical value of $\alpha_2=0{\cdot}1$ in the two-degree case, it is found that for a given sensitivity or static deflection F_0/k_1 the range of frequency for which displacement

is independent of frequency (maximum deviation $+5\%$) is greater in the double system compared with the corresponding single system by a factor of 1·96.

Conversely, for a given range of independence the sensitivity of a double system is 3·85 times greater than that of the corresponding single system.

(iii) *Phase–Frequency Relation*

The expression for the phase angle ϕ_2 as a function of β follows from the solution of the equations of motion. No attempt is made here to determine the conditions limiting phase distortion (departure from linearity in the (ϕ_2, β) characteristic) to an arbitrary figure. Instead Figure 5 shows a graph of this function for $\alpha_2 = 0{\cdot}1$,

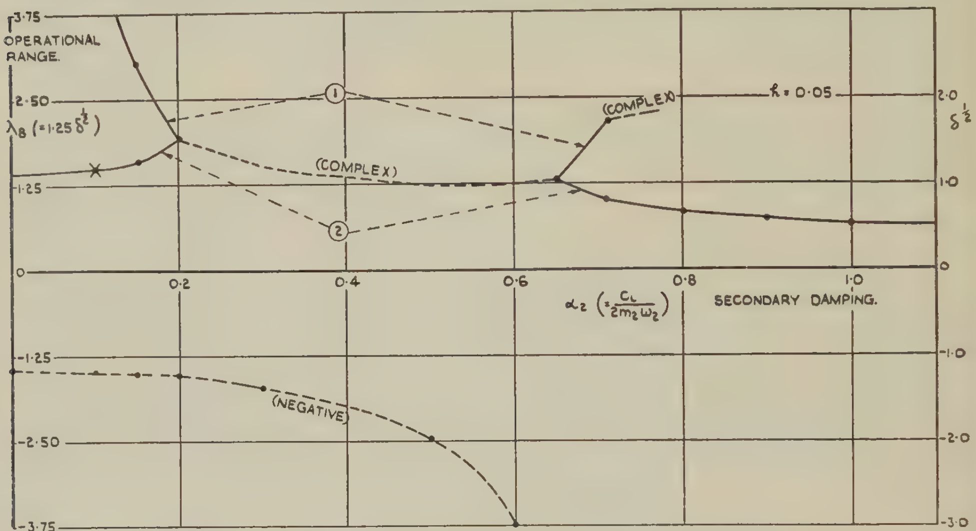

Figure 4. Curve of operational range and secondary damping.

and δ, μ and α_1 derived from branch 2 of Figures 3 and 4. On the same graph is shown for comparison a phase–frequency curve of the corresponding single system under the condition of optimum phase linearity ($\alpha_1 = 0{\cdot}6$) usually accepted as a practical standard. It is noted that in the phase curve for the double systems ϕ_2 is no longer equal to $-\pi/2$ for $\beta = 1$, and that reasonable linearity exists over the operational range defined from Figure 6.

§4. PRACTICAL CONSIDERATIONS

The aim of a theoretical investigation of coupled mechanical systems is to establish that such systems, under certain conditions and within certain limits, may be used as measuring devices.

(i) *Application in Galvanometer Design*

It is suggested that the properties of coupled systems may be used to improve the performance of the mirror type galvanometer. The galvanometer coil, suspension and fluid or electrical damping shall form the first system in the conventional manner. To form the second system the mirror shall be elastically mounted on the coil. For convenience in design, no additional damping shall be used in the second system.

An equivalent value of α_2 may be obtained experimentally, by the logarithmic decrement method, and the corresponding values of δ, μ and α_1 computed. The

effective mass of the mirror and the spring in the second system may be adjusted to satisfy the values of δ and μ: the damping in the first system may be adjusted to satisfy α_1.

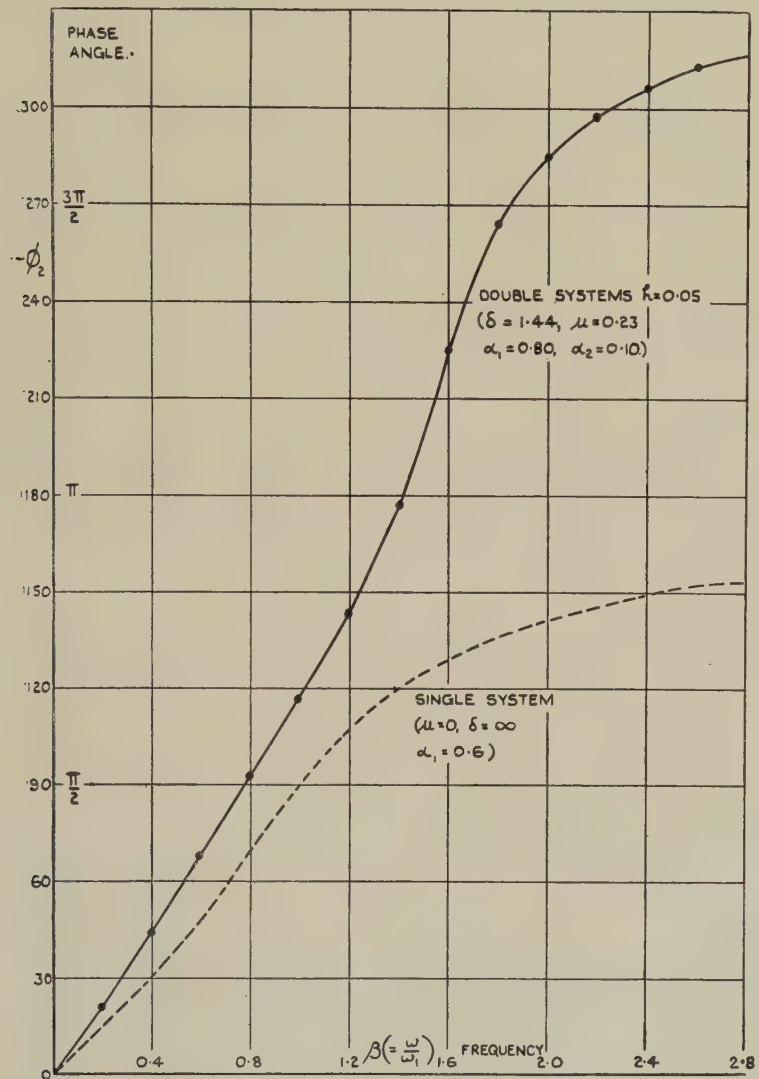

Figure 5. Curve of phase angle and frequency.

In practice the value of α_2 will lie about 0·1 and the curve of Figure 6 has been computed for $\alpha_2 = 0{\cdot}1$ and values δ, μ and α_1 determined from Figures 3 and 4 to illustrate the response of the coupled systems as described. The response $(h = 0{\cdot}05)$ of a single system is shown for comparison. The increased sharpness of "cut-off" in the double system is of practical importance.

(ii) *Application in Accelerometer Design*

It is not intended here to develop fully the theory of the accelerometer application. In this device the acceleration imposes a force upon each mass,

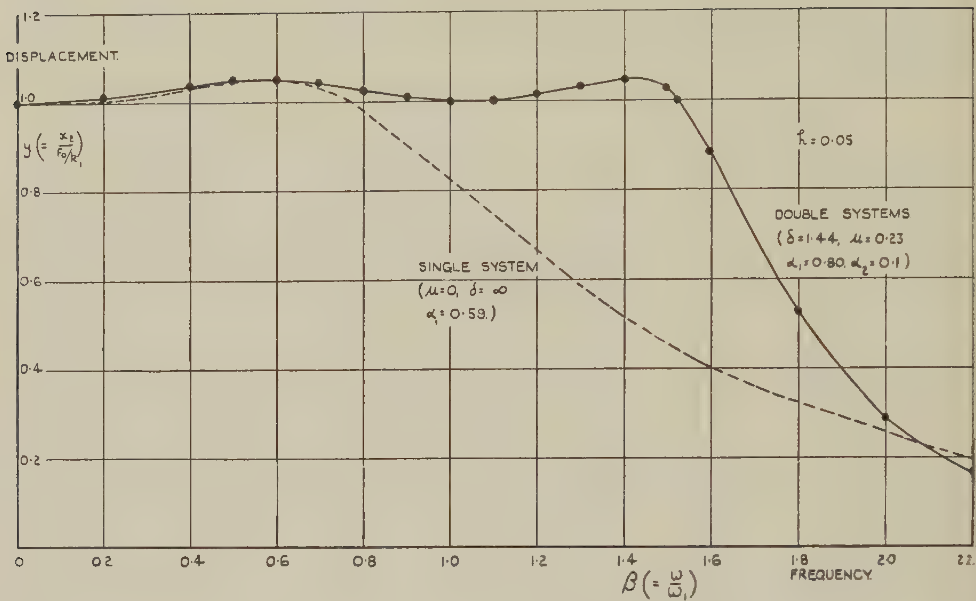

Figure 6. Curve of displacement and frequency.

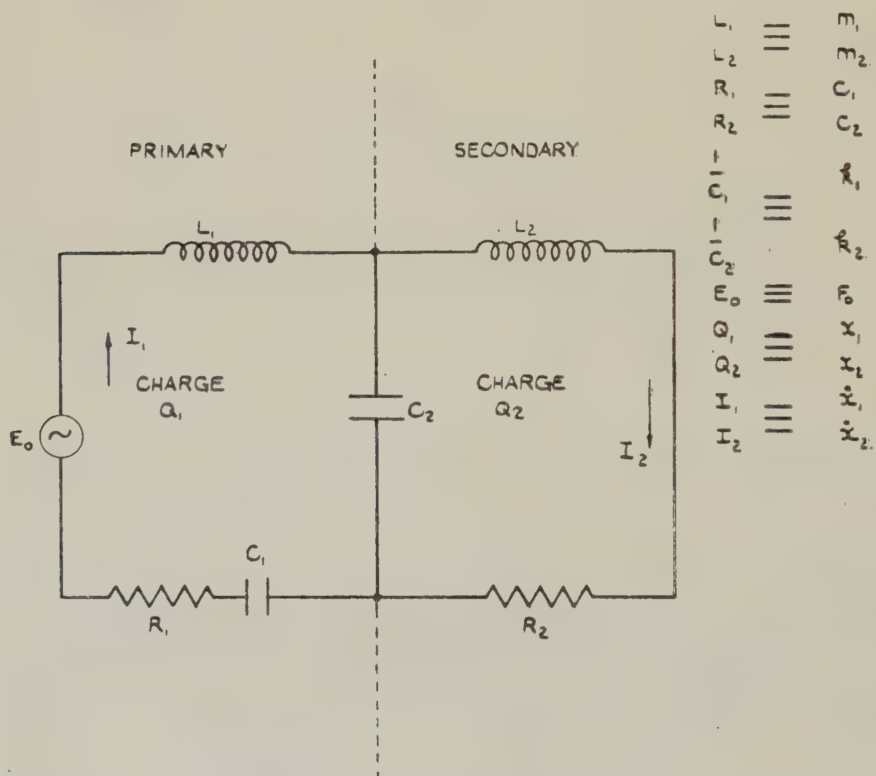

Figure 7. Equivalent electrical circuit. 'Galvanometer' case.

thus modifying the initial equations of motion. The practicability of the application may be investigated by obtaining as before the curves connecting the four parameters. When the accelerometer masses are enclosed in the same damping medium, the behaviour of δ, μ, α_1 and α_2 is governed by a fourth condition, $c_1 = c_2$, i.e. $\alpha_1 = \alpha_2 \mu \delta$.

(iii) *Electrical Analogy*

It is interesting to consider the electrical equivalent of the coupled mechanical systems as defined in §2. Figure 7 shows the analogous electrical circuit and indicates the equivalence of the electrical and mechanical properties.

It is suggested that the electrical method provides a rapid means of verifying experimentally the graphical results obtained in this paper.

§5. CONCLUSIONS

The results obtained from this theoretical investigation demonstrate that the addition of a secondary system to a single degree of freedom system will modify the response to an impressed force of the systems in a manner that is convenient for calculation.

Further, by imposing certain conditions upon the systems the performance as a measuring device may be enhanced. The improvement is obtained as an increase in sensitivity of response for a given operational range of frequency or, alternatively, as an increase in operational range for a given sensitivity.

ACKNOWLEDGMENTS

This paper is published with the permission of the Chief Scientist, Ministry of Supply, and of the Controller, H.M. Stationery Office.

APPENDIX

Key to notation. Suffixes 1 and 2 refer to first and second systems respectively.

m_1, m_2 = mass
c_1, c_2 = coefficient of damping
k_1, k_2 = spring constant
ω_1, ω_2 = natural angular frequency = $\sqrt{(k_1/m_1)}, \sqrt{(k_2/m_2)}$
α_1, α_2 = ratio of damping coefficient to coefficient for critical damping
$= c_1/2\sqrt{(k_1 m_1)}, c_2/2\sqrt{k_2 m_2})$
x_1, x_2 = displacement of mass from equilibrium position
$\delta = \omega_2/\omega_1 \qquad \mu = m_2/m_1$
F_0 = amplitude, ω = angular frequency, of impressed force
$\beta = \omega/\omega_1 \qquad y = |x_2|/(F_0/k_1)$
ϕ_2 = phase angle between impressed force and x_2
h = maximum *increase* from unity of y
λ_8 = upper limit of y independent of β, to variation not more than $(100h)$ %.

Mathematical theory. Consider the arrangement defined in Figure 1 and §2. The mass m_1 is excited by a force $F_0 e^{j\omega t}$; let the displacements of m_1 and m_2 respectively be x_1 and x_2. The simultaneous equations of motion for the systems are

$$m_1 \ddot{x}_1 + c_1 \dot{x}_1 + k_1 x_1 + k_2 (x_1 - x_2) = F_0 e^{j\omega t},$$
$$m_2 \ddot{x}_2 + c_2 \dot{x}_2 + k_2 (x_2 - x_1) = 0.$$

Assuming that the solutions are of the form $x_1 e^{j\omega t}$ and $x_2 e^{j\omega t}$, then

$$(-\omega^2 m_1 + j\omega c_1 + k_1 + k_2)x_1 - k_2 x_2 = F_0,$$
$$(-\omega^2 m_2 + j\omega c_2 + k_2)x_2 - k_2 x_1 = 0.$$

Rewriting in terms of α_1, α_2, δ, μ, eliminating x_1 and separating real and imaginary parts, we obtain

$$\left\{(1+\mu\delta^2-\beta^2)\left(1-\frac{\beta^2}{\delta^2}\right)-4\frac{\beta^2\alpha_1\alpha_2}{\delta}-\mu\delta^2 + j\left[\frac{2\alpha_2\beta}{\delta}(1+\mu\delta^2-\beta^2)+2\alpha_1\beta\left(1-\frac{\beta^2}{\delta^2}\right)\right]\right\}x_2=\frac{F_0}{k_1}.$$

The modulus $|x_2|$ is given by

$$\frac{|x_2|}{F_0/k_1}=\frac{\delta^2}{\{[(\delta^2-\beta^2)(1-\beta^2)-\beta^2\delta^2\mu-4\beta^2\delta\alpha_1\alpha_2]^2+4\beta^2[(\delta^2-\beta^2)\alpha_1+\delta\alpha_2(\mu\delta^2+1-\beta^2)]^2\}^{\frac{1}{2}}}, \quad \ldots\ldots(1)$$

with phase angle ϕ_2 given by

$$\tan\phi_2=-\frac{2\beta[(\delta^2-\beta^2)\alpha_1+\delta\alpha_2(\mu\delta^2+1-\beta^2)]}{(\delta^2-\beta^2)(1-\beta^2)-\beta^2\delta^2\mu-4\beta^2\delta\alpha_1\alpha_2}.$$

In (1) write

$$y=\frac{|x_2|}{F_0/k_1}=\frac{\delta^2}{Z^{\frac{1}{2}}}, \quad \ldots\ldots(2)$$

then

$$Z=[\delta^2-\beta^2 A+\beta^4]^2+4\beta^2[B-C\beta^2]^2,$$

where

$$\left.\begin{aligned} A&=1+\delta^2+\delta^2\mu+4\delta\alpha_1\alpha_2,\\ B&=\delta^2\alpha_1+\delta\alpha_2(1+\mu\delta^2),\\ C&=\alpha_1+\delta\alpha_2,\end{aligned}\right\} \quad \ldots\ldots(3)$$

and, in powers of β,

$$Z=\beta^8+D\beta^6+E\beta^4+F\beta^2+\delta^4 \quad \ldots\ldots(4)$$

where

$$D=4C^2-2A; \qquad E=A^2+2\delta^2-8BC; \qquad F=4B^2-2A\delta^2. \quad \ldots\ldots(5)$$

The general form of the function $y=\delta^2/Z^{\frac{1}{2}}$ is indicated in Figure 2, in which the positive section of the curve is shown. It is now necessary to establish the conditions that y is independent of β (maximum deviation $+(100h)$ %) and to determine the range of β over which these conditions hold.

Let the curve $y=\delta^2/Z^{\frac{1}{2}}$ intersect with the straight line $y=1+h$ at the points λ_1, λ_2, λ_3, λ_4 and with the straight line $y=1$ at the points λ_5, λ_6, λ_7, λ_8. Then the conditions for tangency are

$$\text{(i)} \qquad \lambda_2=\lambda_1, \quad \lambda_4=\lambda_3, \quad \ldots\ldots(6)$$
$$\text{(ii)} \qquad \lambda_7=\lambda_6, \quad \ldots\ldots(7)$$

and the range is given by λ_8.

For $y=1+h$, equation (2) gives $Z-\delta^4/(1+h)^2=0$, whence from (4)

$$\beta^8+D\beta^6+E\beta^4+F\beta^2+G=0, \quad \ldots\ldots(8)$$
$$G=\delta^4[1-1/(1+h)^2],$$

or

$$(\beta^2-\lambda_1^2)(\beta^2-\lambda_2^2)(\beta^2-\lambda_3^2)(\beta^2-\lambda_4^2)=0. \quad \ldots\ldots(9)$$

Applying the conditions (6) and equating coefficients in (8) and (9) we obtain

$$\left.\begin{aligned} D &= -2(\lambda_1^2+\lambda_3^2),\\ E &= (\lambda_1^2+\lambda_3^2)^2+2\lambda_1^2\lambda_3^2,\\ F &= -2\lambda_1^2\lambda_3^2(\lambda_1^2+\lambda_3^2),\\ G &= \lambda_1^4\lambda_3^4. \end{aligned}\right\} \qquad \ldots\ldots(10)$$

Eliminating λ_1 and λ_3,

$$\left.\begin{aligned} E &= \tfrac{1}{4}D^2+2G^{\frac{1}{2}},\\ F^2 &= D^2G. \end{aligned}\right\} \qquad \ldots\ldots(11)$$

Similarly, applying the tangency condition (7) and equating coefficients

$$\left.\begin{aligned} D &= -(2\lambda_6^2+\lambda_8^2),\\ E &= \lambda_6^2(\lambda_6^2+2\lambda_8^2),\\ F &= -\lambda_6^4\lambda_8^2. \end{aligned}\right\} \qquad \ldots\ldots(12)$$

Solving for λ_6 and λ_8 and eliminating

$$\left.\begin{aligned} \lambda_6^2 &= -\tfrac{1}{6}\{2D\pm(4D^2-12E)^{\frac{1}{2}}\},\\ \lambda_8^2 &= -\tfrac{1}{3}\{D\mp(4D^2-12E)^{\frac{1}{2}}\}, \end{aligned}\right\} \qquad \ldots\ldots(13)$$

and

$$27F = -2D^3+9ED\pm(4D^2-12E)^{\frac{1}{2}}(3E-D^2). \qquad \ldots\ldots(14)$$

Combining (11) and (14) and reducing

$$D=\pm 4\sqrt{2}G^{\frac{1}{4}}; \qquad E=10G^{\frac{1}{2}}; \qquad F=\pm 4\sqrt{2}G^{\frac{3}{4}}. \qquad \ldots\ldots(15)$$

Since λ_1, λ_3, λ_6, λ_8 are real, D and F must be negative from (10) and (12).

Eliminating A and B in (5) and substituting for D, E and F from (15)

$$C^8+4\sqrt{2}G^{\frac{1}{4}}C^6+(7G^{\frac{1}{2}}-3\delta^2)C^4+2\sqrt{2}(G^{\frac{3}{4}}-\delta^2G^{\frac{1}{4}})C^2+\tfrac{1}{4}(G^{\frac{1}{2}}-\delta^2)^2=0. \qquad \ldots\ldots(16)$$

Writing $G=H^4\delta^4$, so that $H^4=[1-1/(1+h)^2]$, (16) becomes

$$C^8+4\sqrt{2}H\delta C^6+(7H^2-3)\delta^2C^4+2\sqrt{2}H(H^2-1)\delta^3C^2+\tfrac{1}{4}\delta^4(H^2-1)^2=0. \qquad \ldots\ldots(17)$$

For a variation of y not greater than $+5\%$, from $\beta=0$ to λ_8, $h=0{\cdot}05$, and therefore $H=0{\cdot}549$.

Inserting this value (17) becomes

$$C^8+3{\cdot}11\delta C^6-0{\cdot}89\delta^2C^4-1{\cdot}08\delta^3C^2+0{\cdot}122\delta^4=0,$$

i.e.

$$(C^2-0{\cdot}107\delta)(C^2-0{\cdot}617\delta)(C^4+3{\cdot}83C^2\delta+1{\cdot}82\delta^2)=0.$$

Thus the roots of C^2 are $0{\cdot}107\delta$, $0{\cdot}617\delta$ and two negative roots.

Therefore $C=\pm 0{\cdot}327\delta^{\frac{1}{2}}$, $\pm 0{\cdot}785\delta^{\frac{1}{2}}$; from practical consideration of (3) C must be positive. Summarizing from (5) and ignoring the negative roots of B

$$\left.\begin{aligned} A &= A_0\delta\\ B &= B_0\delta^{3/2}\\ C &= C_0\delta^{\frac{1}{2}} \end{aligned}\right\} \quad \text{where} \quad \left.\begin{aligned} A_0 &= 1{\cdot}767,\ 2{\cdot}79\\ B_0 &= 0{\cdot}806,\ 1{\cdot}08\\ C_0 &= 0{\cdot}327,\ 0{\cdot}785 \end{aligned}\right\}. \qquad \ldots\ldots(18)$$

From (3) and (18)

$$\left.\begin{aligned} 1+\delta^2(1+\mu)+4\delta\alpha_1\alpha_2 &= A_0\delta,\\ \delta^2\alpha_1+\delta\alpha_2(1+\mu\delta^2) &= B_0\delta^{3/2},\\ \alpha_1+\delta\alpha_2 &= C_0\delta^{\frac{1}{2}}. \end{aligned}\right\} \qquad \ldots\ldots(19)$$

Eliminating μ and α_1,

$$(4\alpha_2^3-2\alpha_2)\delta^{3/2}+C_0(1-4\alpha_2^2)\delta+A_0\alpha_2\delta^{\frac{1}{2}}-B_0=0, \qquad \ldots\ldots(20)$$

The roots of (20) are plotted in Figure 3 to illustrate the variation of δ with α_2 for values of α_2 from 0 to 1·0 and for the larger values of A_0, B_0 and C_0 from (18). The alternative smaller values of A_0, B_0 and C_0 give a curve of similar shape but having a smaller real range and therefore of less practical importance.

The variation of μ and α_1 with α_2 may be derived from Figure 3 and (19).

The "operational range" is obtained from (13) and (15), viz. $\lambda_8=8^{\frac{1}{4}}G^{\frac{1}{2}}, (8/9)^{\frac{1}{4}}G^{\frac{1}{2}}$. Discarding the latter ambiguous value and putting $h=0{\cdot}05$, $\lambda_8=1{\cdot}25\delta^{\frac{1}{2}}$.

Using (20) the variations of λ_8 and $\delta^{\frac{1}{2}}$ with α_2 are shown in Figure 4.

Single degree of freedom. When $\mu=0$, $\delta=\infty$ (i.e. $m_2=0$, $\omega_2=\infty$) equation (2) degenerates to

$$y'=\frac{1}{\{(1-\beta^2)^2+4\alpha_1^2\beta^2\}^{\frac{1}{2}}}. \qquad \ldots\ldots(21)$$

Applying the tangency condition as before, $(2\alpha_1^2-1)^2=[1-1/(1+h)^2]$.

Putting $h=0{\cdot}05$

$$\alpha_1=0{\cdot}59,\ 0{\cdot}81. \qquad \ldots\ldots(22)$$

If the curve given by (21) intersects $y'=1$ at $\beta=\lambda_8'$ then $\lambda_8'^2=2(1-2\alpha_1^2)$. Discarding the larger root in (22) since it gives an imaginary value for β in (21), $\lambda_8'=0{\cdot}78$. Comparing this result with the value obtained from Figure 4 for $\alpha_2=0{\cdot}1$ we find $\lambda_8/\lambda_8'=1{\cdot}96$. Thus for $\alpha_2=0{\cdot}1$ the operational range in the double system is greater than that in the corresponding single system by a factor 1·96.

Conversely, since the sensitivity of the first system is inversely proportional to k_1 and therefore inversely proportional to ω_1^2, the sensitivity of a double system is 3·85 times greater than that of the corresponding single system for a given operational range.

REFERENCE

DEN HARTOG, J. P., 1940, *Mechanical Vibrations* (New York: McGraw-Hill), pp. 108–129.

Note on Volt-Dependent Poisoning Effects in Oxide-Cathode Valves

By G. H. METSON
Electronics Division of the P.O. Research Station, Dollis Hill, N.W.2

MS. received 28*th May* 1948, *in amended form* 24*th March* 1949

ABSTRACT. The high vacuum oxide-cathode valve may show cathode poisoning effects when its electrodes are bombarded by electrons of certain discrete energies. Hamaker, Bruining and Aten describe one such effect occurring at about 10 ev. The author confirms this result and describes two other effects occurring at 5·56 ev. and 15·9 ev. The energies of the three effects can be closely associated with the heats of formation of the chlorides, monoxides and sulphates of barium and strontium. It is concluded that the 5·56 ev. effect is due to bombardment dissociation of the monoxides of barium or strontium, the 10 ev. effect to the chlorides and the 15·9 ev. effect either to the sulphates or to a gaseous ionization phenomenon.

§ 1. INTRODUCTION

A CURIOUS poisoning effect on oxide-coated cathodes was noted in 1936 by Headrick and Lederer (1936). The effect occurred when the electrodes of an oxide-cathode valve were bombarded with electrons having any energy between 7 and 25 electron volts. The poisoning reaction was absent when the bombarding energy was less than 5 ev. It was concluded that the poisoning was due to the dissociation of thin films deposited on the electrodes during cathode activation. Chemical analysis showed that the films were carbon compounds and barium compounds—probably oxides.

In 1947 a similar effect was noted by Hamaker, Bruining and Aten (1947) but with a characteristic difference: the poisoning effect occurred only with electron energies greater than 10 ev. Systematic work on the dissociation of chemical compounds by electron bombardment was first undertaken by Jacobs (1946). Jacobs' work resulted in the tentative establishment of a relationship between the minimum electron energy for dissociation and the heat of formation of the compound concerned. The relation between this minimum electron energy (or critical energy) E_c and the heat of formation is $E_c = H/23$ ev., i.e. 23 kg.cal/mole is equivalent to 1 ev. per molecule.

Similar effects were examined by the writer in 1946, and the object of the present note is to extend and reconcile existing information.

§ 2. THE 6–8 VOLT EFFECT

A voltage-dependent effect was first noticed during the examination of commercial pentode valves of the indirectly-heated oxide-cathode type. A typical case may be described in the following manner. The valve was arranged as a diode with control-grid acting as electron collector. With the cathode at a nominal 1,000° K., a diode volt/amp. characteristic was then taken starting with zero voltage on the collector. The characteristic followed a smooth power law curve up to a collector voltage of about 7 volts, after which an abrupt and drastic deviation was observed (see Figure). Similar results were found to occur on a wide range of pentode valves and the phenomenon appeared to be general. It was soon found that the voltage at which the effect occurred was independent of cathode temperature, although the actual magnitude of the effect increased rapidly with decrease of

temperature. Above certain temperatures the effect appeared to be absent altogether. This temperature dependence of the magnitude of the effect is to be expected from common experience of cathode poisoning phenomena. Further work showed that the space-charge current could be held steady for an indefinite period if the collector voltage was maintained at a fraction of a volt below the critical voltage.

To gain quantitative information on the matter a batch of 24 pentode valves of different types was selected for examination. Half of the batch consisted of new valves and the other half of valves which had run for 20,000 hours in service. The

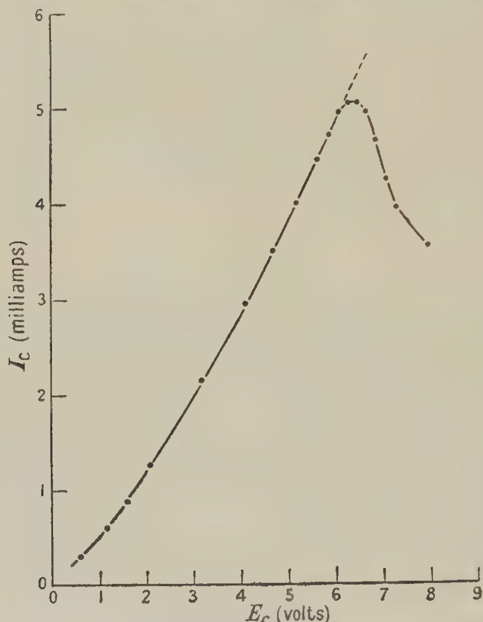

Typical example of 6–8-volt effect.

critical voltage was measured for each tube at a cathode temperature of approximately 900° K. The critical energy was then interpreted as the critical voltage applied between cathode and collector minus the observed value of contact potential plus the mean thermal energy of electron emission from the hot cathode. The measured contact potential was usually of the order of 1 volt and the thermal emergence energy about 0·1 volt. Results for the 24 samples were: critical energy = 5·56 ev., with a standard deviation of 0·28 ev.

§ 3. THE OTHER EFFECTS

In order to separate the several effects it is necessary to understand the reaction of the oxide-cathode valve to a low pressure poisoning attack. If the control-grid of a pentode valve is bombarded for a long period with electrons of 8 ev. energy then a poisoning phenomenon is observed due to the 5·56 volt effect. The effect is due to the evolution of gas resulting from dissociation of a surface film. A proportion of the evolved gas goes to the cathode and poisons it; another portion goes to neutral surfaces in the valve and settles there in the adsorbed state. The gas that enters the cathode is converted to the negative ion state and then tends to re-emerge from the cathode. These negative ions return to the collector, where they become neutralized and are available for a further cycle. There is a chance,

therefore, during each cycle, that a gas atom or ion is permanently removed from the cathode-collector system by adsorption on a neutral surface. In time the whole (or at least the great bulk) of the poisoning gas is ejected, and the cathode recovers from the attack. Prolonged running at 8·0 volts will therefore result in an initial, and possibly drastic, poisoning phase, followed by a slow recovery to the initial emission. Such attacks are described as reversible and have been investigated quantitatively in other work by the writer (Metson 1949).

The control-grid may thus be completely cleared of the film giving rise to the 5·56 volt effect by prolonged bombardment at 8·0 volts. After clearance, the diode volt/amp. characteristic is found to be identical in slope with the original characteristic, although it may be somewhat displaced by contact potential changes.

The conditioned valve may now be examined for a higher order effect. A diode volt/amp. characteristic is taken and a smooth power law curve obtained up to about 10 volts, where an abrupt poisoning phenomenon is observed. The critical energy for this effect was found to be 9·4 ev., the mean value of three observations.

The 9·4 volt effect is now cleared by prolonged running at 11 volts and a search made for still higher order effects. One such effect was observed at a critical energy of 15·9 ev. No further effects between this and 25 ev. could be detected. During this phase of the search the tube gave a smooth characteristic up to 25 volts, at which the diode current was quite steady and independent of time. It seems probable therefore that the effects are limited to 5·56 ev., 9·4 ev. and 15·9 ev.

§ 4. CONCLUSION

If the work of Jacobs is accepted, then an obvious step is to attempt the association of these three critical energies with the heats of formation H of compounds which are likely to occur in the oxide-cathode valve. The Table shows the values of H derived from the critical energies and those of certain compounds taken from a chemical handbook.

Effect (ev.)	5·56	9·4	15·9
Derived value of H	128	216	366
Values of H for probable compounds	BaO 133 SrO 141	$BaCl_2$ 205 $SrCl_2$ 198	$BaSO_4$ 349 $SrSO_4$ 345

Values of H are measured in kg.cal/mole.

From these figures it would appear that the 5·56 ev. effect is due to oxygen poisoning of the cathode, and the 9·4 ev. effect to chlorine poisoning, the gases being developed by dissociation of the monoxides and chlorides of either Ba or Sr or both.

The 15·9 ev. effect must be interpreted with caution as it may well be an example of ionization poisoning (Metson and Holmes 1949) by O^+, Cl^+ or some other positive ion. It is interesting to note however that the cathodes used in the work were of the common BaO–SrO type and contained chlorides and sulphates as minute contaminants.

REFERENCES

Hamaker, H. C., Bruining, H., and Aten, A. H. W., 1947, *Philips Res. Rep.*, **2,** 171.
Headrick, L. B., and Lederer, E. A., 1936, *Phys. Rev.*, **50,** 1094.
Jacobs, H., 1946, *J. Appl. Phys.*, **17,** 596.
Metson, G. H., 1949, *Nature, Lond.*, in press.
Metson, G. H., and Holmes, M. F., 1949, *Nature, Lond.*, **163,** 61.

REVIEWS OF BOOKS

Plastics Dictionary, by THOMAS A. DICKINSON. Pp. xiii + 312. First Edition. (London: Sir Isaac Pitman and Sons, Ltd., 1948.) 25*s.*

This dictionary, which is of American origin, consists of descriptions of materials—polymers, fillers, solvents and products under trade names—together with definitions of scientific and technical terms encountered in the Plastics literature. The cover of proprietary products is indeed comprehensive, both British and Continental materials being included in addition to those of the U.S.A. Many of the descriptions of materials are incomplete and vague, but the author cannot be held responsible for the scanty information which is made available about some products of the Plastics Industry. It is clear, however, that the author has transcribed information from other sources with very imperfect understanding.

The definitions of scientific and technical terms are generally poor and contain so many gross blunders that one has little confidence in the dictionary as a whole. One is concerned not with fine distinctions of meaning or minor blemishes on a substantially sound definition but rather with out-and-out howlers. The following examples are given with the assurance that they are not unrepresentative: *Aldehyde* (p. 12)—A colourless, pungent, volatile liquid produced by the oxidation of ethyl alcohol. Probably the most widely used aldehyde in plastics is *formaldehyde.* All plastics containing aldehyde are collectively known as " aldehydes ". *Alginate fibers* (p. 12)—Fibrous fillers made from *algae. Aliphatic* (p. 12)—Fatty. *Anion-exchange resin* (p. 20)—A resin that is made by the transfer of negative ions within two or more basic ingredients. For example, a phenolic resin can be thus made by the reaction of metaphenylenediamine, hydrochloric acid, formalin, and water. *Azeotropic mixture* (p. 25)—A mixture with the same boiling point at any pressure. *Benzoic acid* (p. 32)—A vegetable compound obtained from benzoin and from various resins. It has a pungent and bitter taste and a somewhat aromatic odour. *Emulsion* (p. 93)—A mechanical mixture of liquids (and sometimes air) made by beating or whipping the liquids together. An emulsion occurs because the liquids are not chemically capable of combining to form another chemical. The particles involved are merely suspended alongside one another. *Glucose* (p. 119)—Any of a class of carbohydrates having $C_6H_{12}O_6$ composition. *Glycol* (p. 121)—A class of artificial compounds intermediate in their properties and chemical relations between alcohol and glycerin. Or a diatomic acid, alcohol being a monoatomic and glycerin a triatomic, which occurs in the form of an odourless liquid with a sweetish taste; it is insoluble in alcohol and water. *Graphite* (p. 121)—A crystalline form of carbon containing traces of iron and silicon oxide. An abrasive, it is sometimes used as a filler for plastic bearings. *Hydroxy-benzyl group* (p. 131)—Phenol and formaldehyde alcohol solutions and their reaction products. *Methylate* (p. 162)—To saturate or mix with methyl alcohol. *pH* (p. 188)—A chemical symbol used to denote the degree of alkalinity or acidity of a substance in terms of the equivalent concentration of hydrogen ions with the sign changed. *Polyvinyl* (p. 227)—Polymerized vinyl.

Substances differing in solubility so widely as *styrene* (p. 280), *hydrochloric acid* (p. 130), *magnesium carbonate* (p. 156), *oxalic acid* (p. 180) and *methane* (p. 161) are described equally as being " more or less soluble in water, alcohol and ether ".

The dictionary is intended for both expert and layman; it may serve to refresh the memory of the expert, but it should not be put in the hands of a layman. K. W. PEPPER.

Vacuum Tube Circuits, by LAWRENCE BAKER ARGUIMBAU. Pp. vii + 668. First Edition. (John Wiley and Sons, Inc., New York; British Agents: Chapman and Hall, Ltd., London, 1948). 36*s.*

It is difficult at first sight to decide for whom Prof. Arguimbau's book is intended. In his preface the author says: "The treatment is intended primarily for those who have studied the physics of vacuum tubes . . . . A knowledge of A.C. circuits, of calculus, and of Fourier series is assumed." In other words, it serves as a " conversion course " for physicists and electrical engineers who wish to become familiar with electronic circuit techniques. However, such readers are likely to get a somewhat false impression of the

relative importance of the various parts of the subject, since the author has tended to give certain advanced topics very detailed treatment, while dismissing lightly matters of rather greater everyday importance to the electronic engineer. For instance, the design and stability of amplitude-controlled oscillators receives thirty pages, as does also the klystron, while only thirteen pages are devoted to amplitude-modulated transmitters. In these pages, also, no mention is made of any system of modulation other than anode modulation.

The author makes considerable use of problems in the text, both to illustrate points already described and also to demonstrate new points to the reader. In fact, to obtain the fullest value from a chapter it is necessary to have worked out the majority of the problems in the chapter. This system is of great value to the student, but is likely to be regarded unfavourably by the practising engineer, who usually prefers to glance rapidly through a new book, thereafter using it mainly for reference.

The subjects which the author treats in detail are in general very well done. Chapter III, Triodes, Pentodes and Linear Amplifiers, and Chapter X, Frequency Modulation, are particularly clear and valuable, and the treatment of Inverse Feedback and Power Amplifiers is sound and practical. The chapters on Transient Response of Video Amplifiers and on Pulses and Television are, however, somewhat sketchy. Other chapter headings include Diodes and Rectifiers, Amplitude Modulation, Oscillators and Microwaves.

The author's style is clear and pleasing throughout. The book is profusely illustrated, both with diagrams to which direct reference is made and also with " thumb-nail sketches " which emphasize points made in the text.

If used in conjunction with one of the standard textbooks on radio engineering, Prof. Arguimbau's book could be of great value to the student. It provides a refreshing and, in most cases, a physical approach to problems which are often treated too formally, and includes much modern material otherwise available only in the literature. A quotation, which might well form the circuit designer's motto, may serve to indicate the author's practical approach : " It is usually possible to solve a difficult problem in a difficult way by brute force and ignorance. However, real advances are made by recognizing difficulties and avoiding them ". K. E. MACHIN.

Textbook of Physical Chemistry, by J. NEWTON FRIEND. Pp. xv + 566. Second Edition. (London : Charles Griffin and Co., Ltd., 1948). 42*s*.

This book is an abridged and revised edition of Dr. Newton Friend's earlier two-volume work, and is intended as a textbook for advanced students. It contains a number of unusual features both in matter and arrangement. The general approach to the subject is descriptive rather than mathematical, and the section on thermodynamics, which is of a relatively elementary character, is relegated to the final chapter of the book. While equations and quantitative expressions are introduced throughout the text, their deduction is often only somewhat sketchily outlined. Most teachers will regard these points as serious criticisms in a work intended for advanced students. At the same time, the book contains a vast amount of information, and a number of interesting topics, such as the mechanism of combustion and flames, which are not usually included in standard textbooks of physical chemistry, are discussed. Furthermore, concepts and ideas which often cause difficulty to students are frequently illuminated by ingenious experiments and illustrations. The reviewer would hesitate to recommend the work as a basic textbook for degree students, but it is a book which they might read with profit for revision purposes and to obtain a view of the subject rather different from that afforded by more conventional texts. A. H.

Principles of Servomechanisms, by G. S. BROWN and D. P. CAMPBELL. Pp. xiii + 400. First Edition. (New York : J. Wiley and Sons ; British Agents : Chapman and Hall, Ltd., London, 1948). 30*s*.

This book is intended to assist graduate and post-graduate study of servomechanisms of all kinds, and is not intended for specialists in a particular field. The subject lends itself well to this broad approach since many techniques common in one field of study can conveniently be carried into another where their use is less common. A typical example is the use of a block diagram and its associated transfer function (or equivalent circuit) to represent a more complex physical object.

This breadth is obtained at the cost of making some of the specialized parts rather lengthy from the point of view of the specialist in that field. For example, the electrical engineer will find much of Chapter 5 unnecessary; and the mathematician's attitude to Chapter 3 would doubtless be similar.

The newcomer to the subject would probably find Chapter 1 too broad for his immediate comprehension and should take as his starting point Chapter 2, which deals with the derivation of equations of motion of mechanical and electro-mechanical systems. The superior properties of closed loop systems are demonstrated, but it is questionable whether Figure 3 is really a fair example of common practice in open loop control.

Chapters 3 and 4 are a largely mathematical excursion dealing with Laplace transforms, frequency responses, vector loci, and the correlation between transient response and steady state sinusoidal response.

Chapter 5 discusses the reduction of complex practical elements to block diagram form, and includes some less familiar mechanical elements as well as electrical elements.

Later chapters are concerned with the design procedures used to ensure satisfactory and specified performance as regards stability, transient response, and freedom from static error. The book also includes a set of problems and an extensive bibliography.

As stated in the Preface, the book deals solely with linear systems and does not discuss the many non-linear effects encountered in mechanical servos as distinct from electronic feedback amplifiers. The approach is mathematical throughout, the relevant equations being deduced at the earliest possible stage. The properties of the system are then treated as being the properties of the resulting equation. The effect of non-linearities on the validity of this procedure in practical cases is not emphasized.

The book is not free from errors, e.g. on page 48 ω is stated to have the dimensions of time; equation (96) on page 84 is stated to be " in dimensionless form ", whereas in fact each term has the dimensions of $(1/\text{time})^2$, and equation (42) on page 104 relates to the response to unit impulse and not to unit step as stated. F. C. WILLIAMS.

Tables of Bessel Functions of Fractional Order, Vol. I. Prepared by the Computation Laboratory of the National Applied Mathematics Laboratories, National Bureau of Standards. Pp. xlii+413. (New York: Columbia University Press, 1948). Price not stated.

The uses of Bessel functions of integral order are familiar to physicists in almost every field, and those of the functions of order half an odd integer are well known in wave-theory. The functions of order $\pm\frac{1}{4}$ and $\pm\frac{1}{3}$ satisfy indirectly the differential equations $y''+p^2x^2y=0$ and $y''+p^2xy=0$.

The present volume gives the functions of the first kind of orders $\frac{1}{4}$, $\frac{1}{3}$, $\frac{2}{3}$ and $\frac{3}{4}$ and of the corresponding negative orders with second differences. A further volume will give the functions of the second kind for the same orders. The argument in every case ranges up to 25, with further tables from which values may be obtained up to 30,000, and the values are given to 10 significant or 10 decimal figures. In addition, the first thirty roots of $J_n(x)=0$ are tabulated, and formulae given for higher roots. A final table assists in interpolation in the order, at a fixed argument.

As is usual in this series, not the least valuable part is the essay on the functions, with an excellent bibliography. J. H. A.

CORRIGENDA

"Temperature Measurements of Flames containing Incandescent Particles", by H. G. Wolfhard and W. G. Parker (*Proc. Phys. Soc.* B, 1949, **62**, 523).

Abstract, line 11. Melting point *should read* boiling point.
P. 525, line 3. Al_2O_3 *should read* AlO.
P. 525, § 3, line 5. Al_2O_3 *should read* AlO.

CONTENTS FOR SECTION A

ABSTRACTS FOR SECTION A

The Physical Basis of Life, by J. D. BERNAL.

32nd Guthrie Lecture, delivered 21st November 1947.

A Stereographic Projector, by A. E. DE BARR.

ABSTRACT. An optical device is described by which the effect of rotation on the stereographic projection of a crystal can be observed directly. The application of the device to the construction of pole figures from x-ray data is described.

A Study of Magnetic Viscosity, by R. STREET and J. C. WOOLLEY

ABSTRACT. A general analysis of magnetic viscosity based on activation energy concept is given. A particular case is considered of the application of the theory to the phenomenon occurring in materials in which bulk magnetization proceeds by the rotational movement of the vectors of single domains, which process, according to a recent theory of Stoner and Wohlfarth, may occur in certain high coercivity alloys. Experiments have been made, using a magnetometer method, with specimens of alnico maintained at various temperatures within the range $-187°$ C. to $250°$ C. The results obtained are found to be in good agreement with the theoretical analysis.

The Decay of ^{170}Tm and ^{186}Re, by P. J. GRANT and R. RICHMOND.

ABSTRACT. The radiations from the active isotopes ^{170}Tm and ^{186}Re have been investigated. ^{170}Tm is found to have a β-ray end-point of $1{\cdot}00 \pm 0{\cdot}005$ MeV. with possible lower-energy groups at $0{\cdot}90 \pm 0{\cdot}015$, $0{\cdot}79 \pm 0{\cdot}025$, $0{\cdot}45 \pm 0{\cdot}05$ MeV. γ-rays with energies $82{\cdot}6 \pm 0{\cdot}5$, 205 ± 10, 430 ± 20 kev. were observed. The 430 kev. radiation is thought to be complex. ^{186}Re is found to have a β-ray end-point of $1{\cdot}090 \pm 0{\cdot}005$ MeV. with other groups at $0{\cdot}95 \pm 0{\cdot}015$ and $0{\cdot}64 \pm 0{\cdot}03$ MeV. Three γ-rays were observed, having energies 700 ± 50, 275 ± 8 and 133 ± 1 kev. The last is assumed te be a mean energy-value of the three low-energy γ-rays found by Cork, Shreffler and Fowler. Decay schemes are suggested for both isotopes.

A Note on the ^{10}B (n, α) ^{7}Li Reaction, by S. DEVONS.

ABSTRACT. It is difficult to explain the observed preponderance of transitions to the excited state of ^{7}Li in the reaction ^{10}B (n, α) ^{7}Li in terms of the usual assumption that the ground state and first excited state of ^{7}Li form a $^{2}P_{3/2},_{1/2}$ doublet. In addition the doublet separation (0·48 MEV.) would be much larger than expected theoretically. If the excited state of ^{7}Li has total angular momentum other than 1/2, one would expect to find, in general, some angular correlation between the direction of emission of the α-particle, that of the subsequent γ-radiation and the polarization of the radiation. The correlations to be expected have been calculated on the assumption that the ground state of ^{7}Li is (3/2, odd), that of ^{10}B (3, odd), or (3, even), and that the compound nucleus ^{11}B has definite $J=5/2$ or 7/2. Results are given for excited states of ^{7}Li with total angular momentum 1/2, 3/2, 5/2 and 7/2 and both even and odd parities.

The Neutrons emitted in the Bombardment of ^{10}B and ^{11}B by Deuterons, by W. M. GIBSON.

ABSTRACT. The photographic plate method has been used in an investigation of the neutrons from the (dn) reactions in ^{10}B and ^{11}B, separated isotopes being used in the targets.

The reaction ^{10}B(dn)^{11}C gives neutron groups at 6·70 MEV. and 4·85 MEV. ; these give an energy release for the transition to the ground state of 6·59±0·10 MEV., and show the existence of a level in ^{11}C at 2·02±0·10 MEV.

The reaction ^{11}B(dn)^{12}C gives well-defined neutron groups at 13·51 MEV., 9·40 MEV. and 4·55 MEV., with a continuous distribution up to 6 MEV. and a small peak at 6·4 MEV. The 13·51 MEV. group gives an energy release of 13·92±0·15 MEV. for the transition to the ground state ; the other groups confirm the existence of levels in ^{12}C at 4·47±0·10 MEV., 9·72±0·15 MEV. and less certainly 7·7 MEV., while the continuous distribution is due to the reaction ^{11}B(dn)3α.

Three-Dimensional Design of Synchrotron Pole-Faces, by C. ROBINSON.

ABSTRACT. An analytical method for the design of a synchrotron pole-face is outlined, the method taking full account of the cylindrical symmetry. Relaxation methods are employed to determine the exact size and shape of the lips correcting for fringing, and are also used to give a final check on the characteristics of the magnetic field. Practical examples of these methods are then given.

Printed by Taylor and Francis, Ltd., Red Lion Court, Fleet Street, London E.C.4